ANALYSIS OF SAGITTAL PROFILE OF SPINE OF ADOLESCENT IDIOPATHIC SCOLIOSIS USING ULTRASOUND

LEE TIN YAN

PhD

The Hong Kong Polytechnic University

2019

The Hong Kong Polytechnic University

Department of Biomedical Engineering

Analysis of Sagittal Profile of Spine of Adolescent Idiopathic Scoliosis Using Ultrasound

Lee Tin Yan

A thesis submitted in partial fulfillment of the requirements for the degree of Doctor of Philosophy

September 2019

CERTIFICATE OF ORIGINALITY

I hereby declare that this thesis is my own work and that, to the best of my knowledge and belief, it reproduces no material previously published or written, nor material that has been accepted for the award of any other degree or diploma, except where due acknowledgement has been made in the text.

_______________________________ (Signed)

______Timothy Lee Tin Yan______ (Name of Student)

ABSTRACT

Radiographic Cobb's angle is the gold standard for evaluation of spinal curvature, however, X-ray is ionizing and is not suggested for repeated scanning. In contrast, ultrasound is non-ionizing and inexpensive, thus more accessible. Ultrasound has been used to evaluate the coronal curvature and transverse vertebral rotation of the spine of patients with adolescent idiopathic scoliosis (AIS). However, no study has reported the reliability and accuracy of ultrasound on sagittal curvature analysis. Since AIS is a three dimensional deformity, the pattern of deformity in the coronal plane may be highly influenced by changes in the axial and sagittal planes due to the effect of coupling in different planes. In addition, characterizing the differences in sagittal profile between normal and scoliotic spines may also provide early detection of vertebrae rotation, and quantifying spinal curvatures in different planes is useful for preoperative planning, postoperative evaluation and monitoring curve progression, thus there is a huge potential of using ultrasound for evaluating the sagittal spinal curvature. The objective of this study was to investigate the feasibility of using ultrasound to evaluate sagittal spinal profile, it was divided into three phases: 1) Phantom study; 2) Human subjects study; and 3) Human subjects study for coronal-sagittal coupling, including the exploratory stage and validation stage.

In the present study, sagittal ultrasound angles were demonstrated to be reliable and valid for assessing sagittal curvature in both phantom and human subject studies. As laminae were observed to have a better visualization in ultrasound images, and no significant differences were revealed in the ultrasound sagittal measurements obtained using spinous processes and laminae as demonstrated in the human subjects study, ultrasound laminae angle was recommended to be used for sagittal

measurement in the future. The reliability of sagittal measurement using ultrasound demonstrated in this study suggested that 3D ultrasound imaging could be a potential non-ionizing tool for evaluating the sagittal profile of patients with AIS. The results of the study also showed that there was a certain level of coupling between the sagittal curvature and coronal curvature. Further studies are worthwhile to investigate whether such coupling has an indication of curve progression. Due to the radiation-free nature of ultrasound, it will also be very meaningful to conduct follow-up investigation of patients with AIS for monitoring sagittal profile changes.

PUBLICATIONS ARISING FROM THE THESIS

Journal Papers

1. **Lee TTY**, Jiang WW, Cheng CLK, Lai KKL, Begovic H, To MKT, Zheng YP, Cheung JPY. A novel method to capture the sagittal profile in spinal deformities: the reliability and feasibility of 3D ultrasound Imaging. Ultrasound Med Biol. 2019;45(10):2725-2735.
2. **Lee TTY**, Cheung JCW, Law SY, To MKT, Cheung JPY, Zheng YP. Analysis of Sagittal Profile of Spine Using 3D Ultrasound Imaging: A Phantom Study and Preliminary Subject Test. CMBBE: Imaging and Visualization 2018. https://doi.org/10.1080/21681163.2019.1566025 (Published)
3. Zheng YP, **Lee TTY**, Lai KK, Yip BH, Zhou GQ, Jiang WW, Cheung JC, Wong MS, Ng BK, Cheng JC, Lam TP. A reliability and validity study for Scolioscan: a radiation-free scoliosis assessment system using 3D ultrasound imaging. Scoliosis Spinal Disord 2016;11:13. (Published)

Conference proceedings

1. **Lee TTY**, Cheung JCW, Zheng YP. Investigation of sagittal profile of spine using 3D ultrasound: A phantom study. 2016 Joint ICBMU & ISMA Conference.
2. **Lee TTY**, Cheung JCW, Zheng YP. Analysis of Sagittal Profile of Spine Using 3D Ultrasound. 2017 International Conference on Biomedical Ultrasound (ICBMU).
3. **Lee TTY**, Cheung JCW, Law SY, Zheng YP. Sagittal spine analysis using 3D ultrasound: a preliminary study using spine phantom. 2017 8th World Congress on Bioengineering.

4. **Lee TTY**, Jiang WW, Cheng CLK, Lai KKL, Begovic H, Samartzis D, To MKT, Cheung JPY, Zheng YP. Radiation-free 3D ultrasound can provide sagittal profile of adolescent idiopathic scoliosis. 2018 SRS 53rd Annual Meeting & Course.
5. **Lee TTY**, Lai KKL, Cheung, JPY, To MKT, YP Zheng. Analysis of sagittal profile of spine using ultrasound imaging in adolescent idiopathic scoliosis with the assistance of radiograph. 2018 SOSORT World Meeting 2018.
6. **Lee TTY**, Lai KKL, Cheung, JPY, To MKT, YP Zheng. A novel approach to sagittal profiling of adolescent idiopathic scoliosis using 3D ultrasound. 2018 The International Research Society of Spinal Deformities (IRSSD).

ACKNOWLEDGEMENTS

I am very grateful to all those people who have helped and supported me throughout my Ph.D. study in PolyU. First and foremost, I would like to express my deepest appreciation to my chief supervisor, Professor Zheng Yong-ping, for his continuous guidance and support throughout my Ph.D. study. He is always very patient in offering me insightful suggestions and comments to improve my research works and enhance the quality of my written materials and presentation skills. It is my great honor to have him as my research advisor and mentor.

I would also like to express my special thanks to my beloved parents for their unconditional support and encouragement throughout my life especially during the study period. This thesis would never have been completed without them. I also owe many thanks to my dear girlfriend, Noel Ho, for giving me so many enjoyable moments and providing me with continuous love and encouragement whenever I encountered difficulties during these years of study.

I would also like to express many thanks to the research members of our group for their precious assistance and comments. Especially, I would like to thank Kelly and Heidi for delivering great quality scanning scans, Meng Qiang for providing the 3D analysis software, Henry and William for technical support, Dr. Jason Cheung and Dr. TP Lam for the valuable comments on my research directions, and Ms Sally Ding for editing the thesis. Last but not least, I would like to express my gratitude to Professor Rene Castelein, for allowing me so kindly during my 2-month visit at University Medical Centre Utrecht.

TABLE OF CONTENTS

LIST OF FIGURES

LIST OF TABLES

LIST OF ABBREVIATIONS

3D: Three Dimensional

AIS: Adolescent Idiopathic Scoliosis

CPB: Centre of Posterior Border

CR: Computed Radiography

CT: Computed Tomography

DICOM: Digital Imaging and Communications in Medicine

ICC: Intraclass Correlation Coefficient

LBP: Low Back Pain

LL: Lumbar lordosis

MAD: Mean Absolute Difference

MRI: Magnetic Resonance Imaging

NCJ: Neurocentral Junction

PT: Posterior Tangent

SD: Standard Deviation

SPA: Spinous Process Angle

TK: Thoracic Kyphosis

US: Ultrasound

USLA: Ultrasound Laminae Angle

USSPA: Ultrasound Spinous Process Angle

XCA: X-ray Cobb's Angle

Chapter 1. Introduction

1.1. Background

Idiopathic scoliosis is a three-dimensional (3D) deformity characterized by lateral deviation, sagittal misalignment and transverse axial rotation of the spine (Hattori et al. 2011, Pope et al. 1984). Among all pediatric spine deformities, adolescent idiopathic scoliosis (AIS) is most prevalent (Cheng et al. 2015, Fan et al. 2016, Fong et al. 2015). Due to the effect of coupling in different planes, the pattern of deformity in the coronal plane may be highly influenced by changes in the axial and sagittal planes (Gum et al. 2007, Hayashi et al. 2009, Sullivan et al. 2017, Villemure et al. 2001). However, most of the AIS studies mainly focus on the coronal plane, indeed additional attention should be paid on sagittal plane deformity and measurements on AIS patients (Deacon et al. 1984, Dickson et al. 1984, Lenke et al. 2001).

Human spine composes of five regions: cervical, thoracic, lumbar, sacrum and coccyx. Thoracic kyphosis and lumbar lordosis are two common sagittal parameters when analyzing sagittal profile. For normal individuals, acceptable ranges for kyphosis and lordosis are from 20 to 50 degrees and 31 to 79 degrees, respectively (Boseker et al. 2000, Bridwell and Bernhardt 1989). Maintaining an optimal sagittal spinal profile helps to maintain spine motor control with minimum energy expenditure, enhance the load tolerance of the spine and increase spinal muscle efficiency (Kim et al. 2006). The sagittal profile of patients with AIS had been shown to be different from normal individuals (Carpineta et al. 2003, Cheung et al. 2018, Schlösser et al. 2014, Schmitz et al. 2011). For instance, reduction of lumbar lordosis and sacrum inclination reduced the natural curvature of the lumbar spine (Makhsous et al. 2013, Alexander et al. 2007, Drzał-Grabiec et al. 2015). In addition, it was demonstrated that alternation of sagittal spinal curvature caused viscoelastic deformation of spinal tissues (Solomonow et al. 2003), higher intra-discal pressure (Wilke et al. 1999) and spine overloading and degeneration (Makhsous et al. 2013, Alexander et al. 2007, Drzał-Grabiec et al. 2015, Beach et al. 2005). Moreover, flattening of the thoracic kyphosis was found to be a risk factor for scoliosis (Roussouly et al. 2013) and reportedly cause diminution of the lung function in patients with scoliosis (Winter et al. 1975). Furthermore, shear loads experienced by vertebrae were altered once the sagittal spinal profile was disturbed, hence facet joints in the posterior portion of the posterior inclined vertebra were unlocked, inducing rotational instability to the spinal column and causing further progression in spinal deformity (Janssen et al. 2011, Schlösser et al. 2014, Castelein et al. 2005, Kouwenhoven et al. 2007). Spinal sagittal imbalance also affects the quality of life of an individual. Previous studies reported that alternation of the lumbar lordosis led to the occurrence of lower back pain (Jackson et al. 2011, Bernard et al. al. 2008, de Jonge et al. 2002), headaches, fatigue and cervical pain (Chow et al. 2007). In some severe cases, social interaction of the patients was affected due to deficient forward gaze (Roussouly and Nnadi 2010). Hence it is important to evaluate the spinal sagittal profile of patients with AIS. Furthermore, characterizing the differences in sagittal profile between normal and scoliotic spines may also provide early detection of vertebral rotation (Schlösser et al. 2014), and quantifying spinal curvatures in different planes is useful for surgical planning and monitoring curve progression (Carlson et al. 2013, Cheung et al. 2013, Vrtovec et al. 2009).

X-ray and magnetic resonance imaging (MRI) are the two commonly used imaging modalities for evaluating sagittal spinal curvature, where using Cobb’s method on radiograph is the gold standard at present (Cobb 1948, Vrtovec et al. 2009, Harrison et al. 2001). The major drawback of radiograph evaluation is that patients are exposed to radiation. Ionizing radiation remains an issue for patients even using EOS, a biplanar X-ray imaging system utilizing reduced dosage, which requires repetitive scanning, on top of the high cost and installation complexity. MRI has been used for spinal deformity evaluation because of its high resolution. However, it is costly and less accessible (Diefenbach et al. 2013). Moreover, patients are required to be imaged in supine position, hence the natural spinal curvature cannot be acquired (Yazici et al. 2011). Furthermore, different topographic methods could only evaluate the spinal curvature in an indirect way instead of measuring the actual curvature of the spine itself.

Free-hand 3D ultrasound imaging, which combines a conventional B-mode imaging system with a position sensor, has been developed over two decades and recently become more popular due to its features of radiation-free, wider accessibility and lower cost in comparison with other 3D imaging modalities (Huang et al. 2005, Huang and Zeng 2017, Mozaffari et al. 2017). Ultrasound evaluation of coronal curvature and vertebral rotation was reported by Suzuki et al. (1989) back to 1980's. Later, a number of 3D ultrasound imaging systems for the coronal plane assessment of scoliosis have been reported by different groups (Cheung and Zheng 2010, Li et al. 2010, Prunama et al. 2010, Chen et al. 2013, Ungi et al. 2014). Cheung et al. (2013, 2015) reported preliminary tests on spinal column phantoms and human subjects based on spinous process angle, and later the same system was used for testing a larger number of subjects, demonstrating high intra- and inter-rater and operator reliability, and good correlation with Cobb's angle (Zheng et al. 2016, Brink et al.

2018). Spinous process angle was also used to investigate the effectiveness of orthotic treatment for patients with AIS (Li et al. (2012). A study utilized tracked ultrasound to localize vertebral transverse processes as landmarks along the spine to measure curvature angles on spine phantoms (Ungi et al. 2014). Huang et al. (2018) further developed this method by continuously monitoring image spatial information to form a continuous curved plane for scoliosis assessment. Centre of laminae methods has also been used for both coronal curvature and vertebral rotation assessment (Chen et al. 2013, Young et al. 2015, Chen et al. 2016, Wang et al. 2016), and all these studies demonstrated that the ultrasound angles obtained were reliable and comparable to the angles obtained from conventional methods. However, no study has been reported on the reliability of 3D ultrasound imaging for evaluating the sagittal spinal curvature.

1.2. Overall Objective and Primary Contribution

The overall objective of this study is to investigate the reliability and validity of using freehand 3D ultrasound system for evaluation of the sagittal curvature of the spine, ultimately providing a radiation-free imaging modality for evaluating and monitoring sagittal spinal profile for patients with adolescent idiopathic scoliosis. To achieve this objective, scanning was performed first on spine phantoms and then on human subjects with different extents of deformity. Intra- and inter-rater reliability of the sagittal ultrasound spinous process and laminae angles, and the comparability of these ultrasound angles with the X-ray Cobb angle were investigated. Preferred ultrasound angles were then applied to a larger group of patients with AIS, in order to investigate whether the coupling relationship observed from traditional radiograph could also be demonstrated using ultrasound, either with or without the aid of X-ray.

An optimal value for sagittal thoracic profile for ultrasound would also be suggested for reference in future sagittal ultrasound evaluation for spine.

The major achievements of this study were summarized as follow:

- Flexible spine phantoms with different degrees of simulated scoliosis were tested to investigate the feasibility of ultrasound on evaluating spinal sagittal curvature under different range of coronal deformation and the relationship between the Cobb's angle and the spinous process angles obtained from X-ray and ultrasound.
- Human pilot tests with different range of coronal deformities were conducted to investigate the reliability of the ultrasound system, with the usage of the specially customized 3D ultrasound software. Sagittal curvatures obtained from ultrasound, using the spinous processes and laminae as reference landmarks, were found to have good correlation with those obtained from traditional Cobb's methods.
- Establishing laminae as a better method for assessing sagittal curvature using ultrasound as the curvatures measured using such landmarks had no significant differences with those obtained from spinous processes, at the same time with better visualization in B-mode images.
- Demonstrating that relative hypokyphosis could be detected in patients with AIS with larger coronal deformities, provided that the same phenomenon was reflected from radiograph, by either with the aid of X-ray or using ultrasound alone.
- Providing a standard thoracic kyphosis value of patients with AIS using ultrasound for future progression study.

1.3. Outlines of the Thesis

This thesis is composed of six chapters. Chapter 1 includes the background information, motivation, objectives, primary contribution and the structure of this thesis. Chapter 2 provides a comprehensive literature review of the related study, including the related issues of AIS and sagittal profile of spine, and different approaches used for evaluating sagittal curvature. In Chapter 3, the experimental materials and methods of the phantom and human subjects tests were described. In Chapter 4, the results obtained from the spine phantom and human subjects were presented. In chapter 5, the results obtained in Chapter 4 and limitations of the phantom and human subjects study were discussed. Finally, in Chapter 6, conclusion from the study was drawn and recommendations on future work were given.

Chapter 2. Literature Review

2.1. AIS Related Issues

2.1.1. Etiology, Diagnosis of AIS

Idiopathic scoliosis is a three dimensional (3D) spine deformity problem (Stokes et al 1987). It is often associated with deviation in coronal plane, sagittal deformation and axial rotational deformities (White et al. 1978, Pope et al. 1984, Hattori et al. 2011). No single cause for idiopathic scoliosis (IS) has been identified at present (Arkin et al. 1949) and it is found to be exclusive to humans (Castelein et al. 2005). Forms of scoliosis reported in other vertebrates are induced using congenital, neuromuscular, cicatricial or experimental methods (Pincott et al. 1982, MacEwen 1973, Beguiristain et al. 1980, Ottander 1963). Generally Idiopathic scoliosis is divided into four stages: 1) Infantile; 2) Juvenile; 3) Adolescent; and 4) Adult idiopathic scoliosis. Adolescent idiopathic scoliosis (AIS) is the most prevalent form of scoliosis which affects 2–3 % of adolescents (Asher et al 2006). Approximately 20 million people are suffered from scoliosis in the United States, and the prevalence of AIS is about 2% to 4% (Good et al. 2009). The prevalence of AIS is about 3% in Hong Kong (Tang et al. 2003). AIS is often diagnosed or detected during the pubertal growth spurt at ages 10–14 years without an identifiable cause (Asher et al. 2006).

At present there are three classification systems. King classification is a two-dimensional system because it only considers lateral deviation in the frontal plane (King et al. 1983). Lenke classification is one of the most commonly used scoliosis classification systems at present, which considers parameters in both coronal and sagittal planes, thus is three dimensional (Lenke et al. 2003). A more recent classification system made by Peking Union College Medicine (PUCM) added the vertebral axial rotation as the third parameter in the classification system, making it a system that can consider three dimensions with an additional vertebral axial rotation in 3D space (Qiu et al. 2005). Lenke Classification labels the primary curve into proximal thoracic, main thoracic and thoracolumbar/lumbar and identifies whether minor curves are structural or compensatory curves by considering the degree of rotation and the curve degrees on standing AP and bending films respectively (Table 2.1). In addition, lumbar spine and sagittal modifier are defined by drawing a sacral vertical line to determine its relationship to pedicles of apical lumbar vertebrae and measuring the thoracic Cobb's angle respectively (Table 2.1).

Table 2.1 *Lenke classification system*

The Lenke classification system for AIS

Curve type	Proximal Thoracic	Main Thoracic	Thoracolumbar/Lumbar	Description
1	Nonstructural	Structural*	Nonstructural	Main Thoracic
2	Structural×	Structural*	Nonstructural	Double Thoracic
3	Nonstructural	Structural*	Structural×	Double Major
4	Structural×	Structural§	Structural§	Triple Major
5	Nonstructural	Nonstructural	Structural*	Thoracolumbar/Lumbar (TL/L)
6	Nonstructural	Structural×	Structural*	Thoracolumbar/Lumbar-Main Thoracic (TL/L-MT)

***Major curve:** largest Cobb measurement, always structural; ×**Minor curve:** remaining structural curves; §**Type4 – MT or TL/L** can be the major curve

Structural Criteria (Minor curves)

Proximal Thoracic	• Side Bending Cobb ≥25° • T2-T5 Kyphosis ≥+20°
Main Thoracic	• Side Bending Cobb ≥25° • T10-L2 Kyphosis ≥+20°
Thoracolumbar/Lumbar	• Side Bending Cobb ≥25° • T10-L2 Kyphosis ≥+20°

Location of Apex (SRS Definition)

Curve	Apex
Thoracic	T2 to T11-12 Disc
Thoracolumbar	T12-L1
Lumbar	L1-2 Disc to L4

Modifiers

Lumbar Spine Modifier	Center Sacral Vertical Line to Lumbar Apex
A	Between pedicles
B	Touches apical body(ies)
C	Completely medial

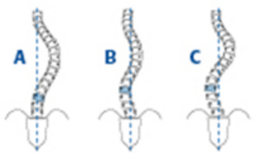

Thoracic Sagittal Profile T5-T12

Modifier	Cobb Angle
- (Hypo)	< 10°
N (Normal)	10° – 40°
+ (Hyper)	>40°

Curve Type (1–6) + Lumbar Spine Modifier (A, B, C) + Thoracic Sagittal Modifier (–, N, +) = Curve Classification (e.g. 1B+):

(https://www2.aofoundation.org/AOFileServerSurgery/MyPortalFiles?FilePath=/Surgery/en/_img/surgery/Add_Material/55/X190/55_X190_i200_700.jpg)

Prior to X-ray assessment, patients with scoliosis would receive a scoliometer screening test to measure angle of trunk rotation with a scoliometer, since scoliometer measurement has a good correlation (r = 0.7) with the Cobb angles (Coelho et al. 2013, Vidal et al. 2013). Information such as gender, age, height, weight, leg length, onset of menarche, family history, and diseases is collected for determining a tentative prognosis. Physical and spinal examinations including forward bending test, neurological examination, spine side-to-side symmetry, shoulder height, iliac crest symmetry, and lateral examination are also conducted. When the hump's angle of trunk rotation is greater than seven degrees measured by Bunnell Scoliometer under forward bending test, the patient is recommended for undergoing the standard radiographic evaluation for suspected scoliosis (Bunnell 1984).

For current clinical practice, Cobb angle on standing postero-anterior X-ray radiograph is the gold standard to evaluate the severity of scoliosis and sagittal curvature of the spine (Cobb 1948) (Figure 2.1a and b). Coronal Cobb angle is defined by the angle between the two straight lines that are drawn on the upper and lower endplate of the most tilted vertebrae of a curve respectively on the coronal radiograph. Patients with spinal curvature in the coronal plane more than 10 degrees are treated as scoliosis (Cobb 1948). Different treatments are applied to different types of AIS patients (Kim et al. 2010). For those with Cobb angle of 20 degrees or less, clinical observation is recommended. Those with immature skeletal and Cobb's angle of between 20 to 40 degrees, brace treatment will be considered. For patients with Cobb's angle greater than 40 degrees and immature skeletal or Cobb's angle greater than 50 degrees and mature skeletal, surgical management may be necessary.

Vertebrae rotation is often observed in patients with AIS with severe scoliosis. At present, the gold standard remains axial computed tomography because of its high resolution (Gocen et al. 1998, Ho et al. 1992, Krismer et al. 1999). Accurate measurement of vertebral rotation may assist in preoperative planning and screw placement for patients with scoliosis.The apical vertebra, the vertebra which is not tilted and most laterally deviated from the central sacral line, and usually presents maximal axial rotation (Lenke 2000), can be visualized with computed tomography (CT), which passes through the vertebral body, both pedicles, laminas, transverse processes, and the spinous process. Yet it can also be assessed using radiographs (Cobb 1948, Nash et al. 1969), ultrasound (Suzuki et al. 1989) and MRI (Birchall et al. 1997). Several techniques have been developed for assessing vertebral rotation: 1) Investigation of spinous process on coronal radiograph (Cobb 1948); 2) Investigating the relative position of convex side pedicle (Nash and Moe 1969); and 3) Image matching method by using multiple landmark methods (Mehta 1973) that estimates vertebral rotation based on relative position of various elements on the vertebrae.

Coronal curvature has been observed to be positively correlated with the vertebrae axial rotation in scoliotic spine, showing that these two components are related to each other (White et al. 1978, Villemure et al. .2001, Gum et al. 2007). Carlson et al. (2013) found out that angle of trunk inclination of the patients with either thoracic or thoracolumbar AIS with mean Cobb's angle of 63 and 48 degrees respectively is positively correlated ($r > 0.7$) with Cobb's angle and apical vertebral rotation angle (with respect to the sagittal plane). Lin et al. (2006) investigated the correlation of individual vertebra axial rotation angle with curvature and torsion from T2 to L4 by using a simplified 3D spine model constructed by two radiographic images in the coronal and transverse planes of scoliosis patients. This preliminary study demonstrated that vertebral rotation is more correlated with the curvature than with the torsion, the correlation coefficients for all investigated vertebrae indeed are small (r < 0.7), which may be due to insufficient subject size (Lin et al. 2006).

Although AIS is a three-dimensional deformity, most of the AIS studies mainly focus on correcting coronal deformity and apical rotation on the coronal and transverse plane in current practice. At present there is only limited information defining the optimization of sagittal profile of the spine, hence additional attention should be paid to sagittal plane deformity and measurements on AIS patients (Deacon et al. 1984, Dickson et al. 1984, Lenke et al. 2001). In addition, investigation on the correlations between the deformity parameters in the three orthogonal planes of the developing immature spine may be helpful to get a better understanding about the initiation and progression mechanism of AIS (Dickson et al. 1984).

(a) **(b)**

Figure 2.1 *Diagram illustrating how Cobb angle(s) is being constructed on (a) coronal and (b) sagittal radiograph respectively.*

2.1.2. Treatment for Patients with AIS

When patients are assigned for brace treatment after diagnosis, they will generally undergo a brace fitting process and follow-up assessment (Negrini et al 2009). The conventional manual method of making a spinal brace is by firstly taking a negative body cast from the patients with AIS (Wong et al. 2003), followed by filling the negative body cast with plaster to prepare a positive cast. Then the positive cast is rectified by removing and adding plaster to certain specific areas of the cast. Finally a spinal orthosis is formed by molding a plastic sheet onto the rectified cast (Wong et al. 2005). The goals for applying brace for patients with scoliosis are reducing the magnitude of the deformity, maintaining spinal balance, and preventing progression of the deformity, where preventing curve progression during adolescent growth spurt is the major objective since it is the high-risk period (Havey et al. 2016, Weinstein et al. 2008). Rigid spinal orthoses have been demonstrated to be effective for most of the cases of moderate AIS, providing that the treatment has been carried out early enough and the brace is worn for long enough every day and under properly applied controlling forces (Wong et al. 2000, Wright 1977, Nachemson and Peterson 1995). When fitting the brace, pads must be placed correctly and adjusted frequently together with the brace for optimal patient outcomes. At present, taking standing X-ray films is the traditional method to assess the effectiveness of bracing on scoliotic curve correction. However, due to the radiation issue, repetitive imaging is not recommended. At present, the existing biomechanical design of spinal orthoses mainly applies external corrective forces by using the 3-point or 4-point pressure systems to support and prevent further progression during the period of puberty of the patients. In addition, according to Euler’s bucking model, length of the spine decreases spine stability while diameter of the spine increases, hence bracing also provides additional time for spine diameter to catch up with skeletal maturity and effectively form a comparatively more stable spinal column (Havey et al. 2016). Other than the effectiveness of the brace, the compliance and appearance of the brace are also important to the patients. Generally, AIS patients are required to wear the orthoses for up to twenty-three hours per day including bedtime (Chu et al. 2006). History taking and physical examination to look for signs of wear are often used to assess the compliance. Application of thermal and force sensors has also been used to reflect the time spent on the orthosis (Lavelle et al. 1996) and force received by the patients (Lou et al. 2002) to further study the compliance of the orthosis. Among different types of scoliosis, patients with severe scoliosis would encounter physically detrimental effects, hence aesthetics becomes another objective when dueling with curve progression with a brace (Negrini et al. 2012). By designing and producing an effective and good-looking brace, spinal pain syndromes and torso aesthetics of the patients may be treated and improved by relieving the curve progression (Negrini et al. 2012). Currently brace effectiveness is still an important area of study for the International Scientific Society on Scoliosis Orthopaedic and Rehabilitation Treatment (SOSORT) and the Scoliosis Research Society (SRS) and the five major areas of study on bracing are: 1) Diagnostic and follow-up issue; 2) Optimization of brace fitting; 3) Investigation of bracing compliance; 4) Monitoring in-brace forces; and 5) Quality of life of the brace wearers.

Once the major curve of these patients reaches a Cobb angle greater than 40 degrees, surgical management may be necessary to prevent further curve progression (Weiss 2008). The current objectives of the surgical treatment for AIS are to maximize the correction of the spinal deformity, achieve balance in the coronal and sagittal plane and axial derotation, and maintain spinal flexibility (Bridwell 1999, Majdouline et al. 2007). There is an increasing trend of the usage of pedicle screws for curve correction (Kim et al. 2004, Suk et al. 2001, Kim et al. 2006), because of their relatively superior major curve correction and biomechanical properties. However, these posterior distraction devices further enhanced the coronal plane correction, resulting in sacrificing the sagittal balance (Potter et al. 2004).

2.1.3. Curve Progression of Patients with AIS

It is also important to define whether scoliotic curves are progressive or not. Progressive scoliosis is defined by a progression of major curve Cobb angle of more than 6° between the first and the latest control (Pruijs et al. 1994) and a Cobb angle between 25° and 50°. While stable scoliosis is defined by a progression of major curve Cobb angle lower than 6° between the first and the latest control (Pruijs et al. 1994), a Cobb angle lower than 25° and a Risser stage ≥ 3 (Skalli et al. 2016).

Various factors have been found to cause curve progression in patients with AIS. Axial and ventral shear forces were found to be one of the significant factors which might cause progression. Vertebrates are normally experiencing predominant axial and ventral shear loads in the vertebrae of the spine due to gravitational and muscle force (Wilke et al. 1997). However, the spinal loading conditions are different for humans. Humans walk in a fully upright posture most of the time during daily activities, the center of mass of the upper body acts straight above the pelvis in human (Hogervorst et al. 2009). For other vertebrates, the center of mass acts in front of the pelvis instead (D’Aouˆt et al. 2002). In a mathematical model in Castelein et al.’s (2005) study, the backward inclined segments of the spine were demonstrated to be subjected to dorsal shear forces other than axial loading. In addition, facet joints are essential to provide rotational stability for the spine, but these joints can only well stabilize shear forces which act on the vertebrae in ventral direction instead of dorsal. A biomechanical in vitro study shows that dorsally directed shear loads were observed larger than ventrally directed shear loads (Kouwenhoven et al. 2007a). The difference could be accounted to the gradual transition of shear force from ventrally directed to dorsally directed in the adaptation of the fully upright posture during walking (Castelein et al. 2005). Such transition of shear force would facilitate rotatory instability (Kouwenhoven et al 2007b) due to the poor functioning of the facet joints and the posterior location of the major spinal muscles and ligaments, which may possibly contribute to axial vertebral rotation (Kouwenhoven et al. 2007a). Kouwenhoven et al. (2008) later on demonstrated that spine under dorsally directed shear loads favored axial vertebral rotation more than ventrally directed shear loads at the mid and lower thoracic in a biomechanical study. Thus the authors hypothesized that dorsal shear loading is a possible enhancer of slight preexistent vertebral rotation (Kouwenhoven 2006a, b, 2007) and progressive vertebral deformation according to Hueter–Volkmann's law (Fritz 2013), which would ultimately lead to progressive scoliosis. Thus backward inclination of vertebrae in the sagittal plane has a prognostic significance in the progression of AIS (Castelein et al. 1992, Schlosser et al. 2014).

Asymmetric growth of the vertebrae could also be one of the factors that may lead to the progression of AIS. In the study of Porter et al. (2000), vertebral canals of skeletons with kyphotic spines were significantly longer than the vertebral length, while such difference could not be observed in normal spine. Guo et al. (2003)

reported that the anterior part of all the thoracic vertebral bodies was found to be longer than the posterior part in magnetic resonance images among girls with AIS, and the ratio of differential growth was found significantly positively correlated to scoliosis severity score. It is hypothesized that the difference is due to the differential growth rate between the vertebral bodies and the posterior elements, which develops thoracic hypokyphosis. The irregular growth can also be accounted for the uncoupled neuro-osseous growth, which was common in AIS patients (Porter 2000, 2001a,b), leading to a comparatively shorter spinal cord (Roth et al 1968). Chu et al. (2006) also found that the ratio of the spinal cord to the length of the vertebral column at the thoracic level smaller in AIS patients than normal individuals. The comparatively faster growth of the vertebral bodies would tether the posterior vertebrae, which eventually causes buckling and rotation of the spine. Such differential growth rate between the vertebral bodies and the posterior elements would lead to hypokyphosis, which is common among patients with AIS. Girls with AIS are found to be taller and more slender than normal controls with the same sex and age (Cheung et al. 2003, Nissinen et al. 1993, Nordwall et al. 1975, Willner 1975) and such differences can be accounted for the flattening of the thoracic kyphosis (Archer et al 1985). Such flattening process happens during adolescent growth spurt and gradually returns back to normal (Cil et al. 2005, Poussa et al. 2005). Since girls mature earlier than boys, they go through peak adolescent growth velocity when the thoracic kyphosis is at its minimum, while boys go through the maximum growth period at a later stage (Dickson et al. 1984). Hence girls have a higher potential from developing thoracic lordosis. Developmental asymmetry was also observed in the intervertebral discs in idiopathic scoliosis. During the development of scoliotic curvature, shifting of the nucleus pulposus to the convex side of the curve could be observed (Bick et al. 1958).

Moreover, fibers of the annulus fibrosis were observed to be extended on the convex side and compressed on the concave side of the curve (Michelsson et al. 1965). The above evidence could explain why degenerative enzymes activity in the discs increased (Zaleske et al. 1985) and elastic fiber network of the annulus fibrosus was sparse and disrupted (Yu et al. 2005) in the discs in idiopathic scoliosis individuals.

Other than growth asymmetry, growth disturbance may also play an important role in the development of AIS. Since curve deformities due to AIS are three dimensional, the growth disturbance caused by curve deformities would also be in three dimensions. A morphometric analysis study of the scoliotic spine stated that the apex height of the scoliotic vertebral bodies was significantly smaller at the concave side and the pedicles were smaller and shorter than those on the convex side (Parent et al. 2002). Growth kinetics between the convex and the concave side of scoliotic vertebrae would become different once scoliosis is developed (Wang et al. 2007), asymmetric loading would have resulted on the epiphyseal plates (Hueter 1862, Volkmann 1882). Asymmetric loading has also been demonstrated to be causative of AIS progression. By applying asymmetric loading on growing vertebrae in animals, AIS-like deformities resulted (Aronsson et al. 1999, Mente et al. 1997,1999, Stokes et al. 1996).

Bone quality also plays an important role in curve progression. Bone mass density and peak bone mass in patients with AIS were found to be lower than those in normal controls (Cook et al. 1987, Cheng et al. 1997, Velis et al. 1989), which could be the combined result of abnormal bone mineralization and bone growth increment during puberty (Lee et al. 2005, Cheung et al. 2006). Furthermore, inverse relationship was observed between curve severity as measured with the Cobb's angle and BMD (Lee et al. 2005), concluding that osteopenia might be an important risk factor of curve progression in AIS.

Preexistent vertebral rotation pattern was found to be existing even in a normal nonscoliotic spine, where mid and lower thoracic vertebrae showed a predominant rotation to right side in humans and quadrupeds (Kouwenhoven et al. 2006a,b). Situs inversus totalis individuals had a reversed rotation trend of vertebrae compared to common individuals (Kouwenhoven et al. 2007), stating that internal organs such as heart play a role in the preexistent rotation pattern. It has later on been found out that this preexistent rotation pattern would be significantly affected by body position, where the rotation during quadrupedal-like position was significantly smaller than that in bipedal and supine position (Janssen et al. 2010). Furthermore, it has been shown that such rotation patterns exist in infantile and juvenile normal humans. Patients with infantile idiopathic scoliosis generally presented left-sided thoracic curvatures (Thompson et al. 1980). Those with juvenile idiopathic scoliosis had left & right sided curves evenly divided (Figueiredo et al. 1981). For Adolescent idiopathic scoliosis (AIS), patients most often had right-sided main thoracic curves in the mid and/or lower thoracic region and left-sided main lumbar curves (Upper thoracic/lumbar) (James et al. 1954, Moe et al. 1970, Ponseti et al. 1950). During infantile stage, a significant leftward rotation was observed in the upper thoracic spine, while in the juvenile stage, significant leftward rotation was only observed in T4 of the upper thoracic spine (Janssen et al. 2011). But in the adolescent stage, the mid and lower thoracic spine demonstrated a significant rightwards rotation (Janssen et al. 2011). The above evidence showed that the mean rotation of the vertebra in the thoracic spine shifts from left to right throughout the initial growth stage. Furthermore, the rotation pattern was found more significantly leftwards in boys than girls (Janssen et al. 2011). However, this phenomenon should be considered as a physiologic process in the normal development of the spine, and an independent process of the pathogenesis of scoliosis (Kouwenhoven et al. 2006b). In addition, though Neurocentral junction (NCJ) activity was believed to be just a passive factor on IS progression (Schlösser et al. 2013) and no conclusive statement has been made on whether neurocentral junction activity would affect progression of IS (Kouwenhoven et al. 2008). There might be a correlation between the NCJ closure and the preexisting vertebral rotation. Neurocentral junction (NCJ) closure starts at L1–L3 at 6 to 7 years old for both males and females. The closure spreads to higher thoracic and L4–L5 and finishes in the mid- and low thoracic spine at 6-9 years old for girls and 7-11 years old for boys respectively (Schlösser et al. 2013). It has been found out that the mean NCJ area kept decreasing starting from the infantile to the adolescent stage (Schlösser et al. 2013). Moreover, the mean NCJ area in the right-hand side in the infantile stage was found larger than that in the left-hand side, and the situation was totally reversed in the juvenile stage (Schlösser et al. 2013).

Other than NCJ closure, there are also factors whose roles in curve progression of patients with AIS are unknown, yet attention is needed. For instance, it has been known that paravertebral muscles are essential to hold the spine upright. Since ligamentous spine alone cannot support vertical compressive forces and buckles at an axial load of only 20 N (Lucas et al. 1961), paraspinal muscle diseases or imbalance would destabilize the spine and likely cause the development of scoliosis (Aprin et al. 1982, Hsu et al. 1983, MacEwen 1974, Fidler et al. 1976, Ford et al. 1984, Riddle et al. 1955). Previous studies showed increased paravertebral muscles EMG activities at the convexity of the curve (Alexander et al. 1978, Cheung et al. 2005). Moreover, a greater proportion of type I muscle fibers was observed in multifidus (Fidler et al. 1976) and in superficial muscles (Ford et al. 1984). In addition, ribs transmit muscle forces from the sternum to the vertebral column through the transverse processes, the costotransverse articulations and ligaments (Kouwenhoven et al. 2008). Experimentally induced elongation of the ribs on growing rabbits asymmetrically resulted in scoliotic curvature of the spine (Agadir et al. 1998) and curvature correction could be done by lengthening the ribs in the shorter side. Incidence of scoliosis in children who underwent thoracotomy was found higher than normal (Kouwenhoven et al. 2008). Role of the spinal cord in the development of AIS remains controversial (Burwell 2001). Neuromuscular disorder reportedly resulted in the development of idiopathic or secondary scoliosis (Aprin et al. 1982, Hsu et al. 1983, MacEwen 1974, Madigan et al. 1981, Piggott 1980). Hence AIS patients were found to have decreased sensory (proprioceptive) input (Pincott et al. 1982) and abnormalities in EEG activity, postural control, and vestibular and somatosensory function (Cheng et al. 1999, Guo et al. 2006, Petersen et al. 1979, Sahlstrand et al. 1979).

2.2. Investigation of Sagittal Profile of Spine and Related Structures

2.2.1. Sagittal Profile of Normal Individuals and Its Importance

At birth, sagittal profile of spine is C-shaped and globally kyphotic (El-Hawary et al. 2016). During growth, physiological curvatures are developed in the sagittal plane, which are likely due to the changes resultants from posture and balance (Cil et al. 2005). Young children have been found to have positive sagittal balance, which decreases throughout childhood and adolescence (Cil et al. 2005). It had been found that thoracic kyphosis increases from 42° in children 3–9 years of age to 48° by age of 10, while lumbar lordosis increases from 44° for children aged 3–9 years to 53° by the age of 10 years (Mac-Thiong et al. 2011a). Generally for normal individuals, the center of C7 vertebral body to the center of upper sacral endplate was found to be very close to the vertical line (Kuntz et al. 2007, 2008; Roussouly et al. 2006). For regional analysis, many parameters have been used in the spine and pelvis and the average values of these values have been widely discussed in different studies. For instance, thoracic kyphosis is between 20° and 50° (Boesker et al. 2000) and lumbar lordosis ranges from 31° to 79° (Bridwell et al. 1989). Some studies suggested reference values of 30° to 50° and 20° to 50° for lumbar mordosis (Bernhardt et al. 1989, Stagnara et al. 1982). Hardacker et al. (1997) stated that acceptable lordosis in the cervical spine was 40° ± 9.7° for normal individuals. Spinal-sacral angle and spinal tilt of normal adult individuals can be expected to be between 110° and 150°, and between 85° and 100° respectively (Mac-Thiong et al. 2010). Pelvic incidence angle measures approximately 52° with a range from 34°to 84° (Van Royen et al. 1998, 2000). This angle is fixed after skeletal maturity. The pelvic tilt angle measures 12° with a range of 5°–30° (Van Royen et al. 1998). This angle changes with compensatory posture and is therefore a postural angle. Sacral slope is approximately 40°with a range of 20°–65° (Van Royen et al. 1998, 2000). Repetitive, strenuous physical activity would cause structural abnormalities in the immature vertebral body (Wojtys et al. 2000). Adolescent athletes with greater cumulative training time demonstrated larger angles of thoracic kyphosis and lumbar lordosis than those lack of sports (Wojtys et al. 2000). Sports with a predominance of forward-bending postures was found to be associated with greater thoracic kyphosis in standing (Rajabi et al. 2007), however no negative effect on sagittal spinal posture was observed in young tennis players (Muyor et al. 2013). Hyperhyphosis was observed in highly-trained young canoeists during standing position (López-Miñarro et al. 2011), but with reduced thoracic and lumbar curvatures. Hyperhyphosis was observed in elite cyclists during standing position but the thoracic spine was straighter on the bicycle than in the standing posture (Muyor et al. 2011). Increased thoracic kyphosis in adolescent elite skiers was observed after five years of intensive training (Alricsson and Werner 2006). A progressive thoracic kyphosis and a flattened lumbar lordosis in adolescent female volleyball players were also reported (Grabara and Hadzik 2009).

Kyphosis and lordosis of the spine help to maintain spine motor control with minimum energy expenditure, enhance load tolerance of the spinal column and increase the efficiency of the spinal muscle (Kim et al. 2006). Modifications of spine sagittal profile are closely related in musculoskeletal spinal issues development (Betsch et al. 2014; Nam et al. 2014). Malalignment in the sagittal plane could lead to significant pain and deformity to the patients. Social interaction would also be affected due to deficient forward gaze (Roussouly and Nnadi, 2010). In addition, alterations in physiological spinal curvatures would possibly lead to an increased risk of injury due to an increase of intervertebral stress (Beach et al. 2005), viscoelastic deformation of spinal tissues (Solomonow et al. 2003) or higher intradiscal pressure (Wilke et al. 1999). Furthermore, flattening of thoracic kyphosis and lumbar lordosis would cause diminution of the lung function (Winter et al. 1975) and decrease the springing function of the spine (de Jonge et al. 2002) respectively in patients with AIS, where the latter effect would cause early disc degeneration and low back pain.

In clinical point of view, the understanding of the regulatory principles of sagittal balance is necessary for achieving good outcomes during treatments for different spinal disorders in the orthopedic rehabilitation field and spine surgery (Mac-Thiong et al. 2003; Cho et al. 2014), especially when treating major spinal deformities in adults such as scoliosis. In addition, it also helps to minimize complications such as adjacent segment disease, sagittal imbalance, pseudarthrosis, and progressive deformity (Mac-Thiong et al. 2010). Quality of life was found to be correlated with sagittal malalignment and loss of LL (Watanabe et al. 2015). Furthermore, preservation of lumbar lordosis is important to avoid early progressive sagittal positive imbalance (Bissolotti et al. 2015) as seen in the ageing process and in other spinal diseases. Neverthelss, adequate restoration of sagittal plane alignment is necessary to improve significantly clinical outcomes and avoid subsequent pseudarthrosis (Farcy et al. 1997; Booth et al. 1999).

2.2.2. Sagittal Compensatory Mechanism

The spinal shape allows equal force distribution across spine column. Disruption of such equilibrium would likely cause deformity (Roussouly and Nnadi, 2010). Compensation mechanism would result in the pelvis and lower limbs. The possibility of rotation of the pelvis around the femoral head's axis is one of the best mechanisms to regulate sagittal balance (Roussouly et al. 2011b). For global sagittal alignment, it can be classified into three stages with respect to the severity of the imbalance: 1) Balanced, compensated balance and unbalances (Barrey et al. 2013). Barrey et al. (2013) also investigated the compensatory mechanism which contributes to keep the sagittal balance of the spine as shown in Figure 2.2. Cervical hyperlordosis is typical compensatory mechanism above a thoracic hyperkyphosis to maintain the horizontality of the gaze. However, such an alternation would lead to an acceleration of degenerative changes in the cervical spine, presence of axial neck pain, foraminal stenosis and development of spondylotic myelopathy. Reduction of thoracic kyphosis is also common during compensation. Decrease of thoracic kyphosis limits anterior translation of the axis of gravity and is commonly observed in young patients with flexible spine. For the elders, spine ageing will occur, the spine will become too rigid and there is no possibility for the patient to reduce the magnitude of the thoracic curve. Hyperextension of adjacent segments is a very common local compensatory mechanism to limit the consequences of lumbar kyphosis on the shift of axis gravity. It can be either global (multi-segment) or local (mono-segment). The advantage of hypertension of these segments is that the upper spine will be placed more posteriorly, however at the same time generating extra stresses on posterior structures, increasing the risk of having retrolisthesis and possibly resulting in accelerated facet joints arthritis. Posterior slippage of the upper vertebra in reference to the lower vertebra, known as retrolisthesis, may also result. It is a 2–3 mm slippage in the lumbar spine and commonly happens at lower or upper part of the kyphotic spine: L5–S1 and upper lumbar spine (L1–L2 and L2–L3). It is generally being underestimated on lying down radiological imaging techniques. The only compensatory mechanism in the pelvis area is pelvis back tilt, which leads to posterior positioning of the sacrum posterior to the coxo-femoral heads. Last but not least, knee flessum correlates strongly with lack of lordosis (Obeid et al. 2011), while ankle extension would possibly induce pelvis shift, which is a key component in maintaining a fixed gravity line-heels offset and is a parameter as important as pelvis tilting (Lafage et al. 2008).

Compensatory mechanism is effective to limit the sagittal unbalance, however at the same time, it could possibly result in adverse effects such as mechanical pain and compromise of neurological structures. To achieve the analysis of sagittal balance and determine the presence of compensatory mechanism, the following three procedures are suggested: 1) Investigate the value of the pelvis incidence, which helps to predict the theoretical values of the spino-pelvic positional parameters; 2) Determine whether the patient is globally balanced by analyzing the positioning of C7 related to the sacrum, the angle between the sacral plate and the line connecting the centroid of C7 vertebral body and the midpoint of the sacral plate, C7 plumbline/sacral femoral distance ratio; and 3) Investigate whether compensatory mechanisms exist in (i) Spinal area such as cervical curvature, thoracic kyphosis and lumbar lordosis and thoracic kyphosis; (ii) Pelvis area ; and (iii) Lower limbs area.

For instance, when an individual possesses in pathological kyphosis, corresponding biomechanical adaptation of the compensatory balance may result. The possibility for compensation to function depends on the location of the kyphosis & length of lordosis and the flexibility of the spine (Roussouly et al. 2011b). If the kyphosis is highly located, the lumbar lordosis is able to compensate the balance; but if the kyphosis extends into the thoracolumbar area, the length of lordosis could be too short to compensate. For a flexible spine, lumbar lordosis is largely curved and the posterior arches are thinner as well as the spinous processes. This would promote a better range of motion; however, it may induce spondylolysis. But when the kyphosis occurs on a rigid spine, the only way for compensation is pelvic tilting, which would result in a downward tilt of the head. In order to correct such posture, the patient would need to tilt the pelvis backwards, extend the hips, flex the knees and dorsiflex the ankles (Roussouly et al. 2010). However, for patients with small pelvic incidence, they have a small capacity for sagittal imbalance compensation through pelvis retroversion (Roussouly et al. 2010, 2011b), which inhibits the restoration of the position of C7 plumb line behind the femoral head in case progressive kyphosis is present in the patient.

Different relationships have been observed between sagittal parameters. Starting from the top of the human spine, cervical angles were found significantly correlated with cervico-thoracic angles and global sagittal alignments (Yu et al. 2013). In addition, significant differences of cervical angles, cervico-thoracic angles and thoracic kyphosis were observed among individuals with no kyphosis, cervical kyphosis, cervical-middle-thoracic kyphosis and cervical-lower-thoracic kyphosis. A hypokyphotic thoracic spine was found to coexist with a kyphosis in cervical spine in idiopathic scoliosis (Canavese et al. 2011). Occipital-C2 angle was found to be significantly negatively correlated with C2-C7 angle, while T1 slope was positively correlated with cervical lordosis (Kaplan et al. (2015). Significant correlation between loss of thoracic kyphosis and cervical kyphosis development was also reported (Hilibrand et al. 1995). The top of thoracic curve on C7 was found to be very stable over the sacrum (Roussouly and Pinheiro-Franco, 2011a). Positive correlation was found between thoracic kyphosis and lumbar lordosis (Van Royen et al. 1998). Lumbar Lordosis mainly depends on sacral slope orientation (Roussouly and Pinheiro-Franco, 2011a). Pelvic incidence was closely related to lumbar lordosis in normal adolescents and adults (Mac-Thiong et al. 2007) and in scoliotic adults (Legaye et al. 1998). Spinal alignment could be affected by pelvic posture (Van Royen et al. 1998). Spino-sacral angle was closely related to sacropelvic balance (sacral slope) and morphology (pelvic incidence) (Roussouly et al. 2006). Sacral slope may increase with negative sagittal balance as a compensatory response (Hong et al. 2015). The above evidence showed that alternation in the sagittal curvature of the spine would lead to global change due to the compensatory mechanism.

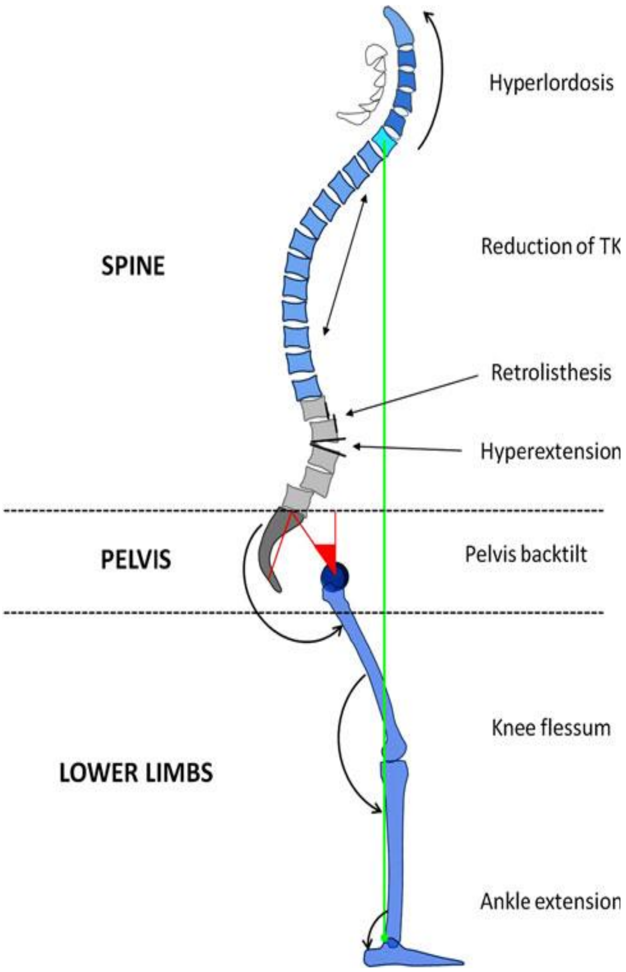

Figure 2.2 *The compensatory mechanism that contributes to keep the sagittal balance of the spine.*

2.2.3. Patients with Significantly Different Spinal Sagittal Curvature

Since spinal deformation does not develop in one plane only, the deformity parameters in different planes may be dependent with each other (White et al. 1978, Villemure et al. 2001, Gum et al. 2007, Hayashi et al. 2009). Hence it is not surprising that different sagittal profiles could be observed in patients with AIS compared to normal individuals.

Scoliosis is also one of the relevant clinical expressions of patients with Parkinson's disease (Doherty et al. 2011, Baik et al. 2009; Schwab et al. 2012). Thoracic kyphosis was found to be positively correlated with lumbar lordosis in groups with or without scoliosis in patients with Parkinson's disesase (Bissolotti et al. 2015). Though lower spinosacral angle was observed in scoliosis group (Bissolotti et al. 2015), no significant difference was found between Cobb angles and any of the spinopelvic and sagittal balance parameters (Bissolotti et al. 2015). Sagittal profile of patients with low back pain (LBP) was also found to be significantly different from normal individuals. Patients with LBP were characterized by a more vertical sacrum and more proximal lumbar lordosis (Jackson et al. 1994). In addition, thoracic kyphosis, thoracic tilt, lumbar tilt, lumbosacral angle, sacral slope, pelvic incidence of adult LBP group were found to be significantly different from normal individuals, with the sacral slope, lumbar lordosis and pelvic incidence being generally smaller in patients with LBP (Chaléat-Valayer et al. 2011**.** However, sagittal parameters were similar between French men and women in the LBP group for the thoracic, lumbar and pelvis regions (Chaléat-Valayer et al. 2011). Adam et al. (1999) stated that the loss of LL was a risk factor for the first time occurrence of serious low back pain (Adams et al. 1999) and degenerative changes for IVD and vertebral body (Schlegel et al. 1996)**.** Hence it was common that spine degeneration was commonly observed in patients with LBP. C7 plumbline was observed to be stabilized or slightly moved forward in patients with degenerated spine (Cil et al. 2005). Moreover, significant reduction of both lumbar lordosis and thoracic kyphosis was observed in patients with disc disease and disc herniation (Barrey et al. 2007). Furthermore, El-Hawary et al. (2016) mentioned that various etiologies could affect sagittal plane alignment such as postural kyphosis, Scheuermann's Condition, congenital kyphosis, myelodysplasia, spinal tuberculosis, posttraumatic kyphosis, syndromic kyphosis, achondroplasia, postsurgical kyphosis and ostlaminectomy.

Patients with AIS were the main focus group of this study. In previous practice, most of the AIS studies mainly focused on the coronal plane, but indeed additional attention should be paid to sagittal plane deformity and measurements on AIS patients (Deacon et al. 1984, Dickson et al. 1984, Lenke et al. 2001). Studies had found that patients with primary thoracic scoliosis were generally hypokyphotic (De jonge et al. 2002, Ilharreborde et al. 2018). Dickson et al. (1984) found that 75% of the apical lateral profiles were found to be lordotic and a mean lordosis of 3° was reported at the apex of the kyphotic thoracic spine of scoliosis patients. The anterior part of the apical vertebrae was higher than the posterior part, with endplate irregularities most often found in the posterior part. A negative correlation was also observed between thoracic kyphosis and the lateral thoracic curves of patients with idiopathic thoracic and double major scoliosis, and the average thoracic kyphosis of these patients was 10 degrees smaller than those without scoliosis in supine position (Schmitz et al. 2001). However, no significant difference was observed in lumbar lordosis between patients with lumbar and double major curves and non-scoliotic subjects. Mac-Thiong et al. (2013) conducted a study on young patients with average 43 degrees Cobb angle and discovered that thoracic kyphosis was significantly lower for patients who possessed thoracic curves than those with lumbar curves, but no significant difference was observed in lumbar lordosis between different curve types.

In addition, no significant change between the groups was observed for the sacral slope, pelvic tilt, or pelvic incidence. Furthermore, the pelvic incidence was significantly correlated with the lumbar lordosis, sacral slope, and pelvic tilt for all the groups. The lumbar lordosis was strongly related to the sacral slope in all cases, but not with the thoracic kyphosis, except in the case of thoracolumbar curves. In addition, there is increasing evidence suggesting that hypokyphosis in the thoracic region and non-uniform growth of the posteroanterior vertebrae mismatch contributes to the development of AIS. Previous study has shown that posteriorly inclined human spine segments would likely lead to a decrement of rotational stiffness, inducing rotational instability to the spine column (Kouwenhoven et al. 2007). Schlösser et al. (2014) and Janssen et al. (2011) demonstrated that patients with mild thoracic scoliosis had a significantly less kyphotic spine and longer and more posteriorly inclined segment from C7-T8 than the normal and those with mild lumbar scoliosis. However, patients with lumbar scoliosis were found to have significantly greater thoracic kyphosis than the normal and those with thoracic scoliosis. In addition, steeper posterior inclination from T12-L2 was observed from patients with lumbar scoliosis. Such hypokypotic phenomenon has further been confirmed in thoracic AIS patients using EOS, a biplanar radiograph modality (Sullivan et al. 2017). Furthermore, elucidation of the timing of the onset of hypokyphosis and scoliosis could provide valuable insight into the curve development of the AIS patients. Nault et al. (2014) observed that patients with progressive AIS were found to have significantly larger angle of the plane of maximal curvature, hypokyphosis, larger apical intervertebral rotation and torsion than non-progressive AIS, with the angle of the plane of maximal curvature demonstrating the most significant difference, by evaluating 3D spinal morphology of progressive and non-progressive patients with similar spinal curve of Cobb angles less than 40 degrees at the first visit. Moreover, the height/width ratio of the vertebrae from T6 to L4 using local and regional measurement was also found higher for non-progressive AIS (Nault et al. 2014). From a study of Ni et al. (2010), thoracolumbar kyphosis was observed in more than 65% of patients with thoracolumbar/lumbar AIS within T11-L2 region. In addition, significant correlations were also observed between apical vertebrae rotation and coronal thoracolumbar/lumbar curvature; and sagittal Cobb angle of T11-L2 thoracolumbar sagittal curve. Moreover, the apex vertebrae in patients with thoracolumbar scoliosis were usually more dorsally inclined.

2.2.4. Factors that Alter Sagittal Curvature of Spine

For young individuals, such as schoolchildren, one of the potential threats that could alter their sagittal profile is carriage of overloaded backpack, which is common among schoolchildren in different regions (Goodgold et al. 2002, Cottalorda et al. 2004). Overloaded backpack has been found to cause back pain and spinal deformities (Moore et al. 2007, Hong et al. 2011, Talbott et al. 2009). Other factors have also been reported to cause deformity in spinal sagittal profile, such as improper practice of elongation exercises (Drzał-Grabiec et al. 2014), hereditary factors (Janssen et al. 2013), patients with idiopathic scoliosis (Roussouly et al. 2013, Yong et al. 2012, Janssen et al. 2011, Hu et al. 2016, Hong et al. 2016), intervertebral disc degeneration (Barrey et al. 2007, Cil et al. 2005), Parkinson’s disease (Baik et al. 2009, Schwab et al. 2012), gender effect (Chaléat-Valayer et al. 2011, Abelin-Genevois et al. 2014, Takács et al. 2015), and age (Hammerberg and Wood 2003, Gelb et al. 1995, Tang et al. 2012, Li and Hong 2004).

The posture adopted by an individual is a key factor that affects the spinal sagittal curvature. Forward-bending posture has become one of the most standard positions to detect scoliosis and has been used as a basis for the screening test in schools recommended by Scoliosis Research Society (SRS) (Stokes et al. 1987). The spinal column changes its profile completely into a long kyphosis during forward bending (Hackenberg et al. 2006). Forward bending in standing position would also result in an increase in the maximum rotation of the surface of the back for the thoracic region and lumbar region with a larger extent. A significant positive correlation in the lumbar region was found between the change in rotation of the surface of the back and the Cobb angle, but no significant relationship was observed between the change of the back surface rotation and the degree of forward bending (Stokes et al. 1987). Minor changes of curvature will be induced in the sagittal plane in the thoracic region regardless of the degree of bending, however, lumbar lordosis is reversed to a kyphosis. This suggested that the thoracic region is less flexible due to the presence of rib cage and stiffer thoracic spine, while lumbar is more flexible due to the increase in rotation of the surface of the back in the lumbar region. Spinal shape also varies during different body postures other than forward bending. An average of 19% correction of the scoliosis angle was induced during supine position (Zetterberg et al. 1983). Mean Cobb angle measured at standing position from Girls with AIS was found approximately 9 degrees larger than that in the supine position, and the difference was 45 degrees in the maximum (Troell et al. 1985). The mean Cobb angle and the rotational angle on a standing radiograph were approximately 16 degrees and 6 degrees larger than those in the supine position respectively (Yazici et al. 2001), suggesting that supine position may spontaneously modify the curves in both the coronal and transverse planes; and error would be introduced when performing analysis on the true extent of rotational deformity if only radiograph in supine position is being measured. Janssen et al. (2010) found that the spine is more kyphotic in the upper thoracic region, equally curved in the mid-thoracic and thoracolumbar region and more lordotic in the lower lumbar region during standing (Janssen et al. 2010). In addition, Salem et al. (2015) found that kyphosis and lordosis angle of patients significantly decreased from standing to prone lying for about 13.4 degrees. Pelvic parameters that relate with hip angle also significantly altered the lumbar lordosis during supine posture (Driscoll et al. 2012). Furthermore, lumbar lordosis was smaller in supine position than in standing position but only for older subjects (Lee et al. 2014). Hence it has been suggested that supine position may spontaneously modify the curves in both the coronal and transverse planes; and error will be introduced when performing analysis on the true extent of rotational deformity if only radiograph in supine position is being measured (Yazici et al. 2001). Moreover, anterior/posterior translations of thoracic cage could cause significant changes in thoracic kyphosis (26 degrees), lumbar curve, and pelvic tilt (Harrison et al. 2002).

Age was also considered as a significant factor which would cause the change of sagittal profile of the spine. An increased risk of the development of spinal deformities had been noticed during periods when extremely rapid growth is assumed, which is around months 6–24, years 5–8 and years 11–14. Cervical spine alignment in patients aged 10 years old shows significantly more lordosis of 6° versus 1° in those older than 10 years, which was possibly caused by the strong influence of craniocervical orientation and thoracic shape (Abelin-Genevois et al. 2014). Asymptomatic children with mean age 3-7 years also had a lower rate of cervical hypolordosis and kyphosis than older patients (Lee et al. 2012). In addition, T1-T2, T10-L2 and L4-S1 are the main different areas in terms of sagittal plane alignment with children younger than 10 years compared to those older (Cil et al. 2005). C7 plumbline was found to have a tendency to move backwards from child until adulthood (Cil et al. 2005), but there was no significant forward displacement of C7 plumbline with respect to sacrum with aging (Mac-Thiong et al. 2010). Cervical sagittal alignment was significantly different between French pediatric patients aged below 11 and those 11 or above (Abelin-Genevois et al. 2014). Pelvic incidence and lumbar lordosis were found to be significantly increased with age in pediatric asymptomatic subjects (Abelin-Genevois et al. 2014). Though hypokyphosis was observed in patients with AIS, thoracic kyphosis and sacral slope were significantly higher in adult patients with more severe scoliosis (Hong et al. 2017). The severity of scoliosis in adults was found to increase with higher pelvis incidence (Roussouly et al. 2013). It had also been demonstrated that spinal sagittal alignment worsens with age in adults (Hammerberg and Wood 2003, Gelb et al. 1995, Tang et al 2012). Early progressive sagittal positive imbalance could be observed in the ageing process (Hammerberg and Wood 2003) and in other spinal diseases such as Parkison's disease (Bissolotti et al. 2014) and degenerative spondylolisthesis (Schuller et al. 2011).

There were also controversial findings about the effect of gender on the patterns of spinal sagittal profile. A study performed three-dimensional reconstruction of radiographs from asymptomatic young adults and found that female's spine was more backwardly inclined than the male spine (Janssen et al. 2009). Abelin-Genevois et al. (2014) found that pediatric asymptomatic female subjects had larger lumbar lordosis than males. Young female tennis players demonstrated significantly larger lumbar lordosis and lower thoracic kyphosis than male players (Muyor et al. 2013). Significant differences of thoracic kyphosis and lumbar lordosis were observed in patients with AIS of different ages and genders (Takács et al. 2015). The cervical sagittal angles and the lumbar lordosis among 150 French pediatric patients were significantly different between boys and girls below 18 years old (Abelin-Genevois et al. 2014). Pelvic tilt was significantly greater and pelvic retroversion began earlier among females for 60-89 age groups, while average T1 slope was significantly larger in males than females from a study investigating standing radiographs of subjects aged above 50 with Cobb's angle less than 25 degrees in coronal plane (Oe et al. 2015). However, Hu et al. (2015) and Mac-Thiong et al. (2010) demonstrated that gender had no effect on pelvis incidence, pelvic tilt, sacral slope, pelvic tilt in their study.

Recently, the influence of a spinal fusion on thoracic kyphosis and overall sagittal alignment has been evaluated. Depending on instrumentation and correction techniques used, postoperative thoracic kyphosis was found to either increase or decrease (de Jonge et al. 2002, Lowenstein et al. 2007, Kim et al. 2006, Vora et al. 2007, Kim et al. 2004). Such alternation in thoracic kyphosis was believed to have an impact in lumbar lordosis because correction of thoracic scoliosis would result in a spontaneous lumbar curve correction, depending on the surgical approach used (Patel et al. 2008, Lenke et al. 1999, Betz et al. 1999, Potter et al. 2005). Flat back syndrome, which is rectification of both thoracic kyphosis and lumbar lordosis, had been increasingly observed in patients after posterior pedicle screws surgery during long term follow up (Thompson et al. 1990, Newton et al. 2010). This syndrome generally includes back pain, degenerative disc disease, and functional disability (La Grone 1999). Newton et al. 2010 had found that anterior and posterior thoracic fusion increased and decreased both thoracic kyphosis and lumbar lordosis respectively at 2-year follow-up. Roussouly et al. (2013) reported that a slight but significant increase of pelvic tilt with a decrease of sacral slope and lumbar lordosis was observed in AIS patients. Kim et al. (2006) suggested that the risk factors which significantly associated with suboptimal sagittal balance 2 years after lumbar spine fusion surgery were: 1) Sagittal imbalance preoperative and 8 weeks postoperatively ≥5 cm; 2) Bigger thoracic kyphosis and pelvic incidence compared with lumbar lordosis (≥45°) before surgery; 3) Lower uppermost instrumented vertebra; 4) Smaller lumbar lordosis compared with thoracic kyphosis (≤20°) at 8 weeks postoperatively; 5) Patients whose age at surgery older than 55 years. In addition, they found out that there was a trend of getting suboptimal sagittal balance after posterior spinal instrumentation and fusion from the thoracolumbar spine to the L5–S1 was observed if the total angle of lumbar lordosis, thoracic kyphosis, and pelvic incidence was ≥45° (Kim et al. 2006). Significant curve correction of the primary scoliosis curve was achieved when the patients underwent posterior only surgical correction and fusion, but significant increase of pelvis tilting had also resulted after surgery (La Maida et al 2013).

2.3. Different Approaches of Sagittal Assessments

2.3.1. Assessment of Patient with AIS on Radiograph Using Cobb Angle

Other than the routine evaluation of the coronal deformity of patients with AIS, evaluation of the sagittal plane was sometimes involved by measuring the thoracic kyphosis and lumbar lordosis using constrained (Boseker et al. 2000, Lee et al. 2011, Schlösser et al. 2014) and non-constrained (Stagnara et al. 1982; Voutsinas et al. 1986) Cobb techniques. For constrained limit vertebrae method, which is commonly used nowadays, thoracic and lumbar vertebrae are defined by the authors. For kyphosis, lower endplate of T12 was always used as the standard in medical literature, but the end of the kyphosis cranial varied from T2 (Boseker et al. 2000), T3 (Lee et al. 2011) and T4 (Schlösser et al. 2014). For lordosis, the angle is commonly defined between two drawn lines to the upper endplate of L1 vertebra and to the lower endplate of the L5 vertebra. But there were also studies using different levels for lumbar lordosis evaluation (Polly et al. 1996). For non-constrained method, the most tilted vertebra needs to be identified to classify thoracic kyphosis and lumbar lordosis (Mac-Thiong et al. 2007). Different from the coronal curvature, at present there is no screening categorization for the sagittal curvature. Rotation was generally evaluated based on the relative position of the pedicles in relation to the underlying vertebral body (Nash et al. 1969) and approximate range of degrees (5-degree interval) represented by each gradation of rotation is determined. However, this method is not a direct measurement of the degree of rotation or the clinical deformity. For cervical measurement, the most typical evaluation methods were occiputo-C2 angle, C2-7 sagittal vertical axis, segmental angle and T1 slope (Oe et al. 2015, Kaplan et al. 2015). Sacropelvic region was also commonly considered when evaluating sagittal balance, in terms of pelvic incidence (PI), pelvic tilt (PT) and sacral slope (SS). There was a geometrical relation between the PI (morphological parameter) and PT/SS (functional parameters), according to the equation: PI = PT + SS (Roussouly et al. 2003).

Other than local measurements, various angular methods had been used to evaluate sagittal global balance, such as 1) Spino-sacral angle: formed by a line from the centre of C7 to the centre of the sacral endplate and the surface of the sacral endplate (Mac-Thiong et al. 2011); 2) Spinal tilt: formed by a line from the centre of C7 to the centre of the sacral endplate and the horizontal surface (Mac-Thiong et al. 2011); 3) spino pelvic tilt: formed by a line from the centre of C7 to the centre of the sacral endplate and a line from the centre of the sacral endplate to the centre of the femoral head (Roussouly and Nnadi, 2010; Mac-Thiong et al. 2011). These angles were typically used to quantify global kyphosis, for instance, severe kyphosis generally implied decreased spino-sacral angle (Mac-Thiong et al. 2011). Chin-brow vertical angle was measured by drawing a line from the brow to the chin and the vertical axis, while the patient stood with hips and knees extended and the neck in a neutral or fixed posture (Bridwell et al. 1989). A classification system has also been established for sagittal global balance evaluation, where no calculation or measurement is involved (Mac-Thiong et al. 2010).

A biplanar X-ray system, EOS 2D/3D imaging system, was recently developed for spine evaluation. It used slot-scanning technology that could reduce the radiation dosage at the same time enhancing image quality (Deschênes et al. 2010). SterEOS 3D, a special 3D construction software, has been developed to accompany the EOS 2D/3D imaging system. This system enabled the generation of realistic 3D models based on a combination of geometric and statistic modelling by a parametric surface 3D reconstruction, and its precision was similar to CT based spinal 3D reconstruction procedure (Mitulescu et al. 2002; Le Bras et al. 2003). Somoskeöy et al. (2012) investigated the accuracy and reliability of the commercial EOS 2D/3D system and sterEOS 3D software under routine clinical circumstances. By predefining end vertebrae before measurements (Dimar et al. 2008; Mok et al. 2008), intra-observer and inter-rater reproducibilities for either 2D or sterEOS 3D measurements were excellent and the results were strongly and significantly correlated with traditional 2D measurement. Other than spine evaluation, the EOS system could be used to investigate other body parts such as pelvic tilt (Lazennec et al. 2011), hip and knee geometrical parameters (Than et al. 2012), acetabular anteversion and inclination (Journé et al. 2012) and musculoskeletal imaging for assessment and follow-up of balance disorder of the spine and of the lower limbs (Wybier and Bossard 2013). However, there were several limitations for the EOS system. Relatively large difference in accuracy was found between the anterior and the posterior vertebral regions, since several anatomical landmarks on the posterior arch such as the transverse and/or spinous processes may be barely visible on the X-ray images, which caused reconstruction error leading to results discrepancies (Mitulescu et al. 2002). In addition, the time needed to reconstruct a detailed 3D spine model was an average of 20 to 30 minutes, and cases with a severe scoliotic curve would definitely require a significantly longer time (Somoskeöy et al. 2012), which was not feasible under routine clinical circumstances.

Moreover, specific devices were needed to maintain the superior limbs and the head of the most unstable patients since movement artefacts due to the long-lasting time of acquisition may lead to the repetition of the examination, resulting in radiation dose increase (Wybier and Bossard 2013). Furthermore, a mild sagittal gap between feet was necessary to avoid superimposition of the lower limbs in the lateral examination, which may induce artificial anterior knee flessum and posterior knee recurvatum

(Wybier and Bossard 2013). EOS also had a limitation for assessing posture. It at present cannot provide study in the supine position, which may be requested in some scoliosis pre-operative assessment (Wybier and Bossard 2013). In terms of cost effectiveness, EOS can be shown to be cost-effective when compared with computed radiography (CR) only if the utilization for EOS is about twice the utilization of CR. However, as CR is widely accepted as the golden standard for spine evaluation method, such estimation would not be possible (McKenna et al. 2012). Also, though EOS applies less radiation dosage during scanning, no evidence shows whether or not these image-related health benefits exist, let alone whether or not they reach the magnitude necessary for EOS to be cost-effective. Furthermore, these extra health gains would be possible only if a sufficient proportion of patients experienced a change in therapeutic management, with a consequent improvement in outcomes, following the use of EOS rather than CR (McKenna et al. 2012).

2.3.2. Sagittal Evaluation Other than Cobb Angle on Radiograph

Other than Cobb angle, different kinds of methods have been used for spinal sagittal angle measurement. Various tangential methods were also introduced for sagittal curvature evaluation. Posterior tangents and Anterior tangents were proposed by Harrison et al. (1996) and Schular et al. (2004), where the curvature was defined by the angle between the two straight lines drawn tangentially to the posterior / anterior vertebral body wall of the end vertebrae. Chernukha et al. (1998) introduced the tangential radiologic assessment of lumbar lordosis (TRALL) method, where the posterosuperior corner of the superior end vertebra, the posteroinferior corner of the inferior end vertebra and the point with the maximal orthogonal distance from the spine were identified for the calculation of the sagittal angle. Another tangent method, namely the Tangent circle method, valuable for evaluating global sagittal geometry was later introduced by Vaz et al. (2002). This method was modified by using two circular arcs and the curvature angle was defined between the straight lines that connected the centers of the circular arcs with the corners of vertebral bodies at both ends of the spine curve and the reference horizontal line. Centroid method was later suggested by Chen (1999), where the angle was defined by two straight lines passing through two vertebral centroids. Followed by computerized centroid method by Briggs et al. (2007), where vertebral body corners from T1 to T12 were manually identified. These methods had been proved to have greater consistency than using Cobb method. Harrison et al. (2001) introduced the Best fit ellipses approach, where an elliptical arc was aligned to the manually identified posterior vertebral bodies' corners using least square technique.

One of the earliest studies which used mathematical models for sagittal curvature measurement was presented by Singer et al. (1990), in which sagittal curvatures were measured by first and second derivative of the sixth-degree polynomial that passed through manually identified anterior and posterior vertebral body contour (Singer et al. 1994). A similar method was introduced in later study, which also used the same landmarks from the vertebral body to evaluate the mean radius of curvature. However, these methods require manual identification of a large number of vertebral landmarks.

Various indexes have also been used to evaluate the thoracic profile of the spine. A spinal line was drawn by connecting the posteroinferior corners of the bodies of the end vertebrae and constructing and additional lines were constructed orthogonally to the spinal line to the posteroinferior corners of the remaining vertebral bodies in the spine curve. The sum of the lengths of these additional lines was considered as Ishihara index (Ishihara et al. 1968). A similar index, Index of kyphosis (Voutsinas and MacEwen 1986), was proposed later, but the sum of additional lines was replaced by the maximal orthogonal distance, which was mainly used for predicting vertebral deformities from kyphosis measurement. The area under curve, which was used as a descriptor of sagittal curvature, was further introduced by Yang et al. (2007), by first manually identifying all postero-superior vertebral body corners, which were then all passed through by spine curve interpolation.

2.3.3. Disadvantages of Current Radiographic Evaluation

Since skeletally immature patients are at risk for curve progression, follow-up posterior-anterior radiographs are necessary for every half a year to one year to monitor the progression (Thomsen et al. 2006). In clinical practice, measuring Cobb's angle from the standing posterio-anterior X-ray radiograph is still the gold standard method to evaluate the severity of scoliosis (Cobb 1948). Routine evaluation and classification of spinal morphology remained predominantly 2D (Lenke et al. 2005; Clements et al. 2011). Sagittal X-ray may somehow be avoided unless necessary to avoid patients from overexposing to radiation. Measurement errors of the intra- and inter-observer reliabilities of Cobb's angle measurement had been reported to be in the range of 3 to 8 degrees using measurement tools (pencils, protractors etc) (Shea et al. 1998, Srinivasalu et al. 2008). These errors were likely due to subjective factors such as end vertebrae selection and observers' skill level (Chockalingam et al. 2002, Stokers et al. 2006). Moreover, routine 2D measurements of thoracic kyphosis erroneously underestimated the preoperative loss of kyphosis in

AIS because of errors associated with axial plane rotation, an inherent component of thoracic scoliosis (Newton et al. 2015). Furthermore, it has been found that there is still a risk of progression for just evaluating and monitoring the Cobb's angle of the patients (Helenius et al. 2003, Tan et al. 2009).

Mass screening or frequent therapy outcome measurements is not recommended due to radiation applied to the patient. In fact, only 10% of patients with curve progression warranted intervention, which means that the rest would expose to unnecessary radiation. Moreover, two radiographs are required and stitched together to produce whole spine view for assessment (Malfair et al. 2010), increasing the risk of radiation exposure. Such radiation accumulated by AIS patients from long-term follow-up may increase the risk of breast cancer in girls with scoliosis (Hoffman et al. 1989, Doody et al. 2000). In addition, radiographic diagnostics in childhood contributed significantly to leukemia and prostate cancer (Schmitz-Feuerhake et al. 2011). Other than radiation issue, another disadvantage of X-ray assessment is that vertebral rotation information in scoliotic spine cannot be directly acquired, since these radiographs do not demonstrate the true magnitude of the 3D spinal deformity present in these patients (Yazici et al. 2001). Though improvements have been made in radiographical technology and techniques to minimize radiation exposure, such as the invention of the EOS system that could provide lower radiation dosage imaging, it was still claimed that long-term health complications remained an inherent risk from limited doses of radiation exposure (Lee et al. 2013). In addition, female patients with scoliosis still had a 4.2% increased risk of breast cancer (Bone and Hsieh 2000). It should be noted that in some countries physiotherapists were not authorized to request X-ray examination (de Oliveira et al. 2012). Hence an alternative system that can accurately measure spine deformity for patients with AIS in all three planes mass screening and longitudinal follow-up during treatments without any hazard of radiation is required in the field.

2.3.4. Sagittal Evaluation of Spine Using Other Methods

For imaging modalities, magnetic resonance imaging (MRI) and computed tomography (CT) are also common for investigating scoliotic spine in the research fields these days due to their high resolutions. However, both MRI and CT are pricey and less accessible (Diefenbach et al. 2013). In addition, MRI requires expertise to operate with long acquisition time, whereas CT requires a higher amount of radiation dosage than traditional radiograph. Moreover, direct measurement of the axial rotation of the spine with a CT scan is inaccurate unless the section is at a right angle to the spinal column, so it is impossible to obtain information on the whole spinal column and the measurement of rotation is disputable. Most importantly, patients are required to be assessed in supine position for both modalities, which could lead to errors in interpretation of the spinal curvature. It had been observed that Cobb's angle derived from the supine posture was significantly and spontaneously corrected from the standing posture (Yazici et al. 2001). Though the results obtained from supine MRI were significantly linearly correlated with the Cobb angles measured on standing x-ray in AIS patients, Cobb angles measured by supine MRI were significantly smaller in both coronal and sagittal planes (Shi et al. 2015, Brink et al. 2017), stating that the parameters from supine and prone scans could not directly be compared to the those from upright radiographs.

Various topographic methods have been used for measuring sagittal curvatures, but they have their own disadvantages. Stereo camera (Figure 2.3a) was used to estimate spine curvature but it was found to be not precise enough and was not able to assess vertebral rotation and visualize the bone architecture (Goldberg et al. 2001). A study using such method even reported differences up to 9 degrees when compared with X-ray Cobb angle measurement (Frerich et al. 2012). A continuous acquisition 3D digitizer called FaroArm (Figure 2.3b) had been used to measure the sagittal spine profile along the spinous processes through sliding on the skin (Salem et al. 2015). It worked by first acquiring 2D sagittal spine models with coordinates, followed by interpolating the data into a five-degree polynomial to obtain thoracic and lumbar angles from the first and second derivative. However, the results were possibly prone to errors since relative positions of the spinous processes were just estimated from the skin surface. A noninvasive anthropometric technique using reflective skin markers (Figure 2.3c) had been used to calculate thoracic kyphosis and lumbar lordosis through obtaining the spatial locations of these markers (Leroux et al. 2000). Schmid et al. (2015) further conducted a study to validate the use of reflective markers, by using radio-opaque markers on patients during radiograph (Figure 2.3d). Repeatable and accurate results would be obtained if palpation was precisely performed on patients. However, it would take a long time for locating the landmarks and attaching the markers to the predefined locations. Lewis et al. (2010) employed inclinometers to determine thoracic kyphosis by placing them over T1/T2 and T12/L1 processes (Figure 2.3e) and demonstrated excellent intra-rater reliability with high ICC and small error using this method. However, there was no certainty that this method was stable over time due to natural variation in postures and accurate palpation was required for every measurement. Chaise et al. (2011) used an adapted arcometer (Figure 2.3f), an aluminium built instrument consisting of a main shaft (Chaise et al. 2011), to measure thoracic kyphosis and lumbar lordosis, and the results were comparable with those from X-ray with good agreement. However, it was not suggested to measure subjects with high BMI since they had high fat levels in the abdominal region and would affect the lumbar measurement. Spinal Mouse (Figure 2.3g) was also used to determine the spinal curvatures and the mobility of the spinal regions with an appropriate degree of accuracy and insignificant intraobserver and interobserver errors (Mannion et al. 2004; Ripani et al. 2008). Though they were easily available and commonly used tools for spinal examination, the results obtained were poor when compared to the standard radiography. Flexicurve (Figure 2.3h), a flexible metallic ruler, was also demonstrated to be able to measure spinal sagittal curvature with excellent repeatability, strong correlation and good agreement with Cobb angle. Prior to angle calculation, palpation and marking of the spinous processes were first performed, followed by folding the flexicurve according to the spine and drawing the contour of the flexicurve onto curve paper with specific spinous processes identified. However, measurement error may arise due to patient positioning, surface palpation of the spinous processes and the misalignment between the flexicurve and the coordinates recorded during paper marking. A motion analysis system based on ultrasound called Zebris (Figure 2.3i), was used to investigate the shape, movement characteristics and mobility of the spine (Zsidai and Kocsis 2006; Takács M et al. 2015). Locations of the spinous processes were recorded through palpation, and were then used to calculate ultrasound angle after curve fitting performed by the built-in algorithm of the system. The ultrasound SPA measured had high test-retest reliability, very good correlation and good agreement with Cobb angle (Takács M et al. 2018). However, the pointing accuracy of the spinous processes had not been investigated and the sample size of the study was small. Judging from the above examples, there is a need for an alternative method to measure the spine curvature with reasonable reliability and repeatability.

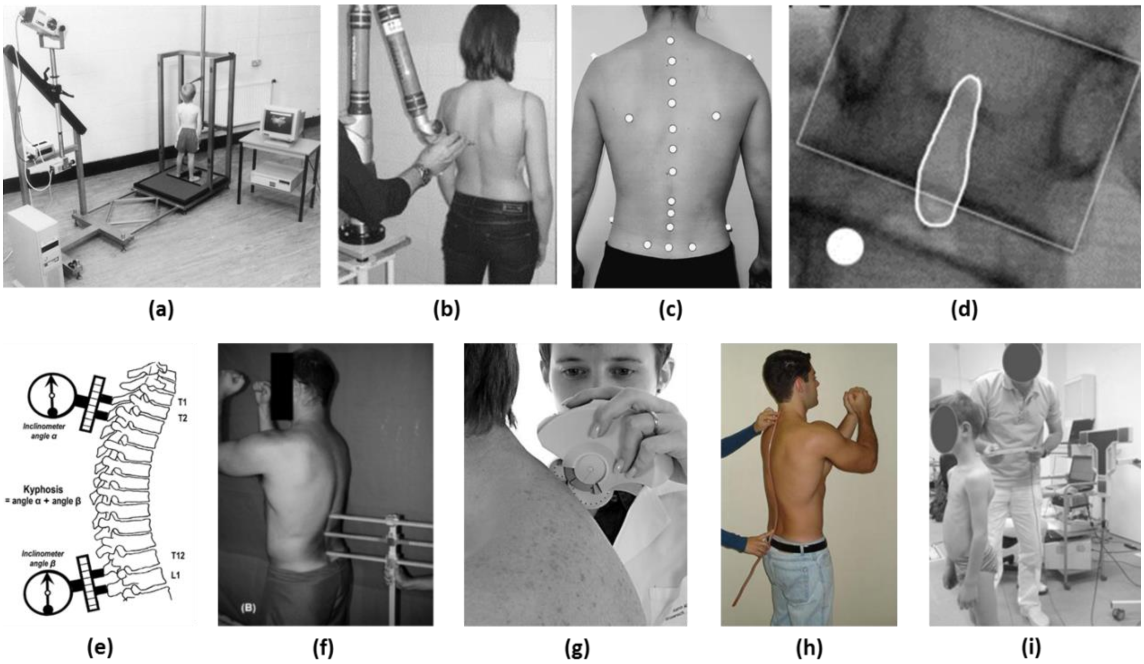

Figure 2.3 *Different non-imaging assessment tools used to assess sagittal curvature of human spine: (a) Stereo camera; (b) FaroArm; (c) reflective skin markers; (d) radio-opaque markers; (e) inclinometers; (f) adapted arcometer; (g) Spinal Mouse; (h) Flexicurve; and (i) Zebris motion analysis system.*

2.3.5. Potential Application of Ultrasound on Sagittal Evaluation of Patients with AIS

The underlying principle of ultrasound is that the bone reflects most ultrasound at the surface of the cortex, giving a clear image and providing valuable information on its shape (Suzuki et al. 1989). Ultrasound imaging can produce acceptable image quality of the posterior spine surface and is more accessible than MRI or radiography. Portable ultrasound machines would allow spine monitoring, even at places without permanent medical imaging devices (Unqi et al. 2014). In addition, cost of installation and the footprint of tracked ultrasound systems are only a fraction of that for radiography systems, which may facilitate wider accessibility and reduce the cost of patient follow-up (Unqi et al. 2014). Hence there is an emerging trend of using freehand 3D ultrasound system for spinal curvature measurement (Nelson et al. 1998, Huang et al. 2005, Fenster et al. 2001; Gee et al. 2003; Cheung CWJ et al. 2010; Purnama et al. 2010).

3D ultrasound was first explored on AIS patients by Suzuki et al. (1989). Spinous processes of the patients were first marked and drawn parallel to the inclination of the vertebrae as seen on an anteroposterior radiograph of the spine. Then the transducer with an attached inclinometer was placed on the spinous process in this line until the image of the laminae became horizontal on the screen. A correlation was found between the Cobb's angle and the vertebra rotation in both thoracic and lumbar curve. Li et al. (2012) investigated the effectiveness of orthotic treatment for patients with AIS using 3D ultrasound in order to enhance the effectiveness of orthotic treatment. SPA was measured from the ultrasound and used as a clinical parameter to estimate the Cobb's angle in order to determine the location of the pressure pad. The results showed that the ultrasound-assisted fitting method of spinal orthosis was effective and beneficial to 62 % of the patients. The intra- and inter-rater reliability of the coronal curvature asymmetry were also investigated on cadaver spinal column phantom (Chen et al. 2013) and patients with AIS (Young et al. 2015). Center of lamina method was used for ultrasound and compared with laser scan using Cobb's method in the study. Coronal curvature measurements were compared to the Cobb angle recorded on the same day. The center of lamina method showed high intra- and inter-rater reliability and moderate correlation with X-ray Cobb. Wang et al. (2015) further investigated the reliability and validity of the centre of lamina methods in clinical setting by comparing to the corresponding MRI measurement on 16 patients with AIS, and similarly, the centre of laminae methods showed high intra- and inter-rater reliability, no significant difference with MRI Cobb and good agreement for coronal angle measurement (Wang et al. 2015). Ungi et al. (2014) utilized tracked ultrasound to localize vertebral transverse processes as landmarks along the spine to measure curvature angles on spine phantoms. Close correlation was found between the tracked ultrasound transverse process angle and the radiographic Cobb measurements (Ungi et al. 2014). In addition, the inter-operator difference of the sonographic transverse process angle was significantly lower than that with radiographic Cobb measurement, though practical usability of the system in this study was yet to be proved. Koo et al. (2014) developed a customized ultrasound system which could identify spinous process from dry bone specimen, by digitizing the spatial position of the spinous process. Different polynomial regression was applied to generate spinal curves, and LOESS (0.4)–posterior deformity angle method was found to best correlate with Cobb's angle.

Cheung et al. (2013) developed a 3D ultrasound imaging method for the radiation-free assessment of scoliosis. Preliminary tests were conducted on flexible spinal column phantoms (Cheung et al. 2013) and 27 human subjects (Cheung et al. 2015). 3D ultrasound volume was obtained through freehand scanning and a virtual 3D model of the spine was formed using the spinous, transverse and/or superior articular processes which were manually chosen. The 3D image was then projected to a 2D plane for X-ray comparison. Ultrasound angles were found to have good linear correlation with X-ray and Bland-Altman showed good agreement between ultrasound and X-ray in both phantom and human studies. The ultrasound system was further modified and improved, and eventually became the commercialized product Scolioscan®. Various studies have been carried out based on Scolioscan® for assessing the curvature of human spine. Previously, we have demonstrated that Scolioscan is reliable for measuring coronal deformity for patietns with AIS in terms of SPA, with excellent intra- and inter-rater and operator reliability, and moderate to strong correlation with Cobb's angle (Zheng et al. 2016), where the results correlated better than Quantec system (R^2 = 0.66) (Goldberg et al. 2001) and the Orthoscan system (R^2 = 0.42) (Knott et al. 2006). Brink et al. (2018) further investigated the reliability and validity of different coronal spinal ultrasound angle measurements using Scolioscan®. Excellent correlations were found between ultrasound and Cobb measurement and no differences in reliability and validity were observed between the ultrasound angles based on the spinous processes and transverse processes. Scolioscan has also been demonstrated to provide reliable information of spinal flexibility and in-orthosis correction of patients with AIS in the prone position (He et al. 2017). The patterns of alternation of coronal curve changes of patients with AIS during forward bending had also been studied, and the patterns of changes between sitting and sitting forward bending postures were found to be highly subject dependent (Jiang et al. 2018).

Other than coronal curvature, ultrasound has also been used in other scoliosis-related researches. For instance, axial vertebral rotation obtained using the center of laminae method showed high intra- and inter- reliability (Chen et al. 2016), and good agreement was found between the laminae ultrasound results with those obtained by the Aaro-Dahlborn method in the magnetic resonance images (Wang et al. 2016). Ultrasonographic evaluation of the Risser sign in patients with AIS was investigated and found to be a reliable method (Thaler et al. 2008). Torlak et al. (2012) further demonstrated that ultrasound could provide Risser sign evaluation with good intra- and inter-rater agreement. Lam et al. evaluated the use of quantitative ultrasound for predicting curve progression (Lam et al. 2011) and determining bone quality (Lam et al. 2013) in patients with AIS. Bone mass density at the femoral head and bone quality in terms of broadband ultrasound attenuation, velocity of sound and stiffness index were found to be significantly lower ($P < 0.05$) in patients with AIS than normal subjects (Lam et al. 2011). Stiffness index was further demonstrated as an independent and significant prognostic factor for AIS and could be considered in addition to other prognostic factors when estimating the risk for curve progression and planning treatment for patients with AIS (Lam et al. 2013).

2.4. Summary

This chapter gives a review of the etiology, diagnosis and treatment for patients with AIS. The human spine is a relatively complex and articulated anatomical structure, with an infinite range of natural biological variability. Though AIS is a 3D spinal deformity, most studies mainly focused on the correction of coronal plane and vertebrae rotation, and the criteria to define optimal sagittal profile were insufficiently investigated. Sagittal Profiles between normal individuals and patients with AIS and other diseases were discussed. In addition, the importance of obtaining optimal sagittal profile was indicated. Potential factors which would cause the disturbance of the sagittal profile of the spine were also discussed and evaluated in detail. Among various sagittal parameters, hypokyphosis has been commonly observed in patients with AIS who possess thoracic scoliosis. Cobb's method and different evaluation approaches on sagittal profile of spine had been discussed for giving an overall picture of the effects of different measurements on the spine. Existing problems of radiograph and the advanced biplanar radiographic EOS have been extensively reviewed. Apart from using radiograph, non-radiation approaches using other imaging modalities, optical systems and other topographic methods have also been reviewed for mapping torso surface and locating vertebrae features to indirectly calculate the spinal sagittal curvature. This leads to the overall objective of this study, which is to investigate the reliability and validity of using 3D ultrasound to accurately measure spinal sagittal curvature for patients with AIS, and to provide optimal criteria for the sagittal profile of these patients by using ultrasound in order to provide mass screening and longitudinal follow-up during treatments without any hazard of radiation.

Chapter 3. Methods

3.1. Spine Phantom Study for Sagittal Curvature of Spine

3.1.1. Ultrasound System

The 3D ultrasound imaging of spine was achieved using an ultrasound scanner (EUB-8500, Hitachi Medical Corporation, Tokyo, Japan) with a linear probe (L53L/10-5) with frequency of 5-10 MHz, an electromagnetic spatial sensing system (MiniBird Ascension Technology Corporation, Burlington, VT, USA) with its sensor mounted on the probe surface, a desktop PC installed with a video capture card (NIIMAQ PCI/PXI-1411, National Instruments Corporation, Austin, TX, USA) and a PC program written using Microsoft Visual Studio 6 with Visual C++ data collection, image processing, visualization and analysis (Figure 3.1) (Cheung, et al. 2015a, Cheung, et al. 2015b). According to the manufacturer, the positional accuracy, position resolution, the angular accuracy and angular resolution of the electromagnetic spatial sensor in terms of root-mean-square were 1.8 mm, 0.5 mm, 0.5 degree and 0.1 degree, respectively.

3.1.2. Spine Phantoms

Four flexible spinal column phantoms featured with soft intervertebral discs allowing deformation (VB84, 3B Scientific, Germany) were used in this study (Figure 3.2). Each spine phantom was scanned using a water-tank scanning approach (Figure 3.1). Plastic frames made of acrylic plates and nylon screws were fabricated for the four phantoms and spatial sensor transmitter to avoid any induced motion by the operator during the scanning process and transportation for X-ray imaging. These spine phantoms were 105cm in height without any deformity. Each of the phantoms was deformed to have four different sagittal curvatures with the presence of scoliotic curvature to simulate different scoliotic conditions. Therefore, in total, 16 different sagittal spinal curvature cases were evaluated.

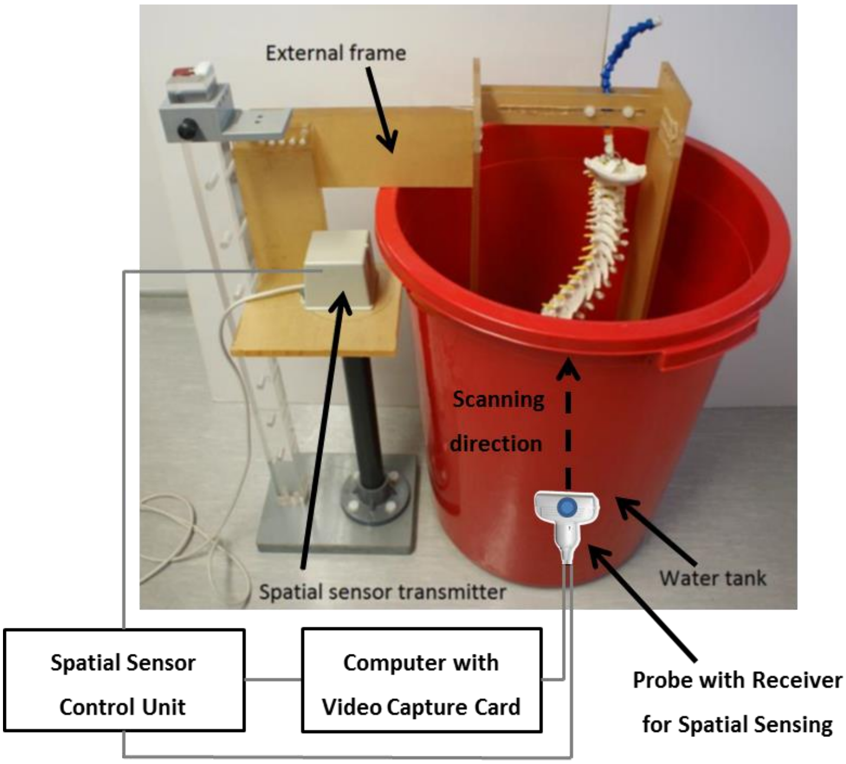

Figure 3.1 *Experimental set-up and system block diagram for the phantom scanning. The grey lines illustrate the connections between the devices.*

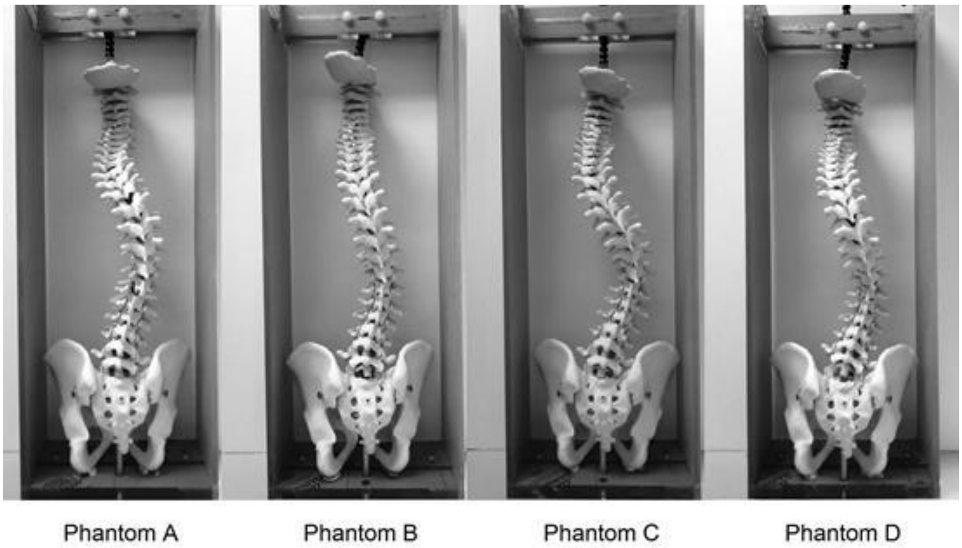

Figure 3.2 *Four flexible spinal column phantoms with different simulated deformity curvatures.*

3.1.3. Study Design and Data Acquisition

All the four phantoms first underwent X-ray chest radiography in lateral positions. The X-ray images were digitized for sagittal Cobb's angle and sagittal SPA measurement using Sante Digital Imaging and Communications in Medicine (DICOM) Viewer free edition version 4.0.13 (Santesoft Ltd, Athens, Greece). To conduct 3D ultrasound scanning, the mounted phantoms were first submerged into a water tank filled with water, with all T1 to L5 vertebrae submerged under water. Prior to scanning, the scanning range was first determined by submerging the probe to the levels of L5 and T1 to define the starting point and ending point respectively. This procedure was exploited for defining the 3D images stack coordinates. During scanning, the probe was oriented with its imaging plane in horizontal plane, and was driven slowly and steadily upwards from L5 to T1 vertebra. The probe's middle line position was maintained to align with the spinous processes of the phantom to ensure that the processes were imaged in the US images during the scanning process. The average scanning time was approximately 1 minute with a frame rate of 10 frames per second, hence around 500 to 700 frames of B-mode images were captured during each scan. After the scanning was completed, the collected ultrasound images (Figure 3.3a) were viewed in 3D with corresponding spatial information (Figure 3.3b). Spinous processes were then manually selected from the stacked ultrasound images using the PC program (Figure 3.4a), where the tips of the processes were manually assigned with a spherical marker in these images using the PC program (Figure 3.4b), and then the spatial information of the processes could be obtained (Cheung et al. 2013, 2015a).

Three sets of data were obtained from the phantom: 1) SPA obtained from 3D ultrasound imaging (USSPA), 2) SPA obtained from sagittal X-ray images (XSPA), and 3) traditional sagittal Cobb's angle (XCA). Both thoracic kyphosis and lumbar lordosis were represented in absolute values for all these angles. The most common radiographic landmarks used in scoliosis measurement are endplates of vertebrae, because they are clearly visible in radiographs. Endplates are not visible in B-mode ultrasound images because the posterior anatomical structure of the vertebrae hinders them from being detected by the ultrasound beam. Indeed one of the most clearly visible vertebral structures by ultrasound is the spinous process. Thus USSPA was evaluated for sagittal spinal curvature using the B-mode images. All the B-mode images were first reviewed manually to identify those images with the echo representing spinous process (Figure 3.4a). Normally multiple images would contain a specific spinous process, then the one with the sharpest echo, often the one located in the middle of all identified images, was selected to represent the tip of the spinous process (Figure 3.4b). Once the location of a spinous process in a specific B-mode image was identified, the 3D spatial coordinates of this location were calculated based on the spatial information of the probe captured by the electromagnetic spatial sensor, a matrix to transfer the location of each pixel in a B-mode image to 3D spatial coordinates (Huang et al. 2005). The spatial coordinates of spinous processes of T2-L4 were identified using this method (Figure 3.4c). Before data analysis, the sagittal profile established from the spinous processes was visually compared with the sagittal shape formed by the spinous processes in the radiograph (Figure 3.4d). The coordinates of the sagittal spinous process profile were then compiled and used to generate a curve using a 5^{th} order polynomial curve fitting algorithm with a custom-designed Matlab program script (Salem et al. 2015). The corresponding slopes of the tangents of T2, T12 and L4 of the generated curves were then obtained. The slopes of tangents of T2 and T12 were used to calculate the thoracic USSPA and those of T12 and L4 were used to calculate the lumbar USSPA.

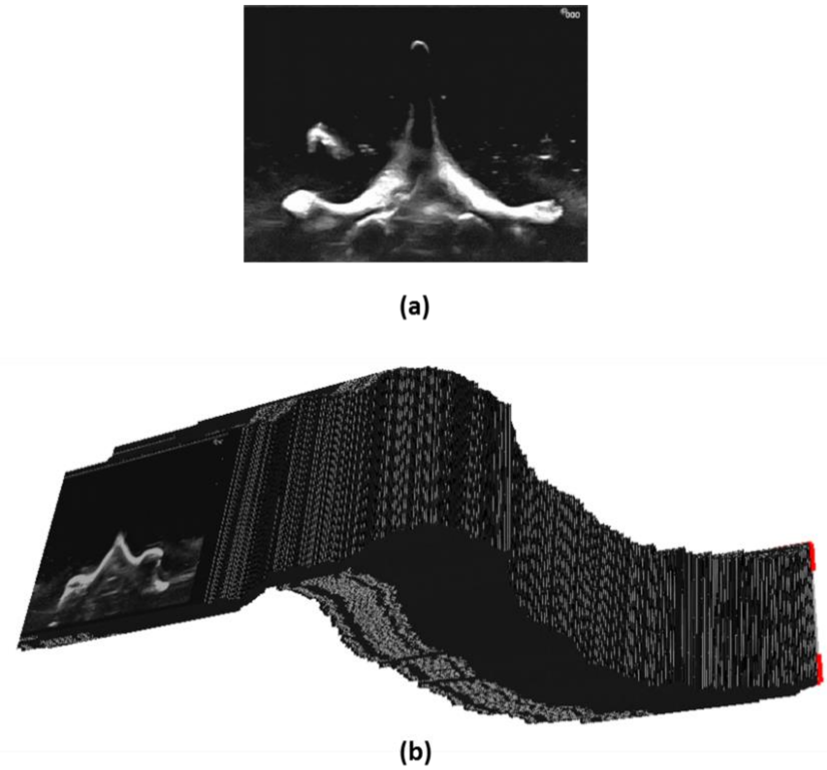

(a)

(b)

Figure 3.3 *(a) A typical B-mode image obtained from the phantom, and (b) 3D ultrasound image series collected from the 3D ultrasound imaging system and stacked according to the orientation and location of each image for further spinous process angle measurement. The spinous process of each vertebra was manually selected from the B-mode images.*

For the Cobb's angle measurement of the X-ray images, thoracic XCA was defined by the angle formed by the straight lines drawn from the upper endplate of T2 vertebra and the lower endplate of the T12 vertebra, whereas lumbar XCA was defined by the angle formed by the straight lines drawn from the upper endplate of L1 vertebra and the lower endplate of the L4 vertebra from the X-ray images (Boseker et al. 2000). The lines were drawn using the Sante DICOM Viewer software and the thoracic and lumbar Cobb's angles were measured from the computer screen using a protractor (Figure 3.5a). For XSPA, image analysis software (Image J ver. 1.49, National Institutes of Health, USA) was used for manually locating the spinous process from T2-L4 in the sagittal radiograph (Figure 3.5b). Similar to the computation of USSPA, the coordinates representing the sagittal plane of the spinous process markers were used to obtain the slope of tangents of T2, T12 and L4 using 5^{th} order curve fitting process to find out the sagittal thoracic and lumbar XSPA.

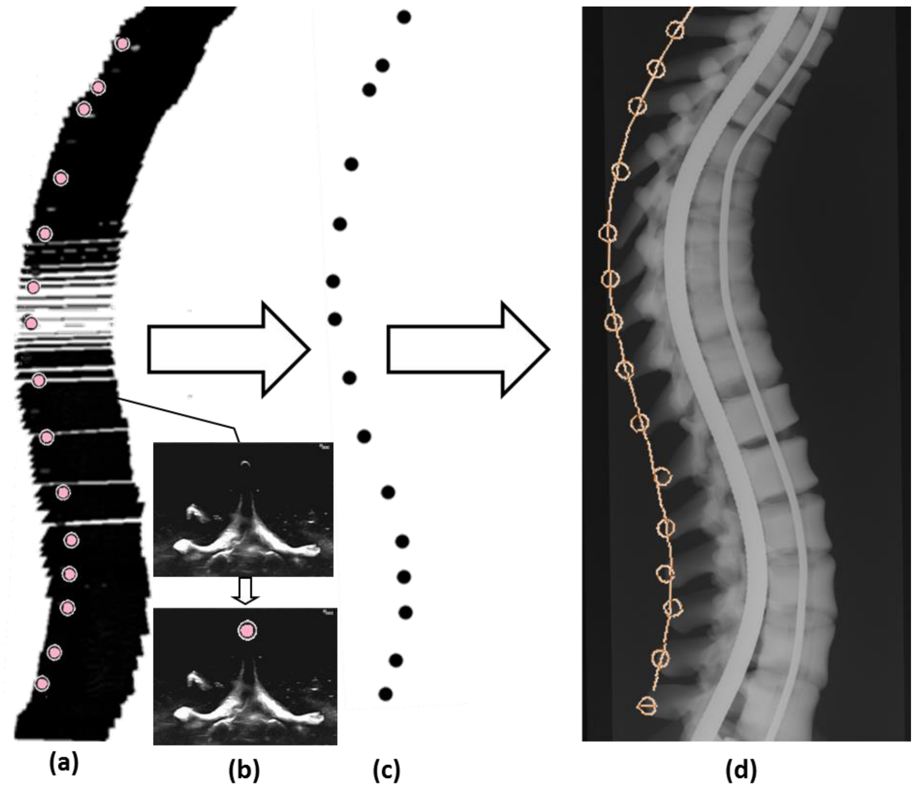

Figure 3.4 *Diagram illustrating spinous processes extracted from 3D ultrasound images. (a) A stack of ultrasound images with spinous processes marked in 3D in corresponding B-mode image, where the black region meaning there was an image stacked and white region without B-mode images; (b) A typical B-mode image containing a spinous process and marked accordingly; (c) Spinous process profile projected in sagittal plane; (d) Corresponding sagittal X-ray image and marked spinous processes. Before data analysis, sagittal spinous process curvature obtained from 3D ultrasound was compared with that from radiograph.*

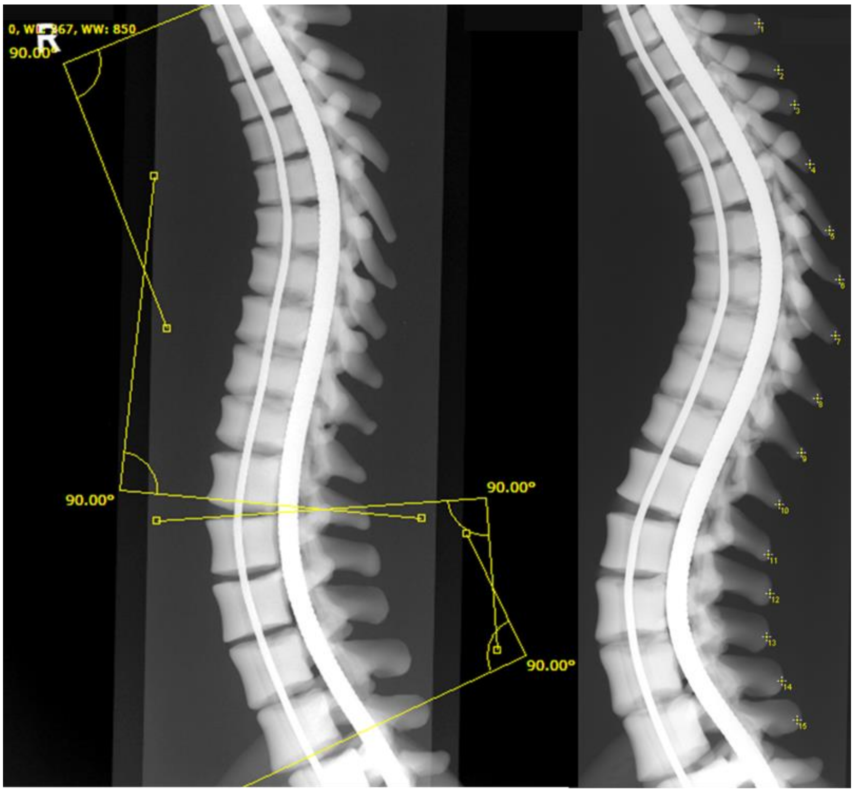

(a) (b)

Figure 3.5 *The two measurement methods of curvature used on radiograph: (a) Cobb's method and (b) spinous process angle by selecting spinous process.*

An operator, named as Operator A, was responsible for conducting the US scanning for twice. Another investigator in this study, named as Rater B, was instructed to obtain two sets of USSPA, XSPA and XCA images respectively at an interval of one week to investigate the corresponding intra-rater reliability. All the second measurements were performed one week after the initial measurements to eliminate bias caused by the effect of memory of Rater B. In addition, Rater B was responsible for acquiring a set of USSPA for the two US scans to test the intra-operator reliability for the US scans. Another rater, namely Rater C, took another measurement from the ultrasound images and X-ray images obtained from the first scan of each phantom to test the inter-rater reliability of USSPA, XSPA and XCA respectively. The correlations of USSPA, XSPA and XCA obtained by Rater B were also tested.

3.1.4. Statistical Analysis

SPSS Version 20.0 (IBM, SPSS Inc., USA) software was used for statistical analysis. The intra-operator reliability for US scanning was analyzed by comparing the first set of USSPA obtained from the first scan with that obtained from the second scan. To investigate the measurement reliability of Rater B for USSPA, XSPA and XCA measurements, the first set of USSPA (first scan), XSPA and XCA measurements was compared with the second set of the corresponding measurements from the same scan or image. Both the intra-operator and intra-rater reliabilities were analyzed using intra-class correlation coefficient (ICC) (two-way random and consistency) (Shrout and Fleiss 1979). To analyze the inter-rater reliability for USSPA, XSPA and XCA, the first set of measurements obtained by Rater B was compared with that obtained by Rater C from the first US scan and X-ray image respectively. The inter-rater reliabilities for all angles were analyzed using intra-class correlation coefficient (ICC) (two-way random and absolute agreement) (Shrout and Fleiss 1979). The Currier criteria for evaluating ICC values were adopted: very reliable (0.80–1.0), moderately reliable (0.60–0.79), and questioned reliable (≤ 0.60). Furthermore, Pearson coefficients were calculated to describe the relationship of the overall sagittal curvature measured (combining thoracic and lumbar angles obtained) for all three angles, with correlation coefficients 0.25 to 0.50 indicating poor correlation, 0.50 to 0.75 indicating moderate to good correlation, and 0.75 to 1.00 indicating very good to excellent correlation (Dawson and Trapp 2004). Mean absolute differences (MAD) and standard deviation (SD) among the three methods were calculated based on the first set of ultrasound measurement to investigate the measurement differences of the methods. Equations describing the line of best-fit through the data of the three methods were also evaluated. The experimental design of this study was illustrated in Figure 3.6 for better understanding. The details of the statistical tests and corresponding data sets used were summarized in Table 3.1.

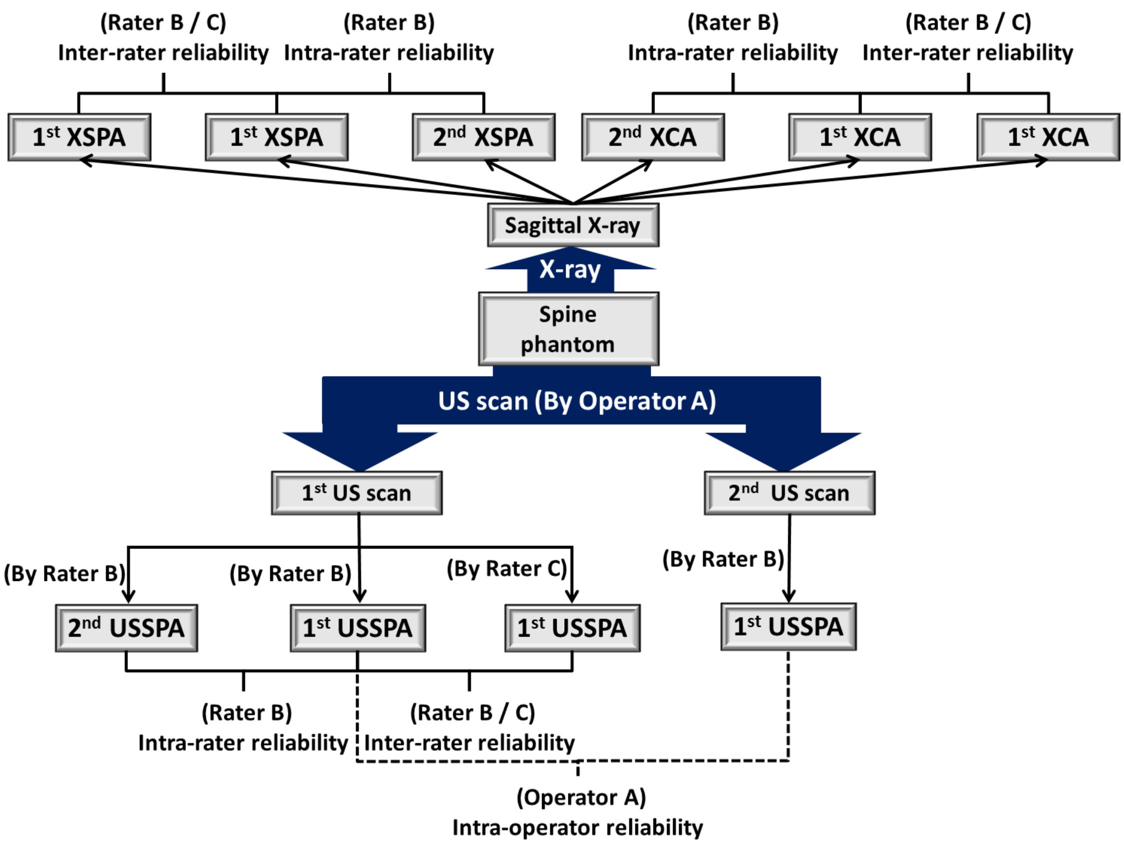

Figure 3.6 *Diagram showing the experiments conducted and the corresponding statistical tests for reliability and repeatability in this study.*

Table 3.2 *Summary of the data sets used in different reliability tests in the phantom study.*

Statistical Test	**Angle being evaluated**	**Result table**	**Remarks**
Intra-rater Reliability	USSPA	Table 4.1	Tests between the two USSPAs obtained by Rater B from the same ultrasound scan
	XSPA		Tests between the two XSPAs obtained by Rater B from the same X-ray image
	XCA		Tests between the two XCAs obtained by Rater B from the same X-ray image
Inter-rater reliability	USSPA	Table 4.2	Tests between the two USSPAs obtained by Rater B and C from the same ultrasound scan
	XSPA		Tests between the two XSPAs obtained by Rater B and C from the same X-ray image
	XCA		Tests between the two XCAs obtained by Rater B and C from the same X-ray image
Intra-operator reliability	USSPA	Table 4.3	Tests between the first set of USSPAs obtained by Rater B from two different ultrasound scans conducted by Operator A

** USSPA: Ultrasound spinous process angle; XSPA: X-ray spinous process angle; XCA: X-ray Cobb's angle*

3.2. Human Subject Study for Sagittal Curvature of Spine

3.2.1. Subjects

Patients diagnosed with AIS were recruited to participate in this test, and all the patients were recruited from a tertiary scoliosis referral center. Patients were requested to receive both ultrasound scanning and X-ray imaging on the same day. This study was approved by the local institutional review board. Signed informed consents were obtained from all the subjects and guardians of the patients aged below 18 prior to the start of the study. Patients with metallic implants and BMI higher than 25.0 $\mathrm{kg/m^2}$ were excluded, as metallic implants would affect the spatial sensing accuracy of the ultrasound probe and high BMI would likely lead to poor image quality in the lumbar region. Other exclusion criteria included: 1) Patients who underwent previous spine surgery; 2) Patients who were wearing a brace during x-ray, and 3) Patients who were allergic to ultrasound gel. In this study we aimed to investigate the reliability and validity of the ultrasound methods for sagittal deformity measurement, thus both USSPA and USLA for all the 21 AIS patients included in this study were obtained from their corresponding sagittal ultrasound images. This number of patients fulfilled the simple approximation that allows the calculation of required sample size of subjects K when the number of replicates n (which was two in this study) is fixed, by setting α set to 0.05 and β (type II error) set to 0.2, while the acceptable and preferred reliability was set as 0.8 and 0.9 respectively (Walter et al.1998).

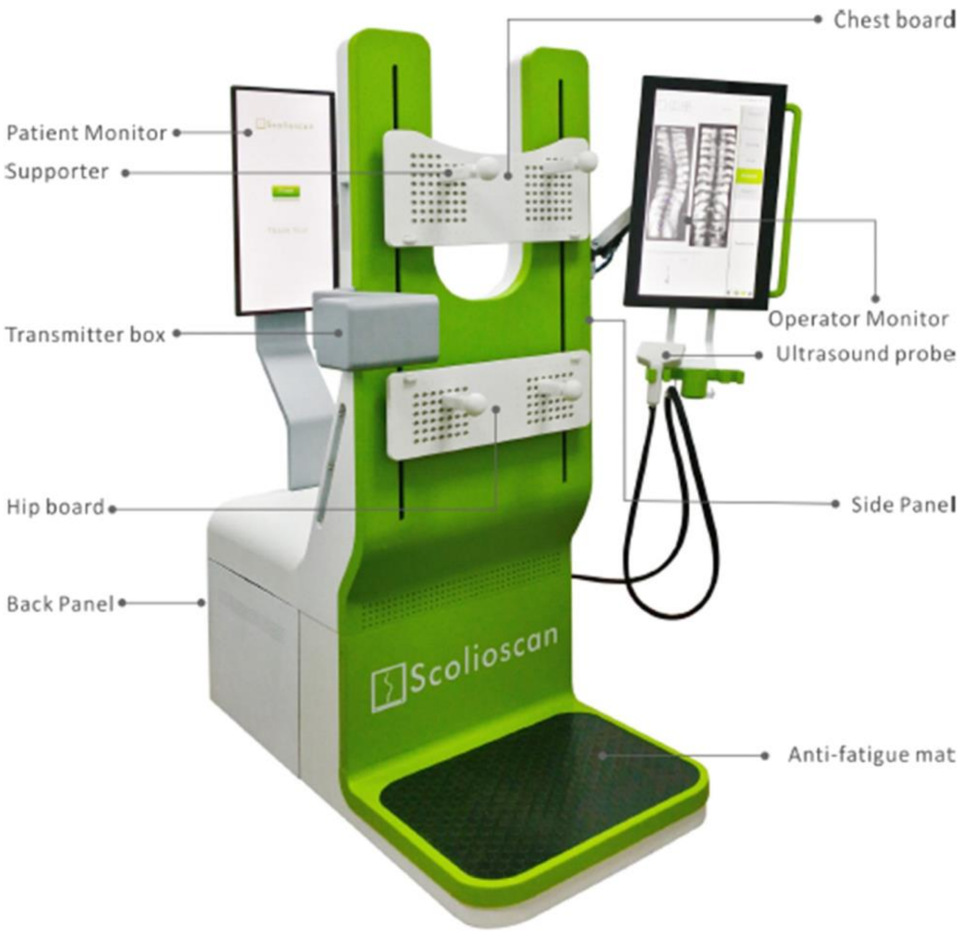

Figure 3.7 *The scolioscan system with its components labeled. The ultrasound scanner, computer and the spatial sensor control box are installed inside the device*

3.2.2. Scolioscan System

The Scolioscan system (Model SCN801, Telefield Medical Imaging Ltd, Hong Kong) was developed based on the 3D ultrasound imaging method reported previously (Cheung and Zheng 2010, Cheung et al. 2013, Cheung et al. 2015, Cheung et al. 2015), but with industrial and ergonomic designs of the hardware and software interfaces. The system included a rigid frame with two movable supporting boards and four supporters to support patients to maintain a stable posture during a test (Figure 3.7). The chest and hip boards could be adjusted by moving up and down to fit patients with different heights, and the four supporters with their length adjustable can be fixed on the boards by inserting to the fixation holes and locked by rotating the supporter by 90°. The locations of boards in vertical direction, the positions of supporters along vertical and horizontal directions, as well as the lengths of supporters could be recorded, and the information could be used in follow-up assessments for the same patient. The 3D ultrasound imaging of the spine was achieved through freehand scanning of the ultrasound probe (frequency of 7.5 MHz, width of 7.5 cm), inside which an electromagnetic spatial sensor was installed to detect the position and orientation of the probe. The electromagnetic transmitter was located inside the transmitter box as indicated in Figure 3.7. The other screen on the back was used to provide information for patients, including a green eye-spot with location set according to the height of the patient to facilitate him/her to keep a stable head and neck posture during scanning. This screen also showed additional information including different steps of evaluation procedures, so as to keep the patient informed of the process, and thus more cooperative.

3.2.3. Testing Protocol

The patient was requested to undress upper garments and shoes before the scanning session and was provided a back-opening dressing gown for ease of scanning. All metallic objects, electronics goods, magnets, and other possible ferromagnetic materials were removed. The patient was asked to stand on the Scolioscan platform for supporter adjustment and the chest and hip boards were repositioned at his/her reasonable height. Two supporters on the chest board and hip board were relocated to align with clavicle anterior concavities and bilateral anterior superior iliac spines respectively. The lengths of supporter’s shafts on both boards were adjusted until they came in contact with the patient. The patient was instructed to maintain a natural standing posture after the adjustment of supporters, and keep eye level horizontal at the level of the eye-spot shown on the patient screen and to focus on the spot throughout the scanning process. Warmed aqueous ultrasound gel was applied to the patient's back by the operator to fill the spinal furrow and to cover the extent of where the probe would sweep. Pre-scanning was performed along L5 and T1, and corresponding adjustment of time gain constant and brightness for B-mode image was conducted to achieve an overall good image quality for the scanning region. After setting the scanning range, the scanning of the spine was conducted by controlling the probe manually, and started approximately from the L5 level and continued to go upward along the spine to the C7 level. The scanning procedure took approximately 30 seconds. After scanning, the collected B-mode image together with the corresponding orientation and position recorded were used for 3D ultrasound volume reconstruction, and the volumes were then transferred to a customized software program for post-processing and generating sagittal ultrasound images for measuring the sagittal curvature. Coronal ultrasound images were automatically formed by obtaining an averaged intensity of all voxels of the ultrasound volume within a selected depth of approximately 10 mm along the anteroposterior direction by using a non-planar re-slicing technique with the skin surface as a reference for selecting the required voxels. The coronal spinous process angle(s) (SPA) were measured by manually drawing the lines on the most tilted part of the mid-line on the coronal image, which represents the shadow of the spinous processes (Figure 3.8), and has been demonstrated to be reliable and repeatable (Brink et al. 2018, Zheng et al. 2016). Since surface references were not available for generating sagittal ultrasound images, they were formed by transferring the ultrasound volume to the customized software (Figure 3.9) and manually selecting the suitable slices along the medial-lateral direction, where the spinous processes and bilateral laminae could be visualized.

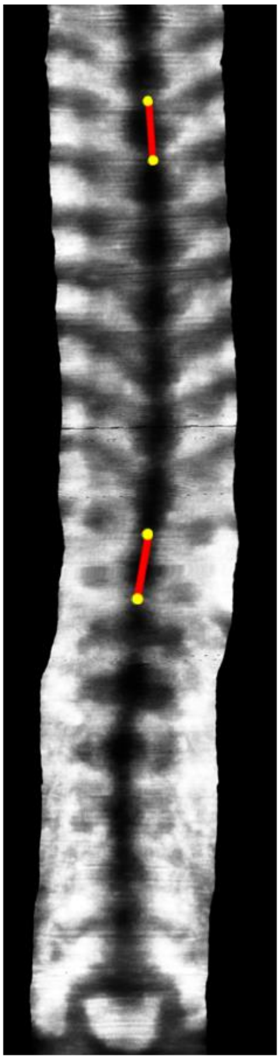

Figure 3.8 *The diagram shows the measurement of coronal ultrasound angle(s)*

Figure 3.14 *Coronal and sagittal ultrasound images and the 3D ultrasound volume obtained from the 3D ultrasound system illustrated by the customized 3D software*

3.2.4.Study Design and Data Acquisition

Two operators were involved to conduct US scanning for each AIS patient. In previous studies on this 3D ultrasound system (Zheng et al. 2016, Brink et al. 2018), scanning repeatability of either the same or different operators has been demonstrated to be reliable, so in this study only one scan was performed for each patient and one ultrasound volume was used for computation during angle analysis. Another three raters, named as Rater 1, Rater 2 and Rater 3, were involved for the curvature measurement. Rater 1 and Rater 2 were responsible for conducting ultrasonic measurements, who were novice researchers with more than 2 years of experience in studying the human spine using 3D ultrasound. Rater 3 was a spine surgeon responsible for radiographic Cobb angle measurements.

For ultrasound, thoracic kyphosis and lumbar lordosis were measured by the SP angle (USSPA) and the laminae angle (USLA). To compute USSPA and USLA, three sagittal ultrasound images visualizing the spinous processes (Figure 3.10a) and bilateral laminae (Figure 3.10b) were first manually obtained by Rater 1 using the customized 3D ultrasound software. The centre of spinous processes and laminae were considered as the landmarks for measuring USSPA and USLA (Figure 3.11a and b). Thoracic USSPA was defined by the intersection angle between the line joining T3 and T4 spinous processes and the line joining T11 and T12 spinous processes, whereas lumbar USSPA was defined by the intersection angle between the line joining T12 and L1 spinous processes and the line joining L4 and L5 spinous processes (Figure 3.12a). USLA was defined by the average of the angle values obtained from the left and right laminae. Thoracic USLA was defined by the averaged intersection angle between the line joining T3 and T4 (left/right) laminae and the line joining T11 and T12 (left/right) laminae, whereas lumbar USLA was defined by the intersection angle between the line joining T12 and L1 (left/right) laminae and the line joining L4 and L5 (left/right) laminae (Figure 3.12b). Both measurements were performed using RadiAnt DICOM Viewer software (Medixant, Poland). Approximate levels of T3, T12 and L5 were indicated by Rater 2 on the sagittal ultrasound image to avoid line misplacement on specific vertebral landmarks.

Thoracic XCA was defined by the angle formed by the upper endplate of T4 vertebra and the lower endplate of the T12 vertebra, whereas lumbar XCA was defined by the angle formed by the upper endplate of L1 vertebra and the lower endplate of the L5 vertebra from the standing posteroanterior X-ray images by Rater 3 (Figure 3.12c)

(Boseker et al. 2000). All raters performed the measurements independently and were blinded to the patients' details.

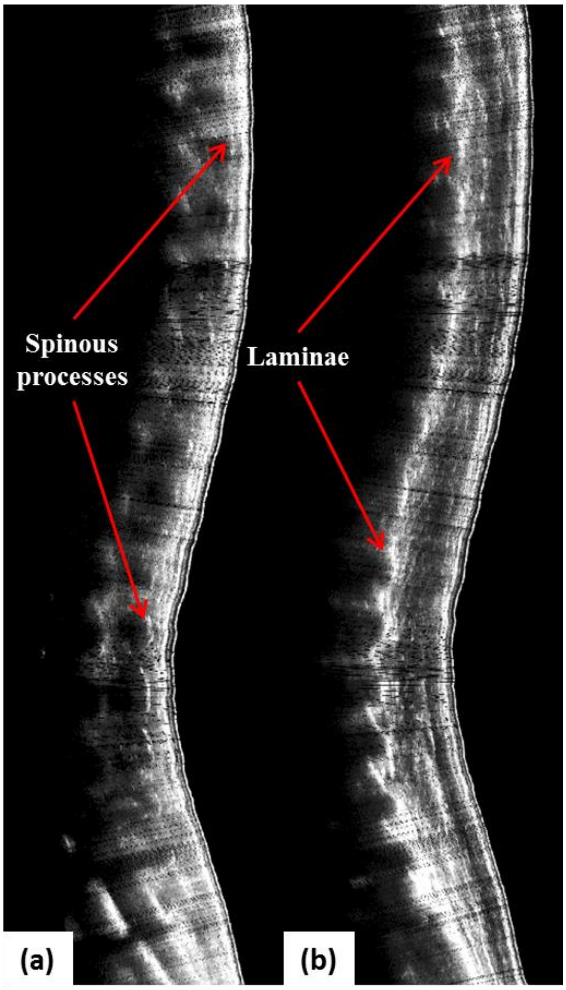

Figure 3.10 *Sagittal ultrasound image illustrating (a) spinous processes and (b) laminae for sagittal measurement.*

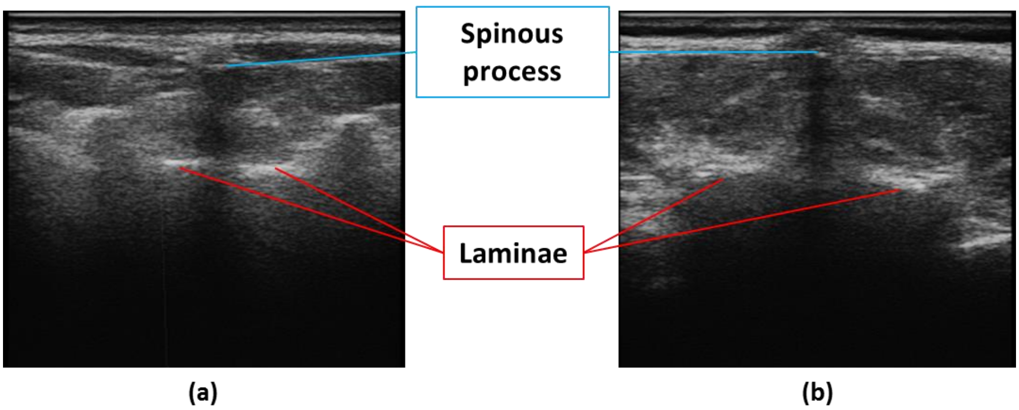

Figure 3.11 *Diagram showing the spinous processes and bilateral laminae of (a) thoracic and (b) lumbar vertebrae.*

3.2.5.Statistical Analysis

Data was reported as mean ± standard deviation (SD). Statistical analysis was conducted using SPSS Version 20.0 (IBM, SPSS Inc., USA) software. Intra-class coefficient (ICC) (two-way random and consistency model) was calculated to evaluate the intra-rater reliability of USSPA and USLA of the two raters (Shrout and Fleiss 1979), by comparing their two measurements made on the same customized sagittal US image individually. The first measurement results obtained by Rater 1 and Rater 2 were compared using ICC (two-wayrandom and absolute agreement model) to determine inter-rater reliability (Shrout and Fleiss 1979). The Currier criteria for evaluating ICC values were adopted: very reliable (0.80–1.0), moderately reliable (0.60–0.79), and questioned reliable (≤0.60) (Currier 1984). Ultrasound measurements were compared with XCA respectively using linear correlation for thoracic curves and thoracic curves. Linear regression equations with intersections were analyzed with correlation coefficients 0.25 to 0.50 indicating poor correlation, 0.50 to 0.75 indicating moderate to good correlation, and 0.75 to 1.00 indicating very good to excellent correlation (Dawson and Trapp 2004). Bland-Altman method was used to test the agreement between XCA and the adjusted ultrasound angles. To measure the differences in agreement for USSPA and USLA, the mean absolute differences (MAD) between XCA and the adjusted ultrasound angles were calculated and compared using paired t-tests. The significance level was set at 0.05.

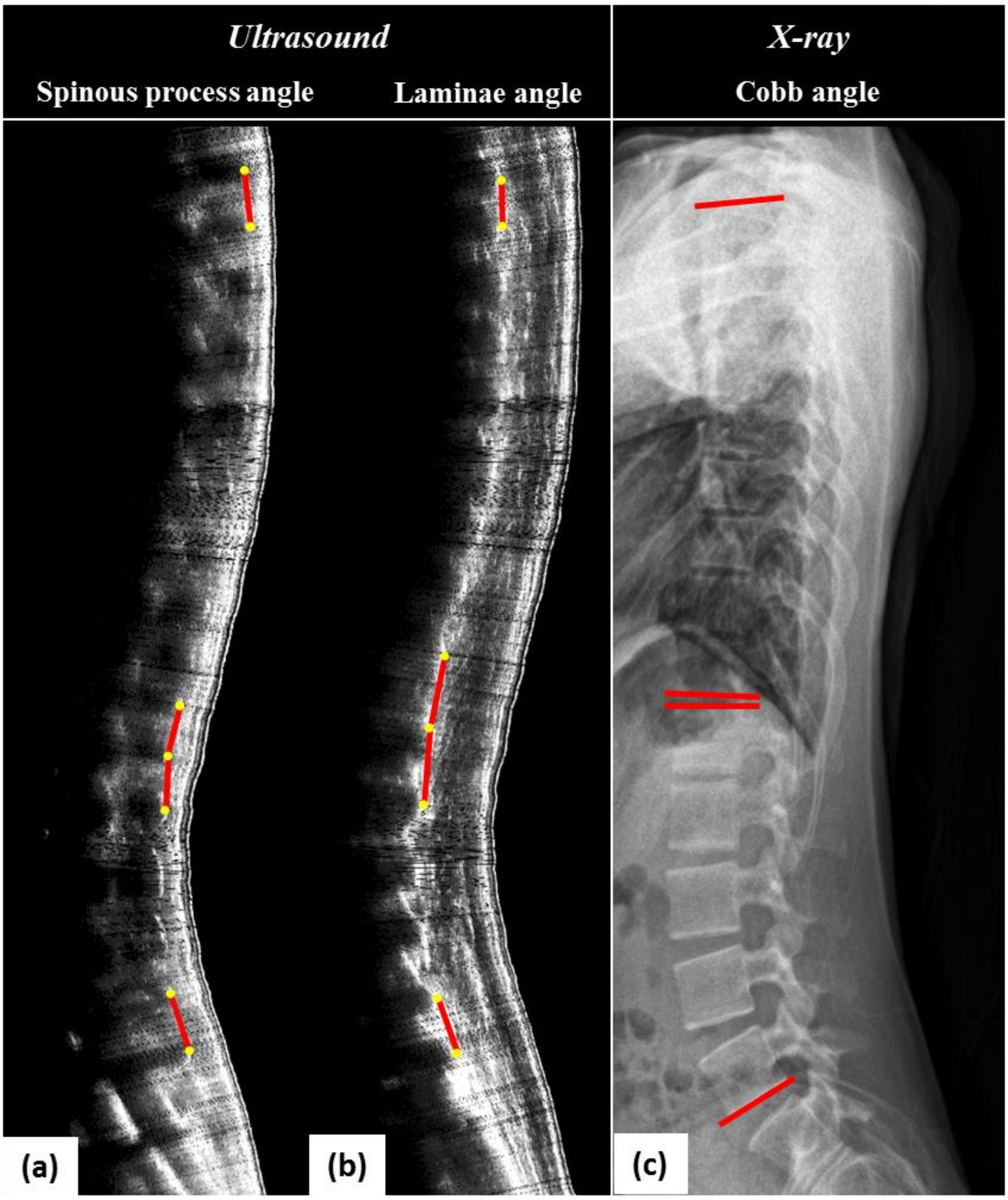

Figure 3.12 *Diagrams showing how (a) Measurement of ultrasound spinous process angle (USSPA); (b) Measurement of ultrasound laminae angle (USLA); and (c) Measurement of Cobb's angle (XCA) were carried out respectively.*

3.3. Human Subject Study for Coronal-Sagittal Coupling

3.3.1.Subjects

Total 300 AIS patients diagnosed with scoliosis and scanned by radiographs were invited for this study. 150 subjects were allocated into the first stage of the study, whereas the second 150 subjects were allocated into the second stage (See details in Section 3.3.2). All these patients were recruited consecutively in the Department of Orthopaedics and Traumatology of The Chinese University of Hong Kong. The study got human subject ethical approvals from both The Hong Kong Polytechnic University (No. 20070321001) and The Chinese University of Hong Kong (No. 2009.622). Informed consent was obtained from all patients (or their parents for those under 18 years of age). The patients received standing plain radiographs within three months before the Scolioscan assessment, and their Cobb angles were measured. Patients with metallic implants and BMI higher than 25.0 kg/m^2 were excluded, as metallic implants may potentially affect the accuracy of ultrasound probe spatial sensing and high BMI may lead to poor image quality in the lumbar region using the current probe.

To study the coupling effect between the coronal and sagittal curves, 115 AIS patients with Cobb < 40° participated in the exploratory stage using the following exclusion criteria: 1) Cobb angle > 40° (N = 25); 2) Special cases: Appeared to be kyphotic in lumbar region in US (N = 3); 3) T3 level was not captured in the ultrasound scans (N = 3); 4) Poor scanning quality in the thoracic region due to the hindrance of the scapula (N = 3); 5) Sagittal X-ray was not available (N = 1). For the validation session, exclusions of patients were made due to: 1) Poor quality due to large rotation (N = 10), possibly caused by large Cobb angle; 2) Special cases:

Appeared to be kyphotic in lumbar region in US (N = 1); 3) T3 / L5 level was not captured in the ultrasound scans (N = 2); 4) Poor scanning quality due to high BMI index (higher than 25.0 kg/m^2) (N = 9); 5) Poor scanning quality in the thoracic region due to the hindrance of the scapula (N = 2); 6) Dropped out during the examination period (N = 1). Hence the total number of subjects involved for the exploratory and validation sessions was 115 and 125 respectively. Figures A.1, A.2, A.3 and A.4 in the Appendices section illustrated the sagittal ultrasound laminae images of patients with single thoracic curve, single thoracolumbar curve, single lumbar curve and both thoracic and thoraco(lumbar) curve of Cobb < 20º and Cobb > 20 º covering from T3 to L5 for reference.

3.3.2.Study Design and Data Acquisition

3D ultrasound imaging system was used for conducting the ultrasound scans and the same scanning protocol as described in Section 3.2.3 was adopted. Since ultrasound can give a clear image of the outline of the laminae (Suzuki et al. 1989) and laminae of the vertebrae had been demonstraed to be a more reliable structure for evaluating spinal sagittal curvature as shown in the pilot study, only USLA would be used for evaluating thoracic kyphosis and lumbar lordosis from the sagittal ultrasound images. This part of the study was divided into two stages: 1) Exploratory stage: To first validate whether ultrasound could detect similar coupling relationship (if exist) using traditional Cobb angle classification, followed by detecting the coupling relationship using SPA classification. A supplementary investigation was also conducted by measuring sagittal angles using different locations of the vertebral bodies on radiograph to study the anatomical effect on the sagittal parameters; 2) Verification stage: To further justify the coupling effect observed in the exploratory stage and to demonstrate ultrasound could detect the coupling phenomenon alone without the utilization of X-ray.

In the exploratory stage, coronal Cobb angles were measured and classified by a doctor in the Department of Orthopedics who has over 10 years of experience in reading radiographs of patients with scoliosis. Curves would be considered as main thoracic if the apex of the curves lied between T6 and T12 disc, and as thoraco(lumbar) if the apex of the curves lied below T12 disc. Sagittal Cobb was measured by the author of this thesis in terms of thoracic and lumbar XCA, whose sagittal X-ray measurements had been demonstrated to have high reliability with another orthopaedic doctor. Two operators were involved for the ultrasound scanning, and one of them (Rater C in human pilot study) was responsible for measuring SPA manually and independently on the coronal ultrasound image, using the manual measurement tool provided by the Scolioscan system. The coronal SPA was then classified into main thoracic or thoraco(lumbar) SPA, where curves would be considered as main thoracic if the apex of the curves lied between T6 and T12 levels, and as thoraco(lumbar) if the apex of the curves lied below T12 level. Thoracic and lumbar USLA was obtained according to the methods described in *Section 3.2.4* as thoracic kyphosis and lumbar lordosis. Both the measurement methods for the sagittal X-ray Cobb and USLA were the same as mentioned in *Section 3.2.4*.

Thoracic kyphosis and lumbar lordosis of the patients with AIS determined using X-ray and ultrasound, which were XCA and USLA respectively, were first classified into two groups based on Cobb angles: 1) Angle of the main thoracic or thoraco(lumbar) Cobb $\leq 20^{\circ}$; and 2) $20^{\circ} <$ Angle of the main thoracic or thoraco(lumbar) Cobb ≤ 40º. Then for SPA classification, thoracic and lumbar USLA of the patients with AIS were classified into two groups: 1) Angle of the main thoracic or thoraco(lumbar) SPA ≤ 17º; and 2) 17º < Angle of the main thoracic or thoraco(lumbar) Cobb. The value of 17º was obtained by substituting Cobb angle of 20º into the linear regression obtained in Figure 4.6 to obtain the equivalent angle of SPA. Similarly, for the validation stage, SPA classification was applied to the second batch of 125 patients, and two groups of patients with AIS were obtained for further analysis.

The anatomical effects of using different locations for sagittal curvature measurement on X-ray were also investigated by two methods other than Cobb (Figure 3.13): 1) Posterior tangent (PT) method (Harrison et al. 1996) and 2) Centre of posterior border (CPB) method. For the PT method, thoracic kyphosis was defined by the angle formed between the posterior border of T4 and T12 vertebra, whereas lumbar lordosis was defined by the angle formed between posterior border of L1 and L5 vertebra from the standing posteroanterior X-ray images (Figure 3.13c). For the CPB method, thoracic kyphosis was defined by the angle formed between the line joining the centre of T3 and T4 posterior border and the line joining the centre of T11 and T12 posterior border, whereas lumbar lordosis was defined by the intersection angle between the line joining the centre of T12 and L1 posterior border and the line joining the centre of L4 and L5 posterior border (Figure 3.13d). All the measurements were performed using RadiAnt DICOM Viewer software (Medixant, Poland).

3.3.3.Statistical Analysis

Sagittal data was reported as mean ± standard deviation (SD). Statistical analysis was conducted using SPSS Version 20.0 (IBM, SPSS Inc., USA). In the exploratory stage, sagittal ultrasound angles were compared with those obtained from X-ray respectively using linear correlation for corresponding Cobb ≤ 20º, 20º < Cobb ≤ 40º and all cases combined. Independent t-tests were used: 1) To compare thoracic kyphosis and lumbar lordosis of X-ray and ultrasound of the patients based on coronal Cobb values (Cobb ≤ 20º and 20º < Cobb ≤ 40º); and 2) To compare thoracic kyphosis and lumbar lordosis of ultrasound based on SPA values (SPA ≤ 17º and 17º < SPA). Pearson correlations between the corresponding coronal and sagittal measurements of the two imaging modalities were also evaluated to describe the relationship between the spinal parameters in the two planes. Similarly in the validation stage, independent t-tests were used to compare thoracic kyphosis and lumbar lordosis based on SPA values (SPA ≤ 17º and 17º < SPA) on the second batch of patients, and finally on all the patients involved in both exploratory and validation sessions. Paired t-tests were used to evaluate the difference in spinal sagittal measurements between ultrasound and the three X-ray methods (Figure 3.13). The significance level was set at 0.05.

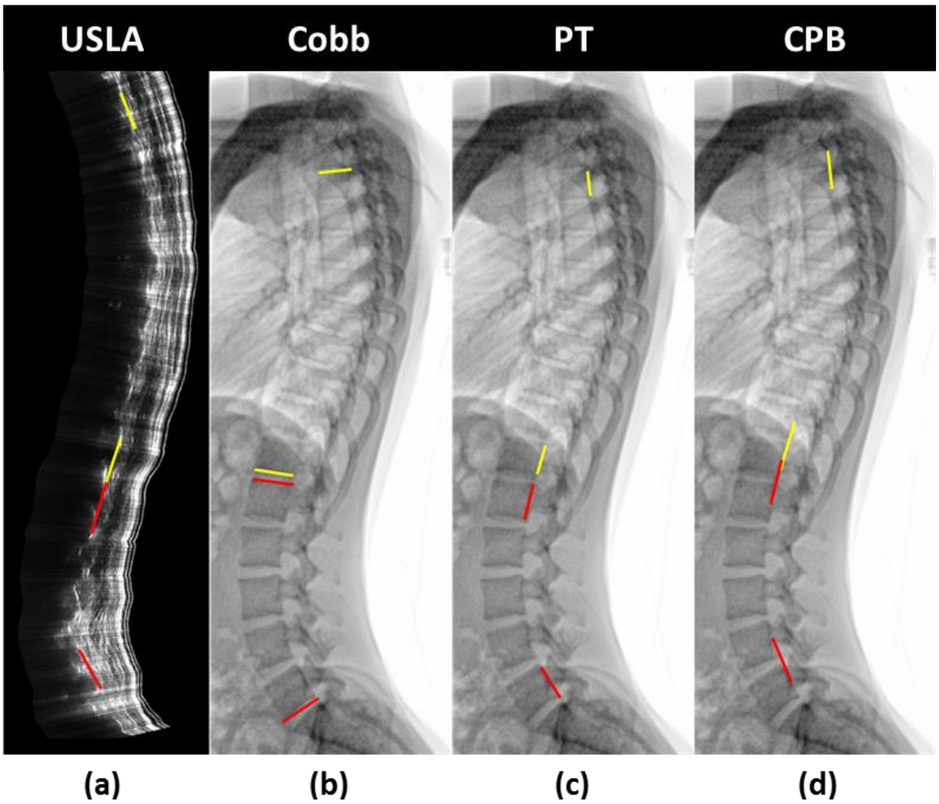

Figure 3.13 *Diagrams showing how (a) Ultrasound laminae (USLA); (b) Cobb; (c) Posterior Tangent (PT); and (d) Centre of Posterior Border (CPB) angles were measured respectively.*

Chapter 4. Results

4.1. Results of Spine Phantom Study

Though 3D coordinates of the spinous processes and coronal plane of the X-ray images were acquired, only the sagittal curvatures of the spine phantoms were analyzed and compared for USSPA, XSPA and XCA since validation of our proposed ultrasound method on sagittal spinal analysis was the focus of this study. The average sagittal curvatures and ranges of the phantoms measured for the three angles by Rater B were: USSPA: 25.6 ± 12.3 degrees (5.5 to 36.9 degrees), 26.5 ± 9.9 degrees (7.6 to 41.3 degrees); XSPA: 23.9 ± 9.7 degrees (4.0 to 36.9 degrees), 25.7 ± 8.6 degrees (11.1 to 39.5 degrees); and XCA: 30.5 ± 8.9 degrees (19.0 to 46.0 degrees), 28.9 ± 5.0 degrees (21.0 to 36.0 degrees) for the thoracic region and lumbar region, respectively.

Raters demonstrated excellent intra-rater and inter-rater reproducibility for USSPA, XSPA and XCA. For intra-rater reliability, the ICC ranged from 0.97 to 0.99 for the angle measured in the thoracic region and from 0.91 to 0.99 for the angle measured in the lumbar region among the three angles (Table 4.1). For inter-rater reliability, the ICC ranged from 0.93 to 0.99 and from 0.86 to 0.98 for the thoracic and lumbar regions, respectively (Table 4.2). In addition, scanning skill for Operator A was found to be very reliable since the ICC values were greater than 0.9 for the results obtained for both the regions (Table 4.3).

Table 4.1 *Intra-rater reliability of Rater B for sagittal curve measurement using the three methods.*

Intra-rater reliability (ICC)	**Thoracic**	**Lumbar**
USSPA	0.985 (0.956 – 0.995)	0.988 (0.966 – 0.996)
XSPA	0.998 (0.994 – 0.999)	0.989 (0.968 – 0.996)
XCA	0.972 (0.921 - 0.990)	0.905 (0.750 - 0.966)

**ICC: Intraclass correlation coefficient; USSPA: Ultrasound spinous process angle; XSPA: X-ray spinous process angle; XCA: X-ray Cobb's angle; Parentheses represent the 95% confidence interval for the coefficient*

Table 4.2 *Inter-rater reliability of the three angles by the two raters.*

Inter-rater reliability (ICC)	**Thoracic**	**Lumbar**
USSPA	0.982 (0.951 - 0.994)	0.908 (0.757 – 0.967)
XSPA	0.989 (0.969 - 0.996)	0.983 (0.953 - 0.994)
XCA	0.930 (0.586 - 0.981)	0.861 (0.651 - 0.949)

**ICC: Intraclass correlation coefficient; Parentheses represent the 95% confidence interval for the coefficient*

Table 4.3 *Intra-operator reliability of Operator A for phantom scanning in terms of spinous process angle obtained.*

Intra-operator reliability (ICC)	**Thoracic**	**Lumbar**
USSPA	0.976 (0.932 - 0.991)	0.911 (0.765 - 0.968)

**ICC: Intraclass correlation coefficient; Parentheses represent the 95% confidence interval for the coefficient*

USSPA, XSPA and XCA were found significantly correlated with each other with $p < 0.05$. The MADs of the thoracic and lumbar angles among the three methods were shown in Table 4.4. Pearson coefficients for XSPA against XCA, USSPA against XSPA and USSPA against XCA were $r = 0.82$, $r = 0.95$ and $r = 0.84$ for thoracic region and $r = 0.72$, $r = 0.89$ and $r = 0.51$ for lumbar region respectively (Table 4.4). The extrapolated linear equation of the comparisons of the thoracic and lumbar angles among the three measurement methods indicated a positive linear relationship (Figure 4.1, 4.2 and 4.3).

Table 4.4 *Best-fit equations and absolute errors obtained from the three methods by Rater B.*

	MAD ± SD (°)			Pearson correlation (r)	
	Thoracic	**Lumbar**	**Overall**	**Thoracic**	**Lumbar**
XCA against XSPA1	6.7 ± 5.5	4.8 ± 4.8	5.8 ± 5.2	0.82	0.72
USSPA1 against XSPA1	2.4 ± 2.4	3.6 ± 2.7	3.0 ± 2.6	0.95	0.89
XCA against USSPA1	5.6 ± 4.3	6.5 ± 5.8	6.0 ± 5.1	0.84	0.51

ICC: Intraclass correlation coefficient; USSPA: Ultrasound spinous process angle; XSPA: X-ray spinous process angle; XCA: X-ray Cobb's angle; MAD: Mean absolute difference; SD: standard deviation; Parentheses represent the 95% confidence interval for the coefficient

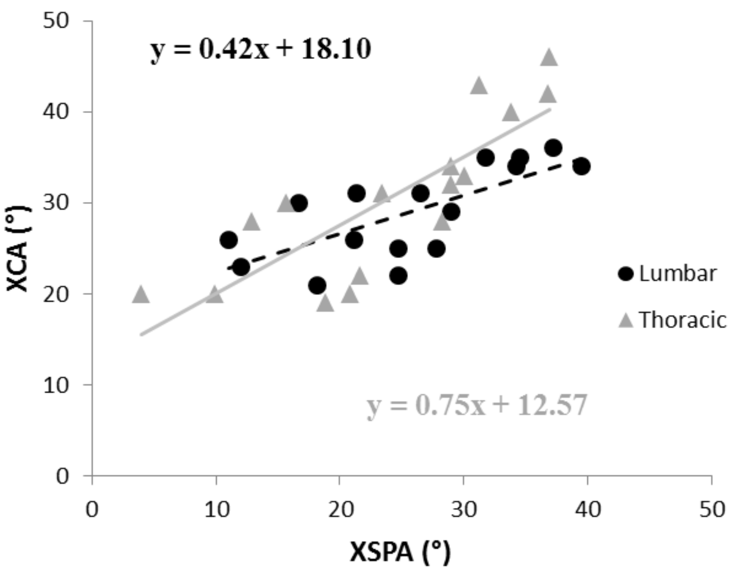

Figure 4.1 *Scatter plot of thoracic and lumbar Cobb's angle against X-ray spinous process angle, with the associated trend line equation. (XSPA: X-ray spinous process angle; XCA: X-ray Cobb's angle)*

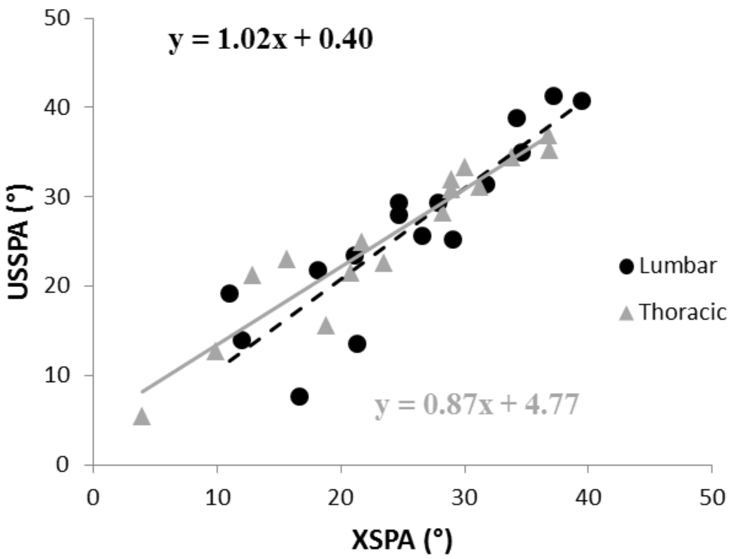

Figure 4.2 *Scatter plot of the thoracic and lumbar ultrasound spinous process angle against X-ray spinous process angle, with the associated trend line equation. (USSPA: Ultrasound spinous process angle; XSPA: X-ray spinous process angle)*

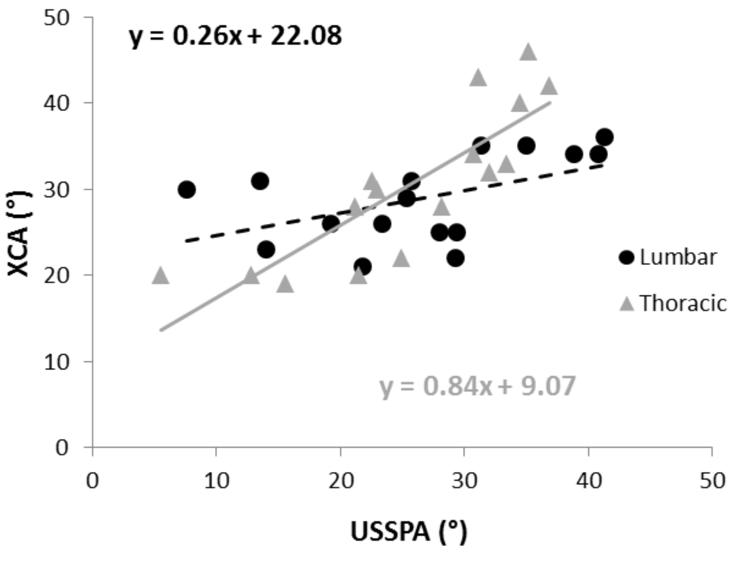

Figure 4.3 *Scatter plot of the thoracic and lumbar Cobb's angle against ultrasound spinous process angle, with the associated trend line equation. (USSPA: Ultrasound spinous process angle; XCA: X-ray Cobb's angle)*

4.2. Results of Human Subject Study

The mean age of the subjects was 15.7 ± 1.3 years (range 12-18 years), with 14 females and 7 males. The mean coronal Cobb angle was 24.5 ± 9.0° (range 11.1 – 41.9°). Thoracic and lumbar XCAs were on average 22.7 ± 14.0° (range 0.7 – 44.6°) and 38.0 ± 12.6° (range 14.7 – 60.0°) respectively. Thoracic and lumbar sagittal ultrasound angles were on average 28.1 ± 10.4° and 18.5 ± 9.2° (USSPA) and 34.6 ± 10.5° and 26.5 ± 12.0° (USLA) respectively.

Intra-rater and inter-rater reliabilities for the ultrasound angles were shown in Table 4.5.

Table 4.5 *Intra-rater and inter-rater reliability of the sagittal ultrasound angles by Rater 1 and Rater 2.*

	Curve	Rater 1 Intra ICC	Rater 2 Intra ICC	First measurement Inter ICC
USSPA	Thoracic	0.98 (0.96 – 0.99)	0.93 (0.84 – 0.97)	0.95 (0.87 – 0.98)
	Lumbar	0.96 (0.91 – 0.98)	0.92 (0.81 – 0.97)	0.94 (0.86 – 0.98)
USLA	Thoracic	0.99 (0.96 – 0.99)	0.97 (0.92 – 0.99)	0.95 (0.88 – 0.98)
	Lumbar	0.98 (0.94 – 0.99)	0.97 (0.92 – 0.98)	0.94 (0.40 – 0.98)

**ICC: Intraclass correlation coefficient; USSPA: Ultrasound spinous process angle; USLA: Ultrasound laminae angle Parentheses represent the 95% confidence interval for the coefficient*

Both USSPA and USLA showed moderate to good linear correlations with XCA (Figure 4.4a and b). Thoracic USLA was found to have the lowest R^2 value (0.574), while lumbar USLA was found to have the highest R^2 value (0.701). The Bland-Altman plot showed a good agreement between the ultrasound angles adjusted with the linear equations and the XCA (Figure 4.5a and b). No significant difference was found between both adjusted ultrasound angles (MAD: USSPA 6.4 ± 4.8° / 6.1 ± 4.4°; USLA 7.5 ± 4.9° / 5.3 ± 4.2°; $p \geq 0.326$ for thoracic / lumbar curves respectively).

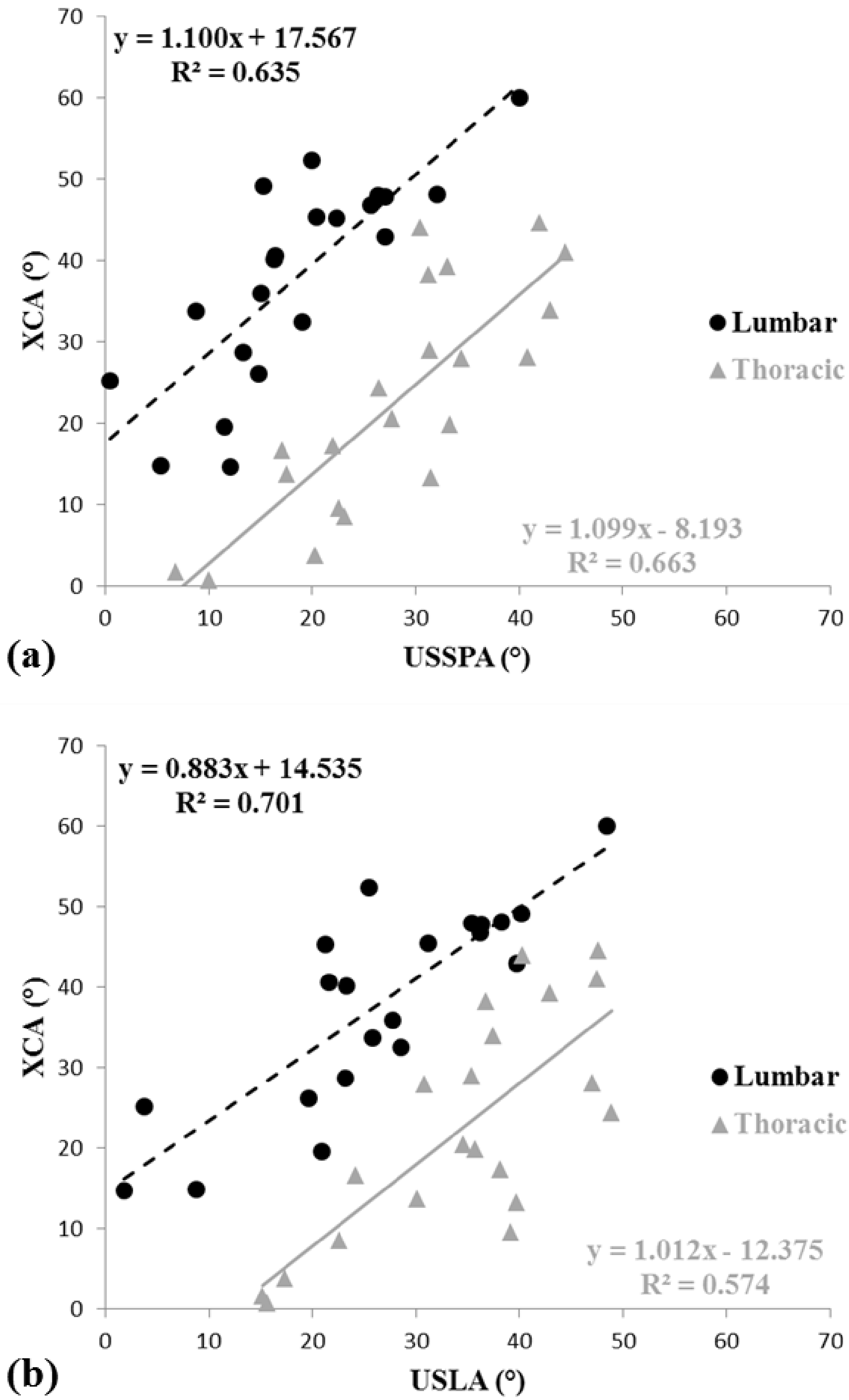

Figure 4.4 *Correlations (R^2) and equations between the X-ray Cobb's angles (XCA) and the two sagittal ultrasound angles based on (a) spinous processes (USSPA) and (b) laminae (USLA), are shown for the thoracic (grey) and lumbar (black) curves.*

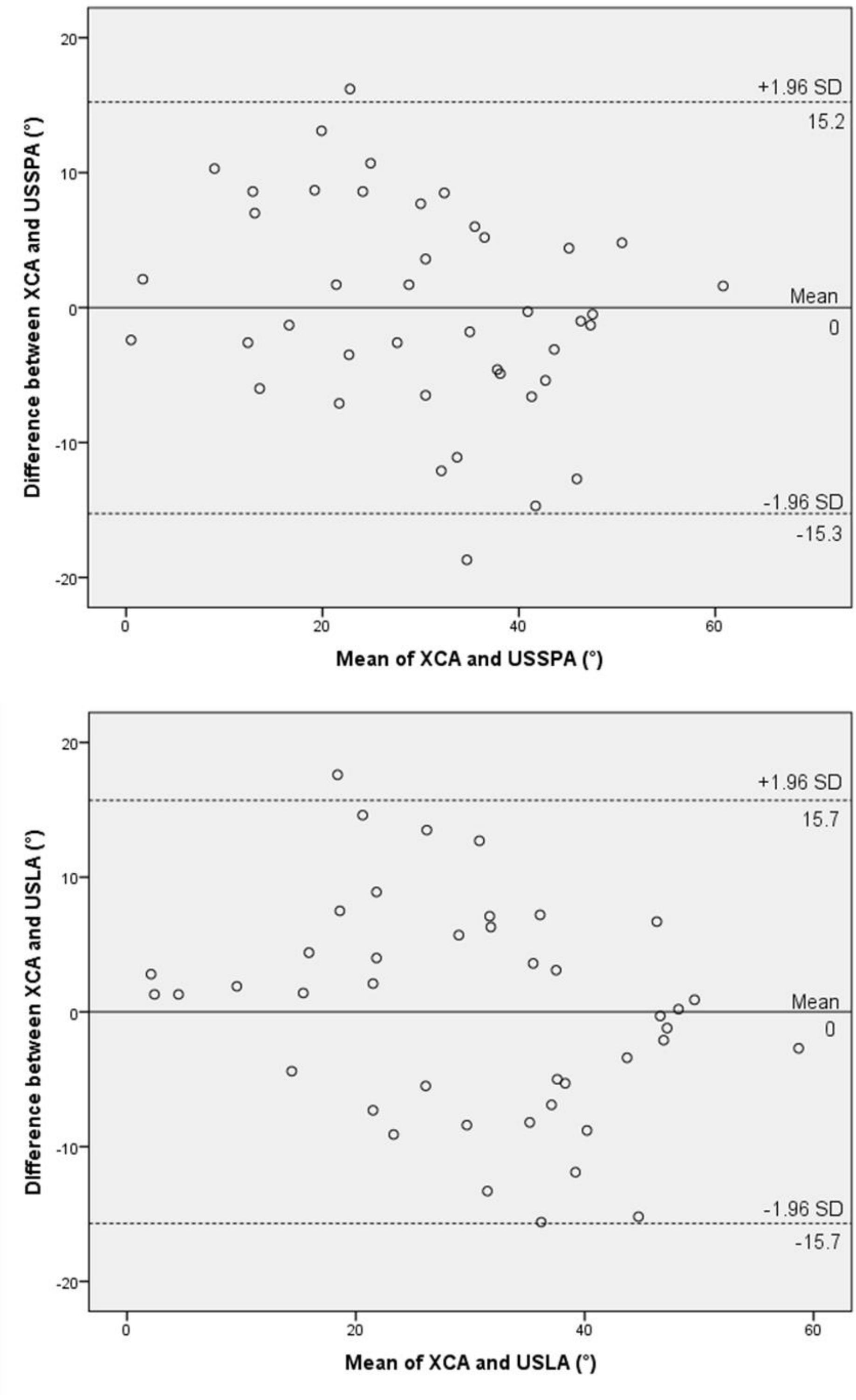

Figure 4.5 *Bland-Altman plots that show the differences between X-ray Cobb's angles (XCA) and the sagittal ultrasound angles corrected with the linear regression equations, including ultrasound spinous process angle (USSPA) and ultrasound laminae angle (USLA). SD: standard deviation*

4.3. Results of Human Subject Study for Coronal-Sagittal Coupling

The correlation and linear regression between SPA and Cobb were shown in Figure 4.6. By substituting Cobb equal to 20º into the regression equation, the corresponding SPA was 17 º.

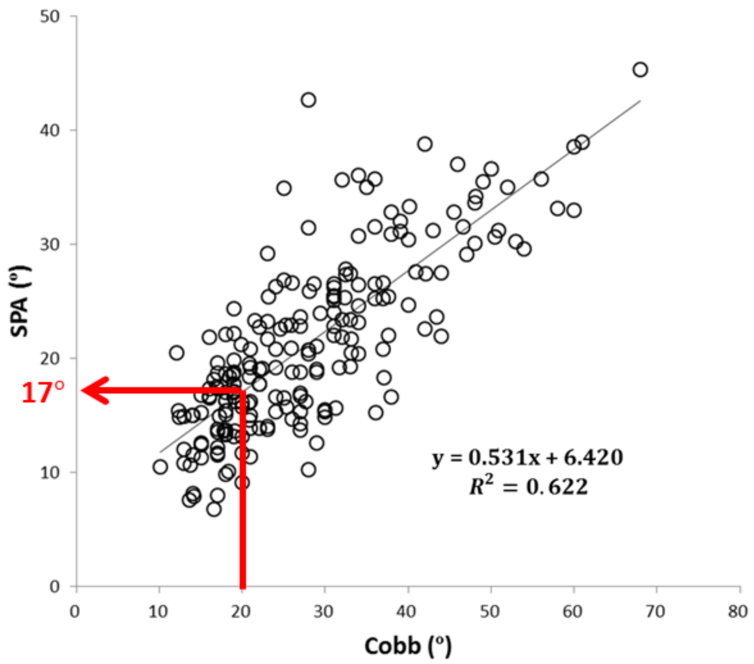

Figure 4.6 *Correlation and linear regression between coronal Cobb and SPA (SPA: Spinous process angle)*

4.3.1. Exploratory Session

The mean age of the subjects was 15.6 ± 3.5 years, with 88 females and 27 males, and the averaged major Cobb angle was 23.2 ± 9.4°. Ultrasound thoracic kyphosis and lumbar lordosis were in average 34.2 ± 10.7° and 27.4 ± 12.3°, while X-ray thoracic kyphosis and lumbar lordosis were in average 25.7 ± 11.6° and 44.8 ± 10.6° respectively. Sagittal ultrasound angles showed moderate to good linear correlations with sagittal Cobb angles for corresponding Cobb ≤ 20º group and all combined cases for all angles (Figure 4.7a and 4.8). Moderate and poor correlations were found between sagittal ultrasound and Cobb angle for 20º < Cobb ≤ 40º group in the thoracic and lumbar angles respectively (Figure 4.7b). All the ultrasound angles were significantly correlated with X-ray Cobb for all angles ($p < 0.001$).

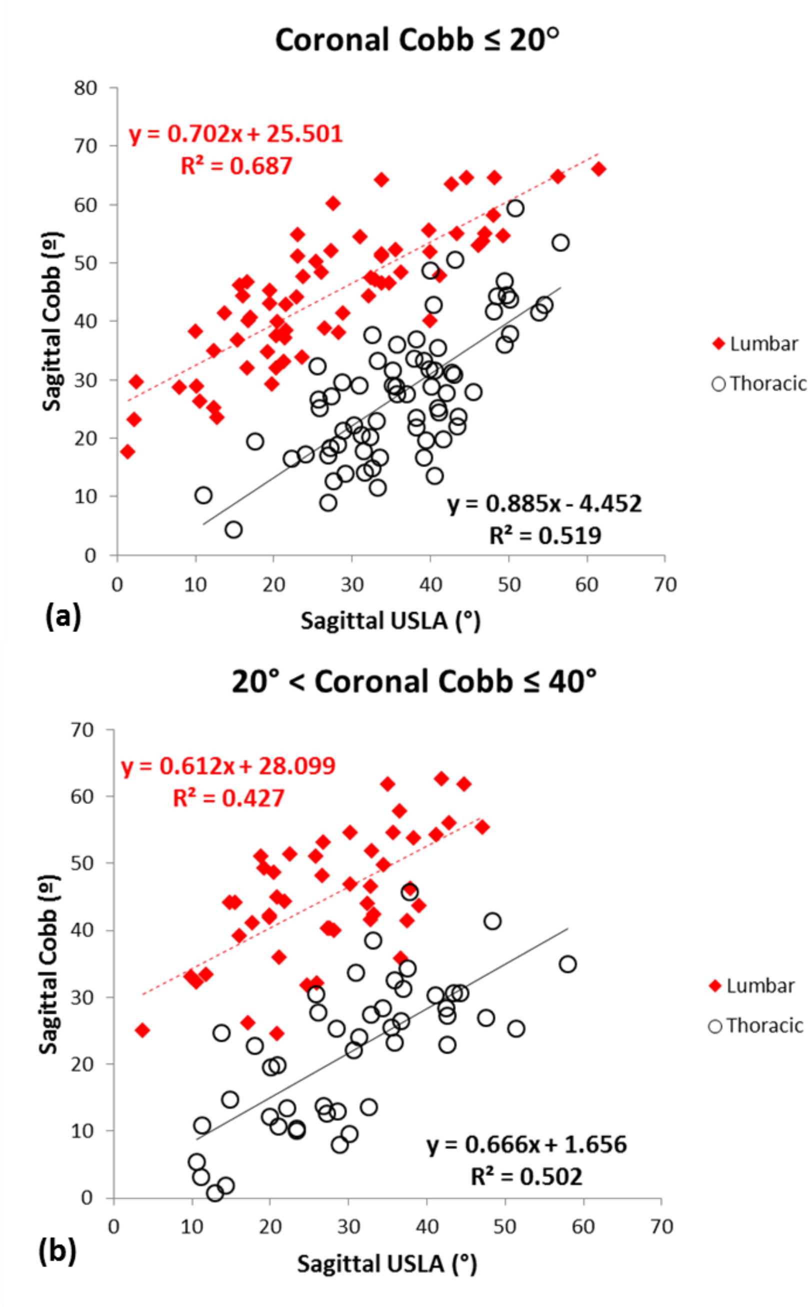

Figure 4.7 *Correlations ($\mathbf{R^2}$) and equations between the sagittal ultrasound angle (USLA) and Cobb angle for subjects with (a) Cobb ≤ 20º and (b) 20º < Cobb ≤ 40º for the thoracic (black) and lumbar (red) curves.*

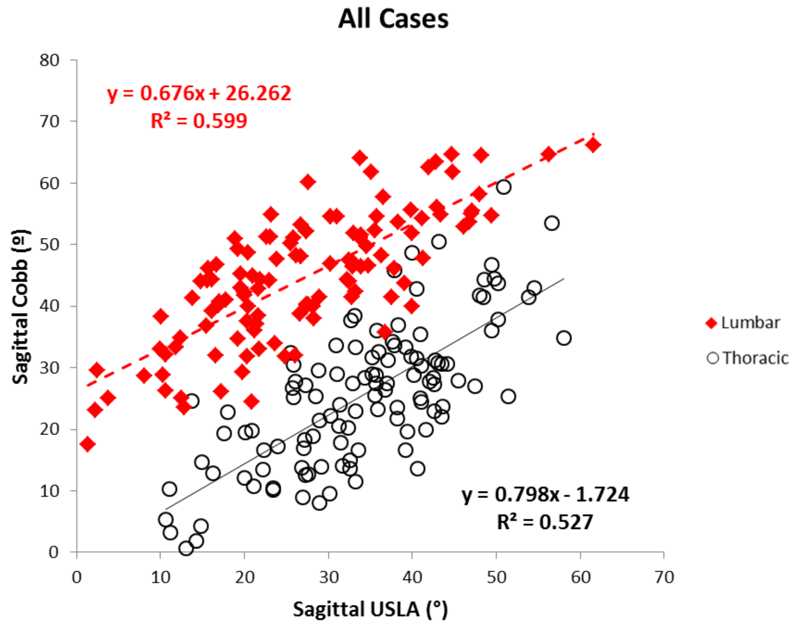

Figure 4.8 *Correlations (* $\mathbf{R^2}$ *) and equations between the sagittal ultrasound angle (USLA) and Cobb angle for all subjects for the thoracic (black) and lumbar (red) curves.*

For the analysis based on cobb classification, thoracic kyphosis obtained from ultrasound and X-ray was significantly larger in main thoracic Cobb ≤ 20º group than that in main thoracic 20º < Cobb ≤ 40º group, but no significant difference of lumbar lordosis was observed between the two main thoracic Cobb group (Table 4.6). No significant difference was observed in the thoracic kyphosis and lumbar lordosis measured by ultrasound and X-ray between the thoraco(lumbar) Cobb groups (Table 4.7). For the analysis based on SPA classification, ultrasound thoracic kyphosis value was also significantly larger in main thoracic SPA ≤ 17º group than that in main thoracic 17º < SPA group, but no significant difference of lumbar lordosis was observed between the two main thoracic SPA groups (Table 4.8). No significant difference was observed from ultrasound lumbar lordosis for both thoraco(lumbar) SPA cases (Table 4.9). Significant correlations (p <0.001) were found between thoracic kypsosis and lumbar lordosis obtained from ultrasound (r = 0.362) and X-ray (r = 0.367). Thoracic kyphosis obtained from ultrasound and X-ray was found to significantly and negatively correlate with ultrasound SPA (r = -0.279) and X-ray main thoracic Cobb (r = -0.322) respectively. However, no significant correlations were observed between ultrasound and X-ray lumbar lordosis with ultrasound SPA (r = 0.174) and X-ray main thoracic Cobb (r = 0.032).

Table 4.6 *Analysis of sagittal parameters according to the main thoracic Cobb angle for ultrasound and X-ray in the exploratory session.*

	Imaging modality	**Main Thoracic Curve**		
		Cobb ≤ 20º	**20º < Cobb ≤ 40º**	***P***
TK (º)	Ultrasound	36.5 ± 9.3	30.2 ± 11.8	***0.004****
	X-ray	27.7 ± 11.4	21.1 ± 11.2	***0.012****
LL (º)	Ultrasound	27.4 ± 13.1	27.5 ± 11.0	0.964
	X-ray	44.5 ± 11.0	45.4 ± 9.9	0.651

The t tests were used to determine the differences between parameters.

**P < 0.05*

TK: Thoracic kyphosis; LL: Lumbar lordosis

Table 4.7 *Analysis of sagittal parameters according to the thoraco(lumbar) Cobb angle for ultrasound and X-ray in the exploratory session.*

	Imaging modality	**Thoraco(lumbar) Curve**		
		Cobb ≤ 20º	**20º < Cobb ≤ 40º**	***P***
TK (º)	Ultrasound	33.6 ± 10.8	35.2 ± 10.5	0.429
	X-ray	26.2 ± 11.6	24.8 ± 11.6	0.533
LL (º)	Ultrasound	27.6 ± 13.7	27.1 ± 10.0	0.797
	X-ray	45.3 ± 11.2	44.2 ± 9.7	0.584

The t tests were used to determine the differences between parameters.

*****P*** *< 0.05*

TK: Thoracic kyphosis; LL: Lumbar lordosis

Table 4.8 *Analysis of sagittal parameters according to the main thoracic SPA angle for ultrasound in the exploratory session.*

Ultrasound	**Main Thoracic Curve**		
	SPA ≤ 17º	**17º < SPA**	***P***
TK (º)	36.6 ± 9.8	29.4 ± 10.7	<***0.001****
LL (º)	26.4 ± 11.9	29.5 ± 12.9	0.201

The t tests were used to determine the differences between parameters.

*****P*** *< 0.05*

TK: Thoracic kyphosis; LL: Lumbar lordosis.

Table 4.9 *Analysis of sagittal parameters according to the thoraco(lumbar) SPA angle for ultrasound in the exploratory session.*

Ultrasound	**Thoraco(lumbar) Curve**		
	SPA ≤ 17º	**17º < SPA**	***P***
TK (º)	35.1 ± 10.5	32.9 ± 10.9	0.287
LL (º)	27.2 ± 12.8	27.7 ± 11.6	0.840

The t tests were used to determine the differences between parameters.

**P < 0.05*

TK: Thoracic kyphosis; LL: Lumbar lordosis.

Thoracic kyphosis and lumbar lordosis measured were all significantly different between ultrasound angle and all three X-ray angles (both p<0.001) (Table 4.10).

Table 4.10 *Sagittal parameters obtained from four different methods and the significance tests for each parameter*

Sagittal Parameters	**Methods Used for Measuring Sagittal angles**				
	USLA	**Cobb**	**PT**	**CPB**	***P***
TK (º)	34.2 ± 10.7	25.6 ± 11.6	28.1 ± 11.2	32.0 ± 11.0	**< 0.001***
LL (º)	27.1 ± 12.1	44.6 ± 10.6	37.6 ± 11.4	33.9 ±10.8	**< 0.001***

The t tests were used to determine the differences between all parameters.

**P < 0.05*

USLA: Ultrasound laminae; PT: Posterior Tangent; CPB: Centre of Posterior Border; TK: Thoracic kyphosis; LL: Lumbar lordosis

4.3.2. Validation Session

The mean age of the subjects was 16.5 ± 3.4 years, with 85 females and 36 males, and the averaged major Cobb angle was 30.5 ± 11.7°. Thoracic kyphosis obtained from ultrasound was significantly larger in main thoracic SPA ≤ 17º group than that in main thoracic 17º < SPA group (Table 4.11). No significant difference was observed in ultrasound lumbar lordosis for both the thoraco(lumbar) SPA groups (Table 4.12). Similar findings were obtained after combining all the subjects' results from the exploratory and validation stage. Thoracic kyphosis was also found to be significantly correlated with lumbar lordosis (r = 0.488) and negatively correlated with ultrasound main thoracic SPA (r = -0.400) (p <0.001). However, no significant correlations were observed between ultrasound lumbar lordosis and ultrasound thorac(lumbar) SPA (r = 0.059).

Table 4.11 *Overall analysis of thoracic kyphosis according to the main thoracic SPA angle for ultrasound in the exploratory and verification sessions.*

Ultrasound	**Stage**	**Main Thoracic Curve**		
		SPA ≤ 17º	**17º < SPA**	***P***
	Exploratory	36.6 ± 9.8	29.4 ± 10.7	**< *0.001****
TK (º)	**Verification**	36.7 ± 7.3	30.4 ± 11.4	**< *0.001****
	Overall	36.6 ± 9.1	30.0 ± 11.2	**< *0.001****

The t tests were used to determine the differences between parameters.

*****P** *< 0.05*

TK: Thoracic kyphosis

Table 4.12 *Overall analysis of lumbar lordosis according to the (thoraco)lumbar SPA angle for ultrasound in the exploratory and verification sessions.*

Ultrasound	**Stage**	**Thoraco(lumbar) Curve**		
		SPA ≤ 17º	**17º < SPA**	***P***
LL (º)	**Exploratory**	27.2 ± 12.8	27.7 ± 11.6	0.840
	Verification	29.9 ± 13.9	32.4 ± 13.6	0.321
	Overall	28.3 ± 13.2	30.7 ± 13.1	0.149

The t tests were used to determine the differences between parameters.

****P*** *< 0.05*

LL: Lumbar lordosis.

Chapter 5. Discussion

5.1. Spine Phantom Study

The reliability of using 3D ultrasound imaging system for the measurement of sagittal spinal curvature was tested and comparisons of the US results with those obtained from traditional X-ray images were made in this study. All the parameters obtained from either X-ray or 3D ultrasound were demonstrated to have excellent reliability. Both USSPA and XSPA were obtained using the spinous process angle. Though the imaging modality was different, the MAD between them was the smallest and the Pearson correlation was the greatest among the three comparisons of the three angles. The difference could be possibly due to the nature of the selection processes of the lateral radiograph and US stack image. Selection of spinous processes was performed from the 2D X-ray image of the spine phantom in the sagittal plane and from the B-mode images of 3D ultrasound volume stack respectively. Thus the perspective difference was one of the major reasons that explained the discrepancies of the results (Vrtovec et al. 2009, Gstoettner et al. 2007). Indeed, a nearly one-to-one relationship was observed between these two parameters, suggesting that they were very much comparable.

Since USSPA was measured using spinous processes and XCA was measured using superior and inferior endplates of the vertebral bodies, lumbar curvatures formed from the spinous processes were likely to be smaller than those measured from vertebrae because the bulky shape of the processes prohibits the lumbar region of the spine phantom for further progression during deformation, while the soft intervertebral structures between the vertebral plates allow larger degrees of deformation. Hence, lumbar USSPA tended to be underestimated compared with

XCA. A study used biplanar radiographs to evaluate the apical thoracic sagittal profile (Hayashi et al. 2009). By comparing the results obtained from the standard lateral projection with those from the "true lateral" view, it was found that the sagittal curvature was significantly greater ($p < 0.001$) in the traditional sagittal view by 10 degrees in average than the "true lateral" view (Hayashi et al. 2009). This suggested that XCA obtained in the study might not be reflecting the 'real' sagittal curvature, but indeed a slightly larger curvature. In addition, the study suggested that the larger the thoracic Cobb's angle in the coronal plane measured, the more kyphotic the thoracic apical profile on the standard lateral radiograph would appear, which would eventually lead to a greater difference in the thoracic apical alignment between the two views (Hayashi et al. 2009). Hence, it is necessary to measure the sagittal spinal curvature using an alternative method instead of using the traditional 2D X-ray projection, and ultrasound could be a potential method for sagittal spinal curvature evaluation.

The Pearson correlations obtained from the phantom study suggested that ultrasound angles in the thoracic regions were more representative than those in the lumbar regions. The differences in the results between the thoracic and lumbar regions might be accounted for the level differences involved for these two regions, where the thoracic vertebrae levels involved to compute the thoracic angle were much more than those for the lumbar angle. Comparison of the mean Cobb values of normal lumbar lordosis in previous studies found out that lesser the vertebral levels involved would likely result in smaller lordosis angle (Stagnara et al. 1982, Fernand and Fox. 1985, Saraste et al. 1985). This effect might be emphasized when using spinous processes for sagittal measurement.

A previous study investigated 39 adolescent girls with double-curved idiopathic scoliosis and reported that the linear relationship between XSPA and XCA was XCA = 0.84*XSPA + 9.63 and XCA = 0.66*XSPA + 33.96 for thoracic and lumbar regions (Delorme et al. 1999), whereas the best-fit equations obtained in our study for XCA against XSPA were XCA = 0.75*XSPA + 12.57 and XCA = 0.42*XSPA + 18.10 for the two regions respectively. Since Pearson correlations obtained in the two studies for both thoracic and lumbar regions were similar and the intra-reliabilities of the measurement in our study were excellent, one of the possible reasons for the discrepancies of the results could be the difference in the calculation of XSPA used in the two studies. However, this could not be confirmed as the calculation details were not described in the previous study (Delorme et al. 1999). In addition, the levels of vertebrae involved for lumbar curvature were different for the parameters, where L1-L4 levels were used for XCA while T12-L4 levels were used for XSPA and USSPA. The reason for such a selection was that we noted the spinous process of T12 (instead of L1) is more aligned with the upper plate of L1, and that of L4 is more aligned with the lower plate of L4. Furthermore, only a single point was selected to represent the spinous process of all vertebrae from T2 to L4 in ultrasound images in this study. However, the spinous process is not a single point, and selection of different locations of the same spinous process may induce variations in curvature measurement.

3D ultrasound imaging, supported by the phantom data, is a potential imaging modality for screening and monitoring the development of individual's sagittal spine profile. It should be always noted that ultrasound and X-ray measurements were based on different structures of the vertebrae, thus it was reasonable that the results of these two modalities did not represent each other. The excellent intra-operator reliability for ultrasound scanning on phantoms as well as excellent intra- and inter-rater reliabilities for angle measurement obtained in this study demonstrated that 3D ultrasound could be used for evaluating sagittal profile on spine phantom. However, water was used as the tissue mimicking background, hence the image quality of ultrasound would be another story when human subjects were being scanned. In addition, for the phantom tests reported in this study, the phantom was fixed thus had no motion, whereas in real subject tests, the subject would likely move forward and backward to change the spinal sagittal profile during the ultrasound scanning. Hence in the following human subjects study, the subject would be stabilized during scanning as introduced by Zheng et al. (2016) for their coronal curvature study. Furthermore, the reliability and validity of ultrasound on sagittal spinal curvature measurement with different deformity curvatures and patterns were conducted in the human subjects test for evaluation of the ultrasound system.

5.2. Human Subjects Study

Traditionally sagittal curvature of spine is evaluated by radiographic Cobb angle, which necessitates ionizing radiation to form the images. Alternative imaging modalities have been suggested to minimize or avoid the radiation issue. Bi-planar stereoradiography utilizes lower dosage of radiation, but it is expensive and not readily available to most medical practitioners. Ultrasound imaging is non-ionizing and relatively cheap. During ultrasound scanning, subjects are maintained in the upright posture, the same as that adopted during traditional radiographic examination thereby providing a real alternative to erect x-ray images. Previous studies have investigated the possibility of ultrasound for assessing the coronal spine curvature, and to the best of our knowledge, the present paper is the first to report the reliability and validity of different sagittal ultrasound angle measurements. Excellent intra- and inter-rater reliabilities were demonstrated for ultrasound sagittal angle measurement, and good to moderate linear correlations were obtained between the ultrasound angles and Cobb angles. The average MAD of the ultrasound measurements was about 6.3°, without significant difference in the different ultrasound measurements. The MADs were higher in the thoracic region for both the ultrasound methods. This is not surprising since spinous processes and laminae in the lower regions of the spine can be identified more easily than the upper regions, which leads to smaller errors during measurement.

The sagittal ultrasound angles obtained were larger in the thoracic curves and smaller in the lumbar curves as compared with their corresponding sagittal radiographic Cobb angles. There were several possible reasons for the discrepancies: 1) The ultrasound measurements were based on SP and bilateral laminae, which are structures located more posteriorly than the vertebral body and where Cobb angle was measured (Brink et al. 2018). Differences in structures used for measurements thus will possibly lead to a different projection of the 3D deformity (Herzenberg et al. 1990). In addition, it has been found that measurements based on posterior vertebral structures would cause the angular value differences (Chernukha et al. 1998); 2) Different positions of arms were adopted for different imaging modalities, where patients were in a relaxed standing posture with arms relaxed at the sides and fists overlying ipsilateral clavicles were adopted for ultrasound and X-ray scanning respectively (Pasha et al. 2016). A decrease in kyphosis and an increase in lordosis were observed when patients adopted the fists overlying ipsilateral clavicles position compared to relaxed standing (Marks et al. 2009); 3) Different levels of vertebrae were involved for X-ray and ultrasound assessments due to different measurement techniques. T3 was involved for the ultrasound measurement, which may possibly lead to the larger value in the thoracic ultrasound angle. We should bear in mind that using traditional Cobb angles alone would not be sufficient to comprehensively study the complex 3D deformity. In addition, sagittal ultrasound images formed in this study were based on the projection of the SP or bilateral laminae selected in the 3D ultrasound volume. This reflected a real sagittal profile of the scoliotic spine rather than the projection on lateral radiographs which was potentially influenced by vertebral rotation and magnitude of deformity. Traditional sagittal Cobb measurements of the thoracic spine in lateral radiographs were found larger than those obtained from 3D view on patients with scoliosis due to axial vertebral rotation (Newton et al. 2015), but in this study the finding was the opposite.

We observed that sagittal curvature analysis using ultrasound required a higher demand on scanning and image quality control in comparison with coronal curvature analysis. Hence additional attention should be paid in the future during scanning, such as using lower frequencies ultrasound for patients with a lumbar curve in order to capture the vertebral structures since they are deeper from the skin surface. Patients with Cobb angles larger than 50 degrees were excluded in this study since spinal sagittal measurement might be prone to measurement error due to the presence of severe rotation (Bao et al. 2018). Spinous processes in the ultrasound images of some patients were deformed for very thin patients due to the protruded scanning trajectories when their backs were being scanned, thus the spinous processes acquired in the ultrasound images were not suitable to compile the USSPA. However, the laminae would not be affected by the above issue, thus the USLA could be used for these types of patients. And since the MADs of the two ultrasound angles were not significantly different, USLA was used in the human subjects study for coronal-sagittal coupling.

5.3. Human Subjects Study for Coronal-Sagittal Coupling

Only the laminae angle was used for evaluating the ultrasound angle in this session. One of the reasons was that spinous processes might not be a good parameter for evaluating scoliotic spine. Since vertebral rotation is likely to exist in deformed spines, it would cause spinous process deviations. The spinous processes increasingly deviate to the concave side during the rotation progression and the ribs also follow the rotation of the vertebrae (Middleditch et al. 2005). Such deviation could lead to developmental asymmetries of the neural arch, rotation of entire vertebra, and isolated deviation (Van Schaik et al. 1989), causing confusion when interpreting the PA radiographs of spine and imitating vertebral body malalignment (Mellado et al.2011a; 2011b). Moreover, since bracing and surgical treatment will be suggested for skeletally immature AIS patients once their major Cobb angles reach 20° and 40° respectively, and thoracic kyphosis of patients with Cobb smaller than 20° was found to be larger than those having Cobb angles from 20° to 40° (Hong et al. 2017), 20° and 40° were set as the border criteria for the sagittal analysis in this study. In addition, for patients with Cobb larger than 40°, the evaluation of the sagittal curvature would be highly affected by the coronal deformity and vertebral rotation, especially for radiograph, hence these patients were not included in this study. Furthermore, T3 was set to be the upper boundary as features of T1 and T2 vertebrae could hardly be observed in the US images, similar to the findings of Young et al. (2015).

Correlation between the thoracic kyphosis measurements by ultrasound and X-ray was higher in the smaller Cobb group than the larger Cobb group, while the correlation between the lumbar lordosis measurements by the two methods was similar for both groups. This suggested that the magnitude of the thoracic curves had a larger effect on causing discrepancies between ultrasound and X-ray than the lumbar curves. The discrepancies could also be accounted for the larger vertebrae rotation of patients with AIS with larger Cobb (White et al. 1978, Villemure et al. 2001, Gum et al. 2007), as rotation in the laminae was found to be greater than that in the vertebral body using CT scans (Suzuki et al 1989). Hayashi et al. (2009) found that the mean apical thoracic sagittal curvature was significantly larger in the standard lateral view than that in the "true lateral" view by an average of 10 degrees, and the magnitude of the thoracic Cobb was also found to be significantly correlated with the thoracic apical sagittal kyphosis in standard lateral view but not in the "true lateral" view. This may suggest that the thoracic apical profile may appear to be more kyphotic on the 2D imaging for patients with larger coronal deformity. Hence in this study, the spinal sagittal profile of patients with large coronal deformation was not investigated as the clinical implications for sagittal profile of severely deformed spine were not significant. In future study, 3D ultrasound analysis would be needed for severe scoliosis cases in order to attain the realistic spinal deformation information (Hayashi et al. 2009).

Patients with larger curve deformity in the main thoracic region were found to be significantly hypokyphotic, but no significant differences were observed in terms of lumbar lordosis among subjects with different lumbar curve deformity, based on the data analysis from either ultrasound or X-ray. This suggested that most of the cases being analyzed had similar behaviour to the case illustrated in Figure A.1, where patients with smaller thoracic deformation had a larger thoracic kyphosis. These findings were similar as those reported in previous studies (Schmitz et al. 2001, De jonge et al. 2002, Thiong et al. 2013, Hong et al. 2017, Ilharreborde et al. 2018). Schlösser et al. (2014) and Janssen et al. (2011) demonstrated that patients with mild thoracic scoliosis had a significantly less kyphotic spine, but those with mild lumbar scoliosis were found to have significantly larger lumbar lordosis compared with the thoracic kyphosis and control subjects. The discrepancies of the findings may be due to the differences of the curve natures of the subjects with AIS involved. Patients with only either thoracic or lumbar curve were invited in their studies, whereas patients with mixed curves were involved in our study. In addition, a negative correlation was revealed between thoracic kyphosis and the thoracic coronal deformation, which was also demonstrated in Schmitz et al.'s study (2001). However, such significant correlation was not shown in the study of Hong et al. (2017). It should be noted that Cobb angle measurement was not categorized when evaluating correlation with thoracic kyphosis and lumbar lordosis.

Patients with larger thoracic curve appeared to be relatively hypokyphotic in radiographic evaluation, and ultrasound was demonstrated to be effective in detecting similar findings in this study. However, it should be noted that sagittal angles measured by ultrasound were larger than those measured by X-ray. The absolute differences between the ultrasound and X-ray measurements decreased from the Cobb method to PT method, and from PT method to CPB method. The mean and SD of the absolute difference between ultrasound laminae angle and central of posterior border angle was 5.8 ± 4.3º and 7.3 ± 5.0º, respectively. The result showed that the discrepancies between ultrasound laminae angle and Cobb angle were caused by the differences of the measurement techniques and the anatomical landmarks chosen for the two modalities. In addition, average inclination between T3 and T4 on radiograph of chronic LBP patients was found to be 4.8º (Harrison et al. 2001), which may potentially lead to the thoracic lyphosis value differences obtained between ultrasound and X-ray since T3 level was involved for ultrasound measurement. A study reported a method similar to the posterior tangent method, the tangential radiologic assessment, for the measurement of lumbar lordosis. The angle measured was found to be 8º to 16º smaller than that by Cobb method (Chernukha et al. 1998). However, it was claimed to be a more reliable method than Cobb for scoliosis measurement since it was not subject to variation in vertebral body contour. Furthermore, the distance between T12 and L5 was too small for lumbar curvature measurement using posterior elements of the vertebrae, hence the curvature measurement would not be representative to radiologic lordosis (Leroux et al. 2000). In future study, S1 might be considered for the evaluation of lumbar lordosis using ultrasound and thus the ultrasound scanning could be started in a more inferior position in order to capture the laminae of S1.

Patients with progressive AIS diagnosed were found to possess significant hypokyphosis by a mean of 4.2º compared to the non-progressive AIS patients (Nault et al. 2014). In addition, increasing severity of major thoracic curve in AIS patients was found to be associated with a progressive loss of thoracic kyphosis (Sullivan et al. 2017). However, such phenomenon could not be proved in this study as randomized controlled cases. A longitudinal study should be carried out on patients with AIS using ultrasound during the first and follow-up visits to investigate whether there is a change between sagittal profiles of the patients and curve progression. The average thoracic kyphosis of AIS patients with thoracic SPA larger than 17 degrees was 36.6 degrees, in both exploratory and validation studies, hence such value could be used as reference in future progression study to investigate whether the initial value of thoracic kyphosis would affect the curve progression in the thoracic region. Spinal ligaments and paravertebral muscles also played an important role in maintaining spinal stability (Kouwenhoven et al. 2008), hence in future study, the correlation between morphologic differences of the spinal muscles and different curve severity could be studied in patients with AIS using ultrasound. Quantifying either spinal curvatures different planes or vertebrae rotation is useful for planning surgery, predicting prognosis and monitoring curve progression (Vrtovec et al.2009, Carlson et al. 2013, Cheung et al. 2013).

It should be noted that ultrasound examination cannot replace the X-ray examination for the evaluation of sagittal spinal curvatures during the diagnosis and annual evaluation of progression. The reliability of sagittal measurement using ultrasound as shown in this study suggested that 3D ultrasound imaging could be a non-ionizing tool to evaluate the sagittal profile of patients with AIS and to give an ultrasound standard of optimal sagittal curvature. 3D ultrasound imaging could also be used to provide a more frequent ultrasound spinal examination for follow-ups, such as monitoring the sagittal thoracic and lumbar curvature, together with coronal curves, to assess the effectiveness of various therapies, which generally can not be done in clinical routine as sagittal X-ray images are not commonly evaluated and are not available in clinics with EOS.

Chapter 6. Conclusion and Future Works

In this thesis, the feasibility and validity of using a non-radiation free-hand 3D ultrasound imaging system for assessing sagittal spinal curvature of a scoliotic spine, together with a customized 3D program, which is compatible to the 3D ultrasound volume, have been investigated. Ultrasound was demonstrated to be reliable and valid for evaluating sagittal curvature of spine, on both spine phantoms and human subjects, in the presence of different ranges of coronal Cobb angle. Ultrasound sagittal curvatures were evaluated using spinous processes and bilateral laminae, which are different vertebral structures compared to those used in traditional Cobb method. Good correlations were obtained between the sagittal curvatures acquired by the two imaging modalities and no significant differences were found between the results obtained using the two different landmarks. Further studies on the patients with AIS using ultrasound suggested that the laminae method should be a more reliable method as the laminae appeared to be clearer in B-mode images, which could avoid unnecessary exclusion of patients due to poor scanning quality. This study was the first to report the feasibility of using ultrasound to assess the sagittal curvature of human spine, based on structures that were different from the traditional Cobb method. Indeed, the ultrasound angles obtained in this study could possibly be more relevant to the real sagittal contour, since the coronal coupling effect would affect the traditional radiographic Cobb measurement on plane radiograph. Therefore, the results indicated that ultrasound using the laminae method might provide a potential clinical tool for assessing and monitoring sagittal curvature of patients with AIS.

This thesis has proposed using USLA for evaluating sagittal spinal parameters of patients with AIS. In future studies, the author will investigate the following issues:

1) The effect of sagittal parameters on the progression of different coronal curves of patients with AIS. Figures 6.1 and 6.2 show the coronal and sagittal ultrasound images of two patients with double-curve AIS acquired during their first and second visit with different degrees of thoracic kyphosis. The images demonstrated that relatively smaller thoracic kyphosis could lead to a larger thoracic curve progression on the coronal plane.

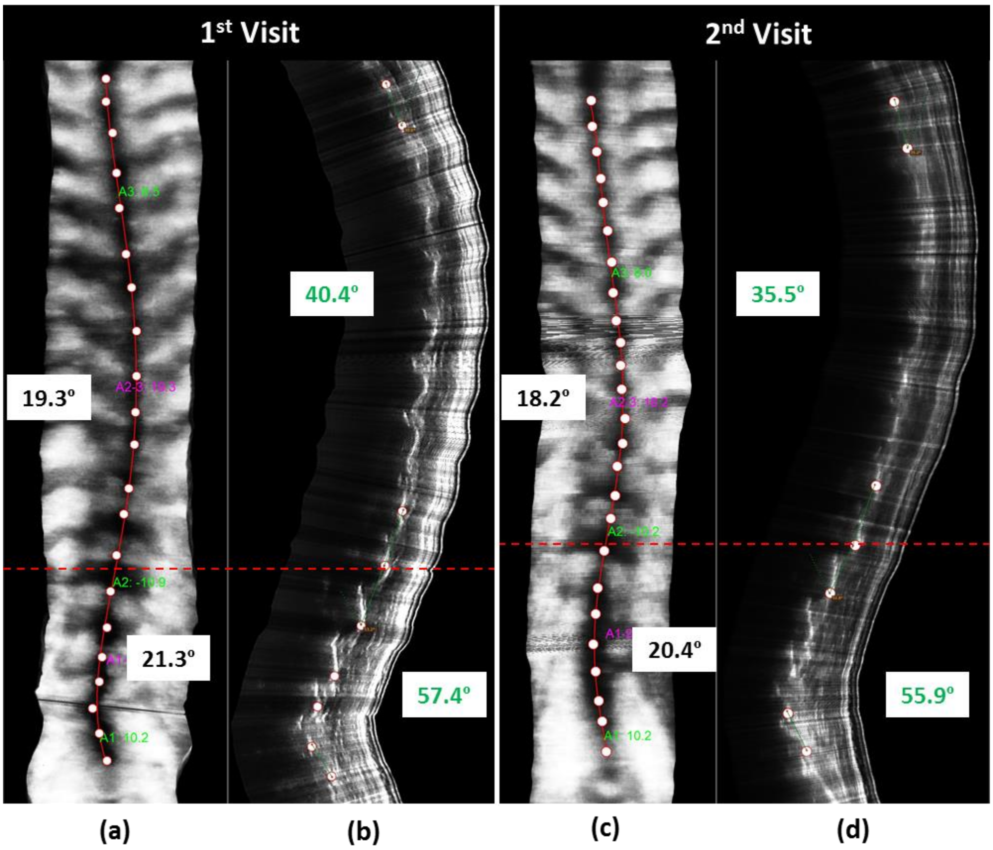

Figure 6.1 *The coronal and sagittal images of a patient with double-curve AIS and relatively larger value of thoracic kyphosis during their first (a and b) and second visit (c and d) respectively. The coronal SPA angles were illustrated in black and the thoracic kyphosis and lumbar lordosis were illustrated in green.*

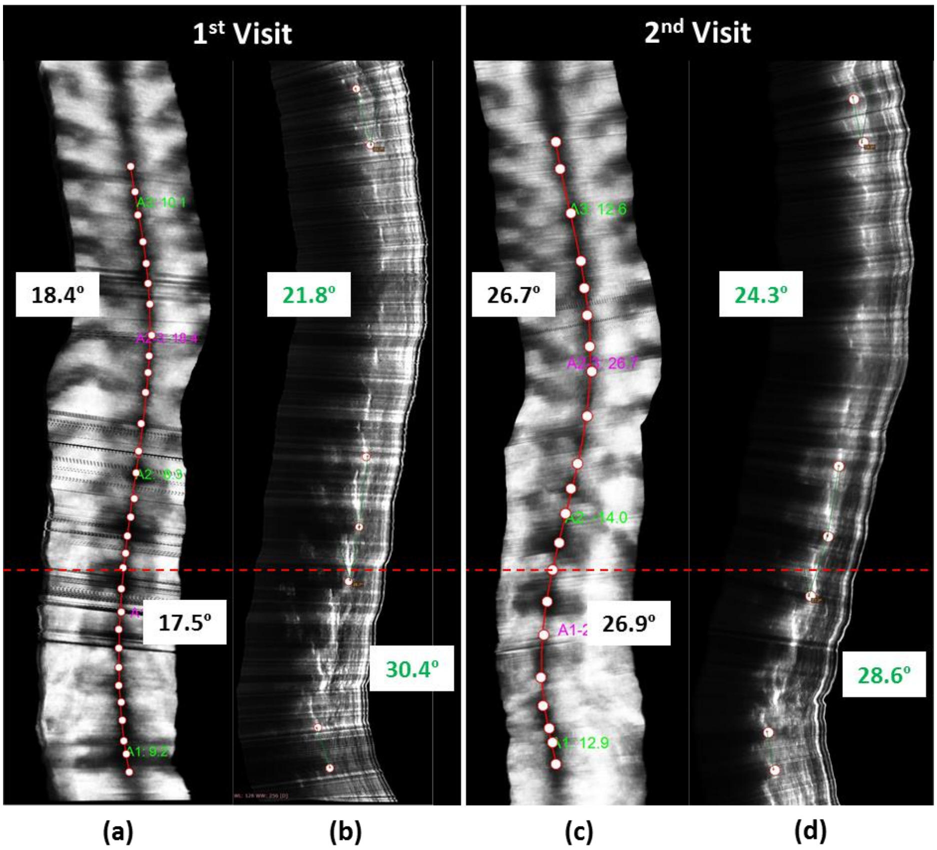

Figure 6.2 *The coronal and sagittal images of a patient with double-curve AIS and relatively smaller value of thoracic kyphosis during the first (a and b) and second visit (c and d) respectively. The coronal SPA angles were illustrated in black and the thoracic kyphosis and lumbar lordosis were illustrated in green.*

2) The 3D alternation of the scoliotic spine during progression, i.e. how the sagittal profile of the spine changes during curve progression.

3) The effect of different positions of arms on sagittal curvature during scanning.

Appendices

A.1. Figures

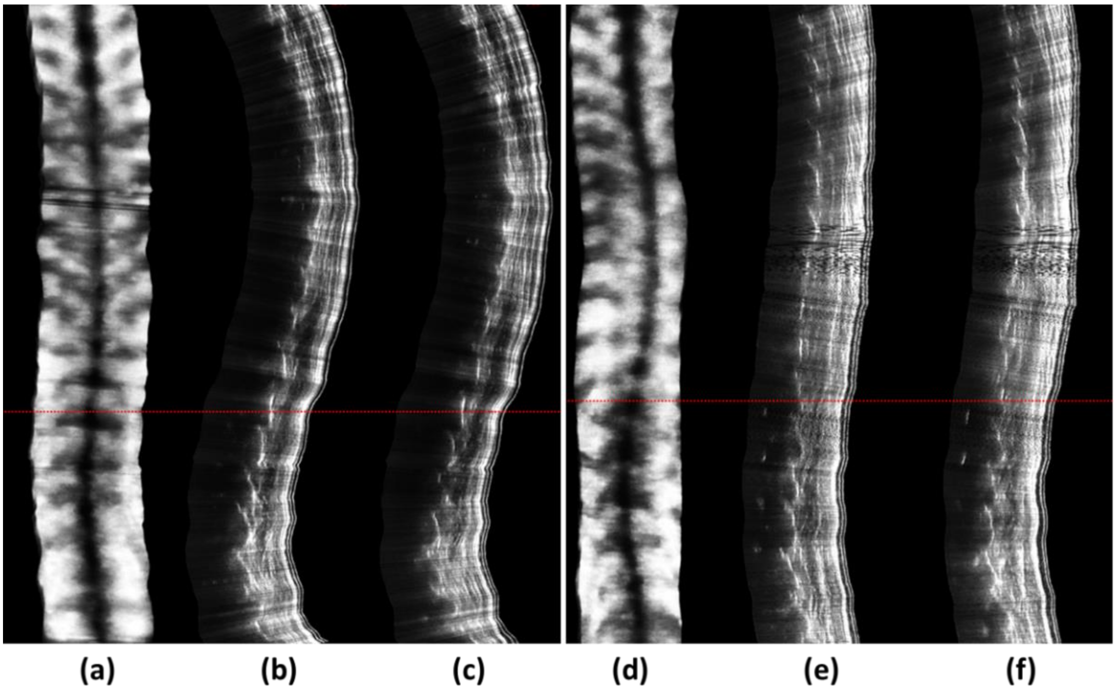

Figure A.1 *The three images on the left were the coronal (a) and sagittal ultrasound images illustrating the left (b) and right (c) laminae of an AIS patient with a single thoracic Cobb less than 20º, whereas the three images on the right were the coronal (d) and sagittal ultrasound images illustrating the left (e) and right (f) laminae of an AIS patient with a single thoracic Cobb larger than 20º. The red line indicates the T12 vertebrae level.*

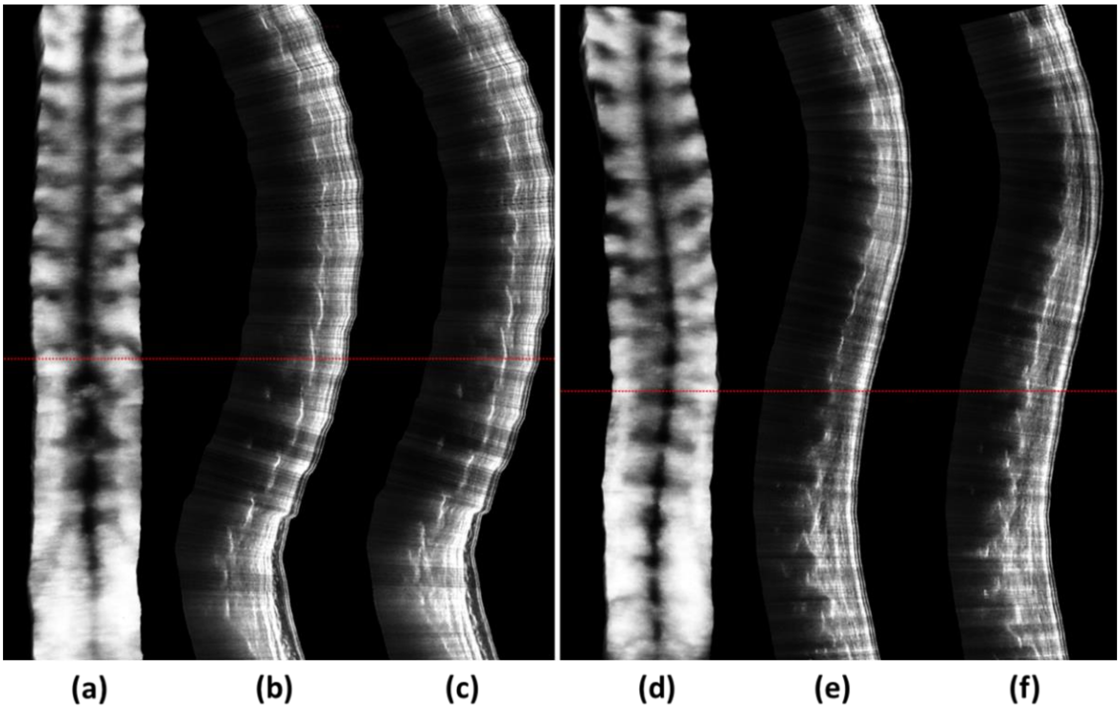

Figure A.2 *The three images on the left were the coronal (a) and sagittal ultrasound images illustrating the left (b) and right (c) laminae of an AIS patient with a single thoracolumbar Cobb less than 20º, whereas the three images on the right were the coronal (d) and sagittal ultrasound images illustrating the left (e) and right (f) laminae of an AIS patient with a single thoracolumbar Cobb larger than 20º. The red line indicates the T12 vertebrae level.*

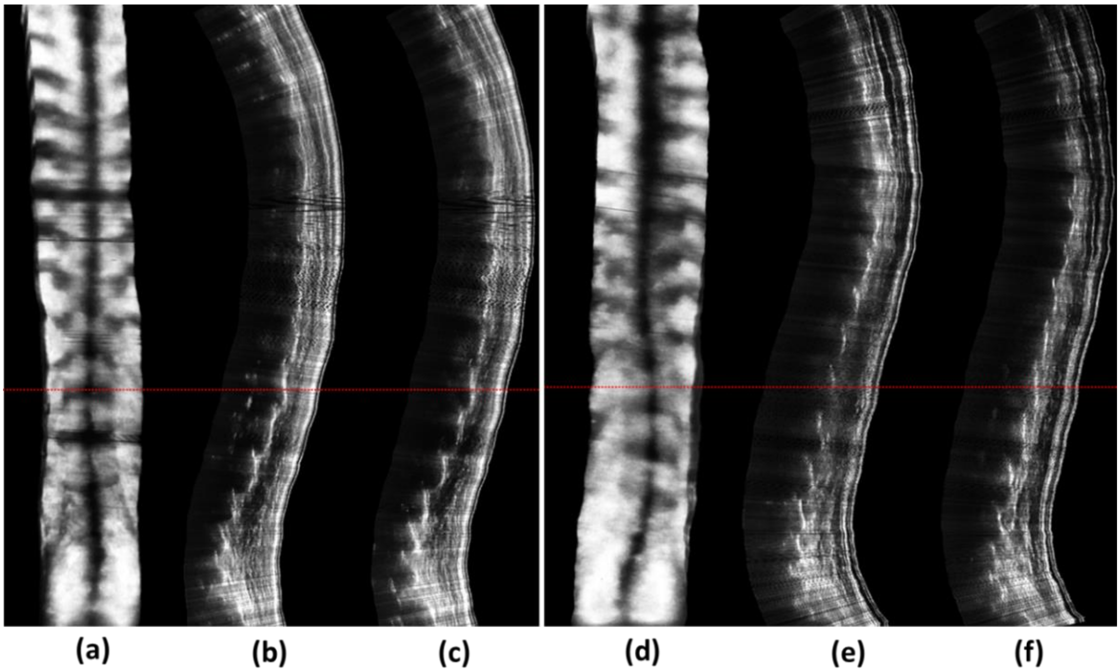

Figure A.3 *The three images on the left were the coronal (a) and sagittal ultrasound images illustrating the left (b) and right (c) laminae of an AIS patient with a single lumbar Cobb less than 20º, whereas the three images on the right were the coronal (d) and sagittal ultrasound images illustrating the left (e) and right (f) laminae of an AIS patient with a single lumbar Cobb larger than 20º. The red line indicates the T12 vertebrae level.*

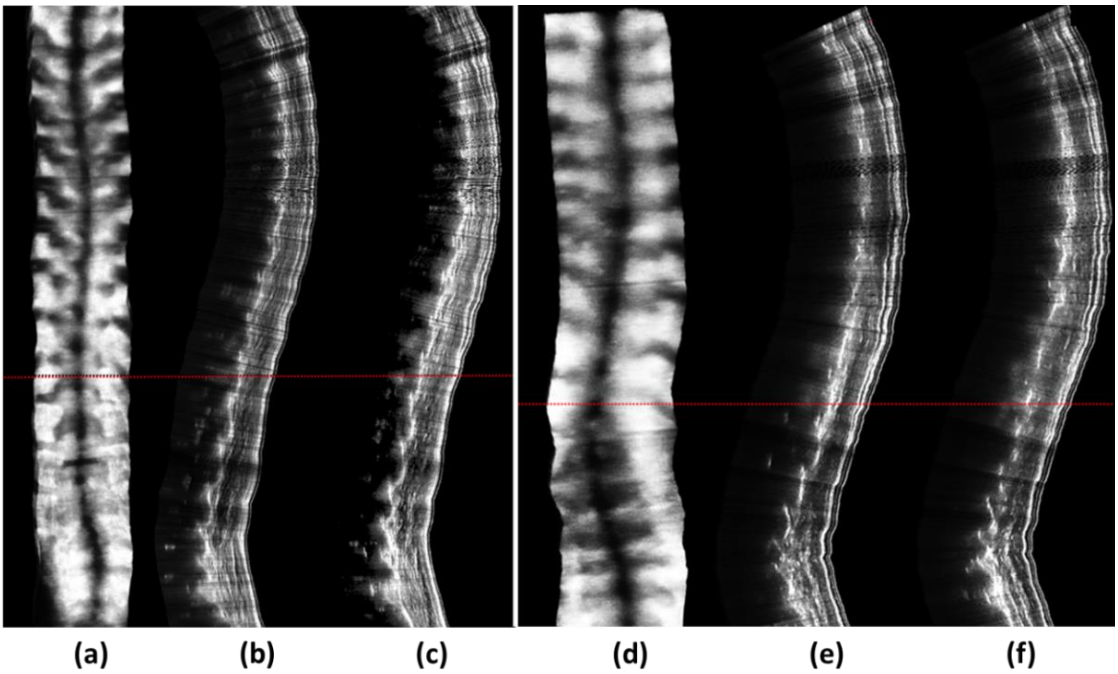

Figure A.4 *The three images on the left were the coronal (a) and sagittal ultrasound images illustrating the left (b) and right (c) laminae of an AIS patient with both thoracic and lumbar Cobb less than 20º, whereas the three images on the right were the coronal (d) and sagittal ultrasound images illustrating the left (e) and right (f) laminae of an AIS patient with both thoracic and lumbar Cobb larger than 20º. The red line indicates the T12 vertebrae level.*

A.2. Data Table

Table A.1 *X-ray Cobb angle of the thoracic and lumbar region measured from the four phantoms of four different curvatures by rater B and rater C.*

	XCA (º)					
	Rater B				Rater C	
	TK		LL		TK	LL
Measurement	1st	2nd	1st	2nd	1st	2nd
Phantom1A	19.2	20.5	31.2	33.3	21.2	30.2
Phantom2A	31.3	35.1	26.5	26.6	32.5	28.3
Phantom3A	20.5	15.4	25.2	24.6	20.5	25.5
Phantom4A	20.0	20.5	25.3	25.4	27.7	26.2
Phantom1B	22.0	25.4	35.3	40.1	27.7	36.4
Phantom2B	20.8	20.2	22.1	22.2	22.8	24.6
Phantom3B	30.1	31.8	21.5	20.3	28.6	23.1
Phantom4B	28.2	30.4	23.1	22.2	29.9	22.3
Phantom1C	42.1	46.2	30.2	34.8	40.5	31.1
Phantom2C	43.4	42.7	36.2	35.2	45.1	33.0
Phantom3C	40.5	40.0	29.6	32.8	41.8	31.5
Phantom4C	46.7	46.1	35.4	35.1	49.2	36.5
Phantom1D	28.5	30.0	31.1	34.2	32.1	35.3
Phantom2D	32.5	35.6	34.2	30.4	32.4	30.0
Phantom3D	34.5	35.6	34.1	32.6	35.9	37.4
Phantom4D	33.4	34.5	26.2	25.3	35.6	19.6

XCA: X-ray Cobb angle; TK: thoracic kyphosis; LL: lumbar lordosis

Table A.2 *X-ray spinous process angle of the thoracic and lumbar region measured from the four phantoms of four different curvatures by rater B and rater C.*

	XSPA (º)					
	Rater B				Rater C	
	TK		LL		TK	LL
Measurement	1st	2nd	1st	2nd	1st	2nd
Phantom1A	18.8	18.1	21.4	21.1	17.4	18.3
Phantom2A	23.5	23.2	21.2	22.9	23.2	22.3
Phantom3A	9.9	9.0	27.8	27.8	9.2	26.7
Phantom4A	4.0	3.8	24.7	24.3	3.8	24.1
Phantom1B	21.7	21.1	31.8	30.6	21	30.9
Phantom2B	20.8	19.3	24.7	23.5	18.8	23.5
Phantom3B	15.7	16.3	18.2	17.4	17.1	17.4
Phantom4B	12.9	13.7	12.0	12.1	8.1	9.1
Phantom1C	36.8	36.1	16.7	18.9	35.9	19.3
Phantom2C	31.2	31.9	37.2	39.0	32.2	38.8
Phantom3C	33.8	33.3	29.0	28.8	33.8	28.9
Phantom4C	36.9	36.9	34.6	36.3	37.2	36.6
Phantom1D	28.3	28.2	26.5	26.5	28.9	26.8
Phantom2D	29.0	29.3	34.2	34.8	28.5	34.2
Phantom3D	29.0	28.3	39.5	39.9	28.8	40.7
Phantom4D	30.0	29.7	11.1	14.3	30.0	12.9

XSPA: X-ray spinous process angle; TK: thoracic kyphosis; LL: lumbar lordosis

Table A.3 *Ultrasound spinous process angle of the thoracic and lumbar region measured from the four phantoms of four different curvatures by rater B and rater C.*

	USSPA(º)									
	Rater B						Rater C			
	TK			LL			TK		LL	
Scan	1st		2nd	1st		2nd	1st		1st	
Measurement	1st	2nd	1st	1st	2nd	1st	1st	2nd	1st	2nd
Phantom1A	15.6	17.2	16.9	13.5	13.8	12.8	17.3	14.0	21.6	11.3
Phantom2A	22.6	21.4	22.1	23.4	21.0	22.7	23.2	22.2	23.2	17.5
Phantom3A	12.8	11.1	12.5	29.4	26.9	29.0	10.1	11.2	27.2	28.9
Phantom4A	5.5	7.1	7.7	28.0	31.9	28.2	6.2	6.4	29.4	25.1
Phantom1B	25.0	26.7	27.1	31.4	34.5	33.2	22.6	23.2	28.9	32.1
Phantom2B	21.5	20.2	19.6	29.3	28.2	27.2	21.4	19.7	28.1	24.4
Phantom3B	23.0	20.1	18.8	21.8	13.5	19.9	21.0	19.6	19.6	16.5
Phantom4B	21.2	18.4	22.7	14.0	15.2	17.1	16.9	18.3	14.1	12.5
Phantom1C	36.9	34.3	37.3	7.6	17.3	8.0	37.5	35.9	17.4	10.9
Phantom2C	31.2	34.8	31.1	41.3	40.3	39.2	32.0	33.9	40.5	39.9
Phantom3C	34.5	33.9	34.7	25.3	26.0	26.0	34.0	33.0	24.0	26.0
Phantom4C	35.2	37.3	36.6	35.0	37.1	36.6	36.7	37.6	30.6	28.8
Phantom1D	28.2	27.0	28.5	25.7	19.9	25.7	28.3	29.3	25.8	22.1
Phantom2D	32.0	32.6	32.5	38.8	39.0	37.8	32.6	32.8	34.5	37.9
Phantom3D	30.8	31.4	31.3	40.8	41.2	41.2	30.5	31.3	44.1	41.3
Phantom4D	33.4	31.6	33.5	19.2	22.8	21.0	31.4	31.7	15.9	20.3

USSPA: Ultrasound spinous process angle; TK: thoracic kyphosis; LL: lumbar lordosis

Table A.4 *Ultrasound spinous process angle of the thoracic and lumbar region measured from the patients of the human subject study by rater 1 and rater 2.*

		USSPA (º)							
		Rater 1				Rater 2			
	Measurement	1st		2nd		1st		2nd	
	Angle	TK	LL	TK	LL	TK	LL	TK	LL
Patients	1	27.7	27.0	27.8	24.3	23.8	29.7	28.3	32.6
	2	30.5	32.1	29.7	35.0	31.3	35.2	28.0	34.2
	3	31.4	20.4	28.1	21.0	29.6	15.6	31.5	21.5
	4	22.0	11.5	20.6	14.3	24.0	14.4	24.2	16.7
	5	44.5	40.0	45.1	37.2	45.6	35.8	49.4	31.1
	6	31.5	20.0	32.6	18.9	35.2	22.9	35.6	18.3
	7	43.0	0.5	41.3	0.6	34.6	3.1	37.4	0.4
	8	17.1	14.8	19.0	13.6	18.9	15.1	25.8	16.3
	9	22.6	22.3	25.1	23.3	26.7	20.9	27.2	24.9
	10	40.8	13.4	37.3	17.1	39.5	11.0	35.3	19.4
	11	31.2	16.4	27.8	12.3	26.3	15.0	29.4	20.9
	12	6.8	12.1	8.3	8.0	8.3	12.0	12.8	10.0
	13	20.3	19.0	20.4	19.7	16.7	24.1	21.7	21.8
	14	26.5	26.4	24.3	28.9	28.7	24.5	29.6	28.5
	15	42.0	15.3	42.8	11.0	44.0	13.9	43.9	12.4
	16	10.0	5.4	8.7	7.1	7.8	9.5	5.4	7.5
	17	34.4	15.0	32.7	16.4	37.4	21.3	30.5	20.2
	18	23.1	8.8	23.5	10.8	20.2	5.4	28.0	8.6
	19	17.6	16.3	19.8	13.2	22.1	15.5	19.7	17.7

20	33.1	27.0	32.9	26.4	36.6	24.1	35.7	27.2
21	33.3	25.7	33.2	24.3	35.8	25.8	34.3	28.0

USSPA: Ultrasound spinous process angle; TK: thoracic kyphosis; LL: lumbar lordosis

Table A.5 *The average ultrasound laminae angle (left and right laminae) of the thoracic and lumbar region measured from the patients of the human subject study by rater 1 and rater 2; and Cobb angle of the thoracic and lumbar region measured from the patients of the pilot test by rater 3.*

		USLA (º)								Cobb (º)	
		Rater 1				Rater 2				Rater 3	
	Measurement	1st		2nd		1st		2nd		1st	
	Angle	TK	LL	TK	LL	TK	LL	TK	LL	TK	LL
Patients	1	34.6	39.7	36.3	35.5	37.3	34.2	32.2	30.5	20.5	42.9
	2	40.3	38.2	40.3	38.5	38.8	31.3	41.1	29.2	44	48.1
	3	35.4	31.2	36.4	30.7	34.4	26.0	35.9	30.6	28.9	45.4
	4	38.2	20.9	39.1	21.9	32.7	18.3	32.3	13.5	17.3	19.5
	5	47.5	48.5	49.1	44.1	47.6	45.7	45.0	44.3	41	60
	6	39.8	25.5	39.3	21.3	39.1	19.6	36.2	19.2	13.3	52.3
	7	37.4	3.8	40.8	6.4	43.6	5.3	39.1	2.3	33.9	25.2
	8	24.3	19.6	24.3	19.0	26.1	16.3	23.1	16.4	16.6	26.1
	9	39.2	21.2	39.6	20.7	38.0	19.9	40.0	17.7	9.6	45.2
	10	47.1	23.2	46.6	22.9	44.3	21.6	45.6	16.9	28.1	28.7
	11	36.8	21.6	34.3	23.5	32.7	20.5	35.2	22.0	38.2	40.5
	12	15.2	1.8	16.2	6.5	11.6	2.0	15.6	6.2	1.7	14.7
	13	17.3	28.5	18.7	29.6	21.0	30.5	20.4	26.8	3.8	32.5
	14	48.9	35.5	51.3	39.1	51.0	32.7	49.1	27.6	24.4	47.9
	15	47.7	40.2	49.0	37.8	47.4	36.6	48.2	38.4	44.6	49.1
	16	15.7	8.8	13.8	12.5	16.6	5.4	18.9	5.0	0.7	14.8
	17	30.8	27.8	33.4	29.0	28.4	22.1	27.0	20.0	27.9	35.9
	18	22.7	25.8	23.4	26.5	29.5	18.3	25.4	18.1	8.6	33.7

19	30.2	23.3	33.7	22.8	30.3	21.0	30.9	21.1	13.7	40.1
20	43.0	36.4	39.2	36.3	37.9	33.4	36.3	30.7	39.3	47.8
21	35.7	36.2	36.4	37.8	33.0	29.3	32.3	28.5	19.8	46.8

USSPA: Ultrasound spinous process angle; TK: thoracic kyphosis; LL: lumbar lordosis

Table A.6 *The Cobb angle, posterior tangent angle and the centre of posterior border angle of the thoracic and lumbar region measured in the sagittal plane, together with the main thoracic and thoraco(lumbar)Cobb angle measured in the coronal plane from the patients in the exploratory session. All angles were measured on X-ray.*

		Sagittal						Coronal	
	Method	Cobb (º)		PT (º)		CPB (º)		Cobb (º)	
	Angle	TK	LL	TK	LL	TK	LL	MT	TL(L)
Patients	1	13.5	45.3	16.9	30.8	19.7	29.7	26.0	18.3
	2	30.6	53.2	37.4	45.6	44.2	33.2	23.0	29.0
	3	34.9	54.5	36.5	50.6	50.9	49.2	22.1	19.9
	4	27.5	40.7	27.3	29.2	33.2	28.0	12.3	18.4
	5	27.7	52.9	35.4	55.7	40.7	44.5	40.0	0.0
	6	19.5	31.9	28.4	19.4	22.8	11.9	27.6	18.9
	7	27.7	61.8	32.4	56.2	39.3	48.8	16.0	20.8
	8	31.2	36.0	29.3	29.9	38.2	24.0	0.0	31.3
	9	16.7	44.3	22.9	40.7	24.7	34.5	13.7	0.0
	10	12.7	34.9	16.3	25.7	20.9	26.5	17.8	0.0
	11	22.2	26.1	26.7	23.9	27.0	21.1	0.0	30.0
	12	29.0	57.8	29.6	51.2	28.7	41.4	0.0	25.3
	13	50.5	63.4	48.1	55.2	54.6	41.9	0.0	18.0
	14	31.3	44.0	34.9	36.4	36.4	24.7	31.7	25.2
	15	36.0	58.2	40.9	53.3	40.5	43.3	11.1	19.1
	16	31.6	46.7	36.0	34.3	33.9	31.4	0.0	0.0
	17	11.5	51.8	24.6	43.6	34.7	35.6	13.9	0.0
	18	5.4	17.6	2.3	12.1	6.6	12.3	21.0	0.0

19	32.4	32.2	29.8	23.1	28.8	18.5	19.0	32.4
20	33.3	40.0	27.2	53.5	26.6	50.2	14.2	0.0
21	34.3	54.8	39.2	45.4	48.7	37.0	36.1	18.2
22	19.4	38.3	21.8	29.8	26.9	22.6	19.0	12.4
23	28.4	35.7	32.1	30.9	31.4	19.3	23.2	20.8
24	24.0	33.9	27.0	29.7	27.0	22.0	22.4	16.9
25	13.7	44.4	16.7	35.3	24.0	30.6	32.0	16.6
26	27.5	48.1	27.8	39.8	36.1	36.2	0.0	30.0
27	8.0	39.2	16.0	29.5	19.5	32.1	20.8	20.7
28	41.7	66.1	43.3	45.0	52.4	44.2	0.0	0.0
29	19.8	41.4	23.4	38.3	25.3	24.6	25.9	0.0
30	23.3	55.4	31.5	49.4	32.7	43.7	31.0	28.6
31	33.6	23.1	34.3	10.1	31.8	2.6	0.0	13.6
32	22.1	54.5	26.5	50.3	30.5	40.7	15.5	29.4
33	17.0	40.1	21.9	56.0	27.7	31.5	15.0	0.0
34	17.2	38.8	17.7	32.7	24.9	28.5	15.0	0.0
35	28.8	32.0	27.4	27.0	30.7	17.6	0.0	16.6
36	33.3	51.2	35.0	41.9	37.9	37.7	17.2	20.0
37	45.8	51.3	34.2	39.3	43.9	26.5	26.0	25.9
38	17.8	41.3	24.6	33.4	23.4	28.3	13.0	19.0
39	14.7	54.5	12.9	42.6	19.4	42.6	27.0	21.0
40	27.4	62.6	28.0	59.3	36.5	47.8	34.0	38.0
41	27.0	51.1	34.2	43.9	37.3	41.0	27.0	31.0
42	43.8	53.7	41.8	43.5	48.9	33.4	18.0	26.0
43	25.1	47.6	29.7	41.3	31.8	35.4	0.0	17.0

44	27.2	38.5	23.6	31.5	28.8	25.1	0.0	14.0
45	29.0	44.2	30.1	36.4	28.4	30.4	0.0	0.0
46	26.4	46.9	27.1	36.3	29.8	33.0	29.0	30.0
47	30.5	46.6	32.6	43.5	29.8	34.3	23.0	0.0
48	37.7	47.1	34.3	38.4	34.7	27.1	0.0	0.0
49	10.1	49.3	11.5	39.3	20.1	34.6	27.0	36.0
50	37.8	46.5	42.9	36.7	44.5	26.9	17.0	19.0
51	28.8	43.0	32.4	36.6	31.8	28.0	18.0	18.0
52	10.4	31.8	15.3	24.1	27.0	21.8	20.1	31.0
53	14.1	37.5	11.5	28.7	14.3	20.4	18.0	17.0
54	23.6	64.5	25.8	55.1	33.8	54.5	17.0	0.0
55	20.6	47.5	24.5	39.4	23.8	37.9	20.0	15.0
56	13.9	41.8	17.8	34.3	21.4	26.7	0.0	37.0
57	4.3	51.1	10.3	48.5	18.3	44.0	18.0	16.0
58	30.6	44.2	34.7	37.2	36.1	20.8	28.0	38.0
59	36.9	41.4	35.7	35.0	37.3	23.5	19.0	21.0
60	12.6	40.2	14.4	28.4	23.8	30.3	39.0	25.0
61	25.5	47.8	23.7	39.7	34.1	30.4	22.0	19.0
62	36.1	61.8	38.4	50.6	37.6	47.2	0.0	25.0
63	9.6	45.0	12.2	42.0	24.0	38.2	38.0	25.0
64	19.7	46.1	22.8	34.4	28.2	25.3	17.0	17.0
65	21.8	56.0	33.7	48.9	31.5	36.8	17.0	22.0
66	13.6	42.8	15.7	30.9	21.0	17.9	26.0	19.0
67	48.7	38.0	40.6	34.5	41.7	25.8	17.3	0.0
68	16.7	54.9	28.3	51.4	29.7	44.2	0.0	15.0

69	41.4	46.5	45.9	38.6	51.4	37.1	24.0	24.0
70	30.8	41.0	30.6	32.0	32.7	24.1	0.0	29.0
71	25.2	52.3	30.9	51.0	27.2	41.5	15.0	0.0
72	18.3	40.3	24.3	35.0	23.7	25.9	0.0	31.0
73	46.8	51.9	43.3	45.6	50.6	34.6	0.0	27.0
74	20.2	26.2	24.2	17.8	29.0	14.4	0.0	0.0
75	19.9	64.7	30.0	56.1	33.5	50.1	20.0	17.0
76	38.5	52.1	43.2	46.4	42.7	39.2	21.0	16.0
77	23.0	32.0	23.1	23.2	26.0	17.1	0.0	22.0
78	25.3	48.3	30.6	44.7	32.3	32.3	24.0	0.0
79	22.9	41.5	33.4	44.2	39.3	36.0	40.0	27.0
80	10.3	28.8	1.6	2.0	9.3	16.2	13.0	0.0
81	42.8	25.1	39.6	16.2	41.8	7.6	18.0	16.0
82	32.6	48.3	26.8	44.0	32.1	31.0	37.0	0.0
83	25.3	28.7	28.9	26.4	29.8	17.5	25.0	0.0
84	44.3	48.7	51.0	39.3	53.4	32.3	0.0	21.0
85	13.6	24.5	17.0	22.8	16.9	15.4	14.0	24.0
86	10.7	33.0	19.9	23.4	27.6	21.5	24.0	31.0
87	24.6	39.9	22.8	28.7	26.2	25.8	32.0	19.0
88	44.5	42.2	39.8	36.7	43.4	28.5	0.0	21.0
89	33.7	54.3	35.3	42.0	36.1	34.3	35.0	31.0
90	41.5	40.0	50.9	40.2	61.3	34.9	0.0	27.0
91	26.7	23.5	27.2	16.8	28.8	10.8	19.0	18.0
92	1.8	37.1	1.5	21.7	6.0	18.6	33.0	0.0
93	12.1	25.0	19.6	18.7	18.6	15.0	34.0	24.0

94	31.8	60.1	35.3	52.3	37.3	50.1	0.0	20.0
95	12.9	33.0	13.1	25.0	17.9	25.2	39.0	0.0
96	28.4	51.0	34.5	40.3	36.7	32.5	31.0	26.0
97	9.0	34.7	7.1	29.5	9.6	25.4	14.0	19.0
98	0.7	29.3	2.6	25.9	14.9	19.6	34.0	0.0
99	16.6	33.3	24.0	31.2	28.7	19.5	15.0	23.0
100	21.4	44.3	26.9	36.6	38.5	32.4	19.0	23.0
101	27.3	29.5	36.0	22.5	38.6	16.3	21.0	0.0
102	35.5	50.2	32.5	44.9	32.5	32.0	15.0	0.0
103	27.9	44.1	26.9	34.4	37.9	17.1	15.0	29.0
104	31.7	51.5	32.2	50.2	39.9	34.8	19.0	0.0
105	24.4	43.7	21.7	33.3	28.4	42.7	0.0	25.0
106	18.9	46.2	28.4	44.3	29.6	36.2	0.0	32.0
107	22.8	55.6	25.2	49.2	24.6	47.5	35.0	0.0
108	59.4	64.6	59.9	51.9	60.6	45.7	0.0	0.0
109	30.3	64.1	34.4	58.1	38.8	52.8	37.0	0.0
110	42.9	55.0	46.4	52.3	50.1	44.8	11.8	0.0
111	14.9	54.7	16.9	38.6	23.6	38.0	0.0	0.0
112	23.7	42.3	22.7	35.3	32.7	31.1	17.0	29.0
113	53.5	53.7	57.4	50.0	60.0	41.6	0.0	13.0
114	29.5	36.8	29.3	31.5	32.5	19.5	18.0	0.0
115	3.2	49.8	6.8	46.1	12.0	38.5	28.0	23.0

PT: Posterior tangent; CPB: Centre of posterior border; TK: thoracic kyphosis; LL: lumbar lordosis; MT: Main thoracic; TL(L): Thoraco(lumbar)

Table A.7 *The average ultrasound laminae angle (left and right laminae) of the thoracic and lumbar region measured in the sagittal plane, together with the main thoracic and thoraco(lumbar) spinous process angle measured in the coronal plane from the patients in the exploratory session. All angles were measured using ultrasound.*

		Sagittal		Coronal	
	Angle	USLA (º)		SPA (º)	
		TK	LL	MT	TL(L)
Patients	1	22.2	19.6	20.5	10.1
	2	44.2	26.8	10.5	21.7
	3	58.1	31.1	17.7	21.2
	4	37.0	17.0	15.4	18.4
	5	26.1	46.2	23.3	19.6
	6	20.2	20.3	16.2	18.5
	7	42.1	35.1	16.5	19.5
	8	42.8	21.2	14.1	15.6
	9	33.6	32.2	10.6	13.2
	10	27.7	12.4	13.6	10.7
	11	30.3	17.2	9.2	14.8
	12	31.0	36.6	17.5	15.7
	13	43.2	42.8	0	13.4
	14	37.1	32.5	19.2	22.9
	15	49.5	48.1	0	13.6
	16	40.6	16.7	6.1	13.8
	17	33.3	40.0	15	19.9
	18	10.7	1.4	13.9	0

19	25.6	10.6	22.6	25.3
20	33.3	40.0	7.9	12.4
21	37.6	23.2	15.2	0
22	17.6	10.1	18.7	14.8
23	34.4	36.7	25.4	18.4
24	31.3	23.6	19.1	17.5
25	26.9	16.2	23.4	18.1
26	35.7	26.8	0	15.5
27	28.9	16.2	14.6	16
28	48.1	61.6	10.1	10.3
29	20.9	28.9	20.9	0
30	35.9	47.2	26.2	26.5
31	37.9	2.2	0	7.6
32	43.5	35.8	23.9	0
33	27.0	16.9	0	9.8
34	24.0	26.6	12.5	19.1
35	40.2	16.6	0	6.8
36	39.2	23.1	14.9	15.7
37	37.8	22.6	14.7	22.9
38	31.5	13.8	10.8	17.7
39	14.9	30.3	13.7	19.2
40	32.9	42.0	24.6	32.8
41	47.5	25.8	16.7	24
42	50.2	38.3	15.4	26.6
43	40.9	23.8	0	18.7

44	27.3	21.7	10	11.5
45	35.3	23.0	0	17.2
46	36.8	30.3	19	15.3
47	25.8	34.8	21.7	19.3
48	32.7	33.0	10.5	8.2
49	23.4	19.2	16.9	35.7
50	50.2	33.9	11.5	13.1
51	35.6	19.6	13.7	15.1
52	23.4	24.8	11.7	22
53	31.7	20.4	9.8	12.2
54	38.2	48.2	0	19.6
55	31.2	32.5	9.1	12.4
56	29.2	20.0	15.3	25.2
57	14.8	33.8	18.6	21.8
58	43.5	15.6	20.7	0
59	38.3	37.6	19.8	20.8
60	27.3	27.4	31.1	34.9
61	35.5	41.3	17.7	18.8
62	35.8	44.8	0	16.5
63	30.2	21.0	30.9	26.8
64	39.5	15.7	8	13.8
65	38.2	42.9	17.3	22.7
66	32.6	21.7	17	0
67	40.0	28.3	0	10.7
68	39.2	43.4	0	14.5

69	48.5	32.9	16.6	26.3
70	43.0	17.8	16.9	21
71	25.8	35.6	16.8	10.5
72	27.2	27.6	0	25.4
73	49.5	33.0	13.3	15.3
74	32.3	10.6	0	10.2
75	41.6	56.3	19.7	24.7
76	33.2	27.4	16.2	16.7
77	33.2	26.0	6.2	13.9
78	51.5	36.4	15.3	0
79	42.6	32.8	24.7	22.8
80	11.1	10.3	14.9	0
81	40.5	12.5	17	17.3
82	36.0	26.2	20.8	0
83	28.5	8.1	11.3	0
84	48.6	20.5	0	11.4
85	40.6	20.9	8.1	5.6
86	21.1	10.0	19.2	25.1
87	13.8	20.5	21.8	24.3
88	49.8	20.0	10.9	15
89	31.0	41.2	25.5	0
90	53.9	28.2	15.1	14.3
91	25.8	12.9	17.1	22.1
92	14.3	21.4	23.4	22.1
93	20.0	3.8	23.1	20.8

94	39.9	27.6	0	16.1
95	28.6	21.4	32	24.5
96	42.5	18.9	18.8	0
97	27.0	19.3	15	22.2
98	13.0	19.8	20.4	20.4
99	22.4	11.9	12.6	14
100	28.9	21.9	17.7	23.2
101	42.7	2.5	10	10.6
102	40.9	25.5	15.2	0
103	45.5	14.9	11.3	12.6
104	35.3	33.9	16.6	16.8
105	41.1	39.1	0	22.6
106	28.2	37.9	35	42.6
107	18.0	39.9	0	20
108	50.9	44.7	0	26.6
109	41.1	33.8	0	6.8
110	54.6	47.1	8.4	0
111	32.6	49.4	13.5	18.8
112	43.6	33.3	36.6	37
113	56.7	46.8	13.7	12
114	28.8	15.5	16.3	0
115	11.2	34.5	31.4	29.2

USLA: Ultrasound Spinous Process angle; SPA: Spinous process angle; TK: thoracic kyphosis; LL: lumbar lordosis; MT: Main thoracic; TL(L): Thoraco(lumbar)

Table A.8 *The average ultrasound laminae angle (left and right laminae) of the thoracic and lumbar region measured in the sagittal plane, together with the main thoracic and thoraco(lumbar) spinous process angle measured in the coronal plane from the patients in the exploratory session. All angles were measured using ultrasound.*

		Sagittal		Coronal	
		USLA (º)		SPA (º)	
	Angle	TK	LL	MT	TL(L)
Patients	1	39.7	29.5	19.5	24.8
	2	36.3	14.4	15.2	11.7
	3	7.6	14.5	22.0	27.8
	4	27.1	32.7	15.8	0.0
	5	50.0	41.5	20.3	34.7
	6	34.2	27.4	0.0	20.7
	7	26.4	10.4	0.0	11.7
	8	24.4	23.9	23.2	26.4
	9	34.7	41.7	0.0	6.0
	10	26.8	21.8	12.3	10.6
	11	42.3	16.7	0.0	9.4
	12	20.7	2.4	22.6	22.5
	13	24.0	23.9	20.9	18.3
	14	29.1	42.6	13.6	24.2
	15	25.2	16.7	36.4	28.7
	16	29.1	27.8	19.7	23.0
	17	44.5	33.1	13.2	20.2
	18	50.1	25.5	13.2	12.3

19	7.9	7.7	26.8	17.9
20	34.6	46.3	0.0	10.2
21	24.2	37.4	41.0	34.6
22	21.2	30.4	17.6	23.7
23	28.7	30.1	11.4	18.2
24	47.1	67.2	0.0	23.3
25	31.4	32.0	7.3	9.4
26	33.3	35.4	18.8	22.5
27	25.2	39.4	21.2	25.6
28	29.1	22.9	18.2	22.9
29	39.5	35.7	32.5	0.0
30	39.8	46.4	0.0	21.0
31	30.3	9.5	19.3	9.7
32	33.4	37.4	15.5	17.3
33	18.0	45.6	0.0	19.8
34	35.8	57.3	9.5	14.9
35	23.9	10.7	13.9	17.8
36	32.1	20.6	35.8	46.0
37	28.8	46.0	23.2	0.0
38	31.0	23.2	23.0	17.9
39	19.5	13.0	21.6	21.3
40	23.8	6.5	17.3	15.4
41	34.2	39.7	16.6	21.7
42	28.3	40.1	17.8	19.7
43	28.1	30.9	19.5	24.8

44	18.6	13.3	20.3	0.0
45	36.4	44.4	12.5	14.3
46	26.3	49.3	15.0	24.0
47	13.4	18.2	22.4	17.1
48	31.7	20.8	14.3	11.0
49	37.1	46.0	16.6	20.1
50	42.1	42.1	8.3	6.6
51	7.1	22.3	17.3	21.9
52	41.0	62.9	14.1	21.8
53	43.8	37.9	14.8	20.8
54	10.9	25.6	35.6	27.7
55	48.6	37.8	8.4	6.9
56	37.7	29.6	19.9	24.8
57	20.2	11.7	27.4	20.5
58	26.0	34.5	13.8	16.4
59	34.7	24.8	33.9	32.1
60	42.7	44.7	11.2	13.5
61	34.0	27.9	0.0	15.3
62	34.8	45.1	0.0	16.3
63	38.8	43.6	17.0	24.1
64	30.6	47.5	9.0	20.7
65	40.9	36.8	0.0	32.3
66	39.1	32.6	14.3	11.5
67	37.5	25.4	14.2	18.1
68	13.1	11.4	33.4	36.5

69	36.1	30.6	16.4	20.9
70	13.9	24.2	24.9	38.4
71	34.0	2.9	0.0	19.7
72	29.3	23.1	18.5	36.3
73	19.8	28.7	18.4	16.2
74	33.2	40.9	33.8	18.3
75	38.2	47.7	10.3	17.8
76	56.5	30.0	21.6	26.4
77	33.9	3.9	0.0	4.3
78	42.6	41.8	16.3	22.2
79	34.6	37.3	25.2	0.0
80	23.1	15.4	0.0	3.4
81	28.8	21.4	13.0	0.0
82	45.2	52.8	27.5	22.7
83	40.2	39.5	13.9	25.5
84	41.8	25.7	14.8	0.0
85	42.9	25.4	13.0	16.8
86	47.3	52.9	30.7	21.6
87	17.5	34.8	26.6	21.3
88	51.0	45.0	14.4	23.2
89	20.2	40.9	35.8	25.2
90	33.0	30.6	31.4	30.2
91	25.0	18.4	18.8	18.6
92	14.1	26.5	21.5	11.0
93	33.8	23.3	0.0	16.2

94	26.9	38.8	20.8	27.3
95	20.3	41.7	19.6	16.9
96	36.7	6.0	14.1	11.7
97	40.4	46.7	16.0	22.0
98	48.0	38.6	0.0	16.5
99	38.8	23.5	26.5	26.5
100	38.5	37.5	19.7	21.9
101	33.8	44.8	15.6	17.9
102	47.5	40.3	0.0	27.5
103	48.1	44.4	10.8	7.7
104	31.1	27.3	8.5	16.9
105	47.7	28.7	0.0	13.0
106	36.7	30.3	10.7	15.2
107	27.7	20.4	34.6	26.1
108	43.2	37.8	10.2	11.4
109	33.9	15.7	18.6	18.6
110	35.2	41.7	16.1	21.3
111	28.1	23.7	34.3	33.7
112	19.5	24.7	33.3	25.8
113	30.5	22.7	11.5	30.6
114	32.8	54.4	16.3	12.7
115	49.5	54.0	18.2	31.5
116	25.0	44.9	14.4	17.4
117	25.1	27.6	22.5	22.1
118	14.0	20.7	28.3	22.4

119	56.3	40.3	19.0	26.8
120	23.4	50.4	18.1	16.8
121	31.7	34.4	23.2	26.7
122	17.2	15.9	23.8	32.3
123	32.2	33.4	28.2	21.7
124	4.0	7.6	35.9	0.0
125	53.4	64.7	0.0	20.4

USLA: Ultrasound Spinous Process angle; SPA: Spinous process angle; TK: thoracic kyphosis; LL: lumbar lordosis; MT: Main thoracic; TL(L): Thoraco(lumbar)

A.3. Information Sheet

Figure A.5 *Information sheet provided for the patients who participated in the study*

Informed Consent Form_PhaseIII V2

CONSENT FORM

Use of the Scolioscan for Quantitative Evaluation of Spinal Deformity –
A Validity Study on Patients with Scoliosis
Version: PhaseIII_ConsentForm_v2
Date: 4-Sep-2015

I, Name: ________________________ , HKID No. ______________ , Scoliosis Clinic No. ______________agree to participate in the above named research study. I understand that the study will be carried out as described in the Information Statement a copy of which I have retained. I realize that whether or not I decide to participate will not affect my medical care and treatment for Scoliosis. I also realize that I can withdraw from the research study at any time and do not have to give any reason for withdrawal. Such a withdrawal from the study will not affect any on-going treatment that I am receiving at the hospital. I can gain access to my data file at any time. The identity of myself will not be revealed without my consent to anyone other than the investigators conducting the study. Future quotation and presentation of the data will be made in an anonymous way. I have had all my questions answered to my satisfaction.

**Delete if appropriate (at 8 locations)*

(1) Signature of patient: ________________________ Date : ______________

Name of Patient: ____________________________ ID No.: ______________

Date of Birth: ______________________________

Home Address:____

____

Home Phone No.: ____________________________

(2) Signature of parent: ________________________ Date: ______________

Name of parent:_____________________________ ID No.: ______________

Relationship with the study child: __________________

(3) Signature of Doctor/Researcher: __________________Date: ______________

Name of Doctor/Researcher: ____________________________

Contact Person: Dr Tsz Ping Lam (Tel: 2632) or Ms. Tsang Ka Ling, Echo (Tel: 2632)
Department of Orthopaedics and Traumatology, The Chinese University of Hong Kong.
For enquiry regarding patient's right, please contact The Joint CUHK-NTEC CREC by phone 2632 or email to crec@

Page 1 of 1

A.4. Consent Form

Figure A.6 *Consent form provided for the patients who participated in the study*

Informed Consent Form_PhaseIII V2

同意書

三維超聲評估系統對脊柱側彎病症的定量評估
版本: PhaseIII_ConsentForm_v2
修訂日期: 4 / 9 /2015

本人____________________, 香港身份証號碼____________________, 病歷卡號碼________________同意參與上列研究計劃. 本人明白此計劃將會參照“研究詳情”進行, 本人亦擁有一份“研究詳情”. 本人明白參與此項目與否是不會影響 本人將來接受的治療。本人亦明白隨時可以中途退出這項計劃而不須提供任何理由，并不會影響本人將來的治療。

本人可以隨時翻閱個人檔案。個人私隱將受到保密。研究結果將以不記名方式發表。

本人已充份明白是項科研計劃，并且提出的有關問題已獲得滿意答覆。

(1) 參加者簽名 ____________________ 日期 ____________________

參加者姓名 ____________________ 身份證號碼 ____________________

出生日期 ____________________

住址 ____

____

電話 ____________________

(2) 家長簽名 ____________________ 日期 ____________________

家長姓名 ____________________ 身份證號碼 ____________________

與受試者關係 ____________________

(3) 醫生/研究員簽名 ____________________ 日期____________________

醫生/研究員姓名 ____________________

如有任何問題、困難或事故，可聯絡：林子平醫生（電話：2632- ）或曾嘉玲小姐（電話: 2632- ）
如對病人權益有疑問，請致電 2632 或電郵至 crec@ 聯絡香港中文大學－新界東醫院聯網臨床研究倫理聯席委員會

共一頁

References

Abelin-Genevois K, Idjerouidene A, Roussouly P, Vital JM, Garin C. Cervical spine alignment in the pediatric population: a radiographic normative study of 150 asymptomatic patients. Eur Spine J 2014;23(7):1442-8

Adams MA, Mannion AF, Dolan P. Personal risk factors for first-time low back pain. Spine 1999;24(23):2497-50

Agadir M, Sevastik B, Sevastik JA, et al. Induction of scoliosis in the growing rabbit by unilateral rib-growth stimulation. Spine 1988;13:1065-9

Dimeglio A, Canavese F and Bonnel F. Normal Growth of the Spine and Thorax. The growing spine. Chapter 4. P.48-80

Alexander MA, Season EH. Idiopathic scoliosis: an electromyographic study. Arch Phys Med Rehabil 1978;59:314-5

Alricsson M, Werner S. Young elite cross-country skiers and low back pain-A 5-year study. Phys Ther Sport 2006;7(4):181-4

Ames CP, Blondel B, Scheer JK, Schwab FJ, Le Huec JC, Massicotte EM, Patel AA, Traynelis VC, Kim HJ, Shaffrey CI, Smith JS, Lafage V. Cervical radiographical alignment: comprehensive assessment techniques and potential importance in cervical myelopathy. Spine 2013;38(22):S149-60

Aprin H, Bowen JR, MacEwen GD, Hall JE. Spine fusion in patients with spinal muscular atrophy. J Bone Joint Surg Am. 1982;64:1179-87

Archer IA, Dickson RA. Stature and idiopathic scoliosis. A prospective study. J Bone Joint Surg Br 1985;67:185-8

Arkin AM. The mechanism of the structural changes in scoliosis. J Bone Joint Surg Am 1949;31:519-28

Aronsson DD, Stokes IA, Rosovsky J, Spence H. Mechanical modulation of calf tail vertebral growth: implications for scoliosis progression. J Spinal Disord 1999;12:141-6

Asher MA, Burton DC. Adolescent idiopathic scoliosis: natural history and long term treatment effects. Scoliosis 2006;1(1):2

Aylott CE, Puna R, Robertson PA, Walker C. Spinous process morphology: the effect of ageing through adulthood on spinous process size and relationship to sagittal alignment. Eur Spine J 2012;21(5):1007-12

Baik JS, Kim JY, Park JH, Han SW, Park JH, Lee MS. Scoliosis in patients with Parkinson's disease. J Clin Neurol 2009;5(2):91-94

Bao H, Liu Z, Bao M, Zhu Z, Yan P, Liu S, Feng Z, Qian B, Qiu Y. Predicted final spinal height in patients with adolescent idiopathic scoliosis can be achieved by surgery regardless of maturity status. Bone Joint J. 2018;100-B(10):1372-1376.

Barrey C, Jund J, Noseda O, Roussouly P. Sagittal balance of the pelvis-spine complex and lumbar degenerative diseases: a comparative study about 85 cases. Eur Spine J 2007;16:1459-67

Barrey C, Roussouly P, Le Huec JC, D'Acunzi G, Perrin G. Compensatory mechanisms contributing to keep the sagittal balance of the spine. Eur Spine J 2013;22 Suppl 6:S834-41

Beach TA, Parkinson RJ, Stothart JP, Callaghan JP. Effects of prolonged sitting on the passive flexion stiffness of the in vivo lumbar spine. Spine J 2005;5(2):145-54

Beguiristain JL, De Salis J, Oriaifo A, Cañadell J. Experimental scoliosis by epiphysiodesis in pigs. Int Orthop 1980;3:317-21

Bernhardt M, Bridwell KH. Segmental analysis of the sagittal plane alignment of the normal thoracic and lumbar spines and thoracolumbar junction. Spine 1989;14:717-21

Betsch M, Wehrle R, Dor L, Rapp W, Jungbluth P, Hakimi M, Wild M. Spinal posture and pelvic position during pregnancy:a prospective rasterstereographic pilot study. Eur Spine J 2015;24(6):1282-8

Betz RR, Harms J, Clements DH III, Lenke LG, Lowe TG, Shufflebarger HL, Jeszenszky D, Beele B. Comparison of anterior and posterior instrumentation for correction of adolescent thoracic idiopathic scoliosis. Spine 1999;24:225-39

Bick EM, Barash ES, Lehman L. Congenital scoliosis without vertebral anomaly; the vertebral histology of two cases. Clin Orthop 1958;12:285-90

Birchall D, Hughes DG, Hindle J, Robinson L, Williamson JB. Measurement of vertebral rotation in adolescent idiopathic scoliosis using three-dimensional magnetic resonance imaging. Spine 1997;22:2403-7

Bissolotti L, Donzelli S, Gobbo M, Zaina F, Villafañe JH, Negrini S. Association between sagittal and scoliosis in patients with Parkinson Disease: A Cross-sectional study. Am J Phys Med Rehabil 2016;95(1):39-46

Bissolotti L, Gobbo M, Villafane JH, Negrini S. Spinopelvic balance: New biomechanical insights with clinical implications for Parkinson's disease. Eur Spine J 2014;23(3):576-83

Boesker EH, Moe JH, Winter RB, Koop SE. A determination of the normal thoracic kyphosis: a roentgenographic study of 121 normal children. J Pediatr Orthop 2000;20:796-8

Bone CM, Hsieh GH. The risk of carcinogenesis from radiographs to pediatric orthopaedic patients. J Pediatr Orthop 2000;20:251-4

Booth KC, Bridwell KH, Lenke LG, Baldus CR, Blanke KM. Complications and predictive factors for the successful treatment of flatback deformity (fixed sagittal imbalance). Spine 1999;24(16):1712-20

Boseker EH, Moe JH, Winter RB, Koop SE. Determination of "normal" thoracic kyphosis:a roentgenographic study of 121 "normal" children. J Pediatr Orthop. 2000;20(6):796-8

Bridwell KH, Bernhardt M. Segmental Analysis of the sagittal plane alignment of the normal thoracic and lumbar spines and thoracolumbar junction. Spine 1989;14:717-21

Bridwell KH, Betz RR, Capelli AM, Huss G, Harvey C. Sagittal plane analysis in idiopathic scoliosis patients treated with Cotrel–Dubousset instrumentation. Spine 1990;15:921-6

Briggs AM, Wrigley TV, Tully EA, Adams PE, Greig AM, Bennell KL. Radiographic measures of thoracic kyphosis in osteoporosis: Cobb and vertebral centroid angles. Skeletal Radiol 2007;36(8):761-7

Brink RC, Colo D, Schlösser TPC, Vincken KL, van Stralen M, Hui SCN, Shi L, Chu WCW, Cheng JCY, Castelein RM. Upright, prone, and supine spinal morphology and alignment in adolescent idiopathic scoliosis. Scoliosis Spinal Disord. 2017;12:6

Brink RC, Wijdicks SPJ, Tromp IN, Schlösser TPC, Kruyt MC, Beek FJA, Castelein RM. A reliability and validity study for different coronal angles using ultrasound imaging in adolescent idiopathic scoliosis. Spine J. 2018;18(6):979-85

Bunnell WP. An objective criterion for scoliosis screening. J Bone Joint Surg Am 1984;66(9):1381-7

Burwell RG. Comment to “The pathogenesis of idiopathic scoliosis: uncoupled neuro-osseous growth?” by R. W. Porter. Eur Spine J 2001;10:482-7

Canavese F, Turcot K, De Rosa V, de Coulon G, Kaelin A. Cervical spine sagittal alignment variations following posterior spinal fusion and instrumentation foradolescent idiopathic scoliosis. Eur Spine J 2011;20(7):1141-8.

Carlson BB, Burton DC, Asher MA. Comparison of trunk and spine deformity in adolescent idiopathic scoliosis. Scoliosis 2013;8(1):2

Castelein RM, van Dieen JH, Smit TH. The role of dorsal shear forces in the pathogenesis of adolescent idiopathic scoliosis: a hypothesis. Med Hypotheses 2005;65:501-8

Castelein RM, Veraart B. Idiopathic scoliosis: prognostic value of the profile. Eur Spine J 1992;1:167-9.

Chaise FO, Candotti CT, Torre ML, Furlanetto TS, Pelinson PP, Loss JF. Validation, repeatability and reproducibility of a noninvasive instrument for measuring thoracic and lumbar curvature of the spine in the sagittal plane. Rev Bras Fisioter 2011;15(6):511-7

Chaléat-Valayer E, Mac-Thiong JM, Paquet J, Berthonnaud E, Siani F, Roussouly P. Sagittal spino-pelvic alignment in chronic low back pain. Eur Spine J 2011;20 Suppl 5:634-40

Chen W, Le LH, Lou EH. 2016. Reliability of the axial vertebral rotation measurements of adolescent idiopathic scoliosis using the center of lamina method on ultrasound images: in vitro and in vivo study. Eur Spine J 25(10):3265-73

Chen W, Lou EH, Le LH. Using ultrasound imaging to identify landmarks in vertebra models to assess spinal deformity. Conf Proc IEEE Eng Med Biol Soc 2011;2011:8495-8

Chen W, Lou EH, Zhang PQ, Le LH, Hill D. Reliability of assessing the coronal curvature of children with scoliosis by using ultrasound images. J Child Orthop 2013;7(6):521-9

Chen YL. Vertebral centroid measurement of lumbar lordosis compared with the Cobb technique. Spine 1999;24(17):1786-90

Cheng JC1, Guo X, Sher AH, Chan YL, Metreweli C. Correlation between curve severity, somatosensory evoked potentials, and magnetic resonance imaging in adolescent idiopathic scoliosis. Spine 1999;24:1679-84

Cheng JC, Guo X. Osteopenia in adolescent idiopathic scoliosis. A primaryproblem or secondary to the spinal deformity? Spine 1997;22:1716-21

Chernukha KV, Daffner RH, Reigel DH. Lumbar lordosis measurement. A new method versus Cobb technique. Spine 1998;23(1):74-9; discussion 79-80

Cheung CJ, Zhou GQ, Law SY, Lai KL, Jiang WW, Zheng YP. Freehand three-dimensional ultrasound system for assessment of scoliosis. J Orthop Translat 2015;3(3):123-33

Cheung CS, Lee WT, Tse YK, Lee KM, Guo X, Qin L, Cheng JC. Generalized osteopenia in adolescent idiopathic scoliosis–association with abnormal pubertal growth, bone turnover, and calcium intake? Spine 2006;31:330-8

Cheung CW, Law SY, Zheng YP. Development of 3-D ultrasound system for assessment of adolescent idiopathic scoliosis (AIS): and system validation. Conf Proc IEEE Eng Med Biol Soc 2013;2013:6474-7

Cheung CWJ, Zheng YP. Development of 3-D Ultrasound System for Assessment of Adolescent Idiopathic Scoliosis. In: Lim CT, Goh JCH, ed. WCB 2010, IFMBE Proceedings 31, 2010:584-7

Cheung J, Halbertsma JP, Veldhuizen AG, Sluiter WJ, Maurits NM, Cool JC, van Horn JR. A preliminary study on electromyographic analysis of the paraspinal musculature in idiopathic scoliosis. Eur Spine J 2005;14:130-7

Cho KJ, Kim YT, Shin SH, Suk SI. Surgical treatment of adult degenerative scoliosis. Asian Spine J 2014;8(3):371-81

Chockalingam N, Dangerfield PH, Giakas G, Cochrane T, Dorgan JC. Computer-assisted Cobb measurement of scoliosis. Eur Spine J 2002;11(4):353-7

Chu WC, Lam WW, Chan YL, Ng BK, Lam TP, Lee KM, Guo X, Cheng JC. Relative shortening and functional tethering of spinal cord in adolescent idiopathic scoliosis? Study with multiplanar reformat magnetic resonance imaging and somatosensory evoked potential. Spine 2006;31(1):E19-25

Cil A, Yazici M, Uzumcugil A, Kandemir U, Alanay A, Alanay Y, Acaroglu RE, Surat A. The evolution of sagittal segmental alignment of the spine during childhood. Spine 2005;30:93-100

Clements DH, Marks M, Newton PO, Betz RR, Lenke L, Shufflebarger H; Harms Study Group. Did the Lenke classification change scoliosis treatment? Spine 2011;36:1142-5

Cobb JR. Outline for the study of scoliosis. In American Academy of Orthopaedic Surgeons, Instructional Course Lectures. St Louis, CV Mosby, 1948, pp. 261-75

Coelho DM, Bonagamba GH, Oliveira AS. Scoliometer measurements of patients with idiopathic scoliosis. Braz J Phys Ther 2013;17(2):179-84

Colonna PC, Vom Saal F. A study of paralytic scoliosis based on five hundred cases of poliomyelitis. J Bone Joint Surg Am 1941;335-53

Cook SD, Harding AF, Morgan EL, Nicholson RJ, Thomas KA, Whitecloud TS, Ratner ES. Trabecular bone mineral density in idiopathic scoliosis. J Pediatr Orthop 1987;7:168-74

Currier DP. Elements of research in physical therapy. 3rd edn Williams & Wilkins 1984, Baltimore, pp 160-71

D'Aouˆt K, Aerts P, De Clercq D, De Meester K, Van Elsacker L. Segment and joint angles of hind limb during bipedal and quadrupedal walking of the bonobo (Pan paniscus). Am J Phys Anthropol 2002;119:37-51

Dawson B, Trapp RG. Basic and Clinical Biostatistics. 4th Ed. New York: Lange Medical Books/McGraw-Hill; 2004

de Jonge T, Dubousset JF, Illés T. Sagittal plane correction in idiopathic scoliosis. Spine 2002;27(7):754-60

de Oliveira TS, Candotti CT, La Torre M, Pelinson PP, Furlanetto TS, Kutchak FM, Loss JF. Validity and reproducibility of the measurements obtained using the flexicurve instrument to evaluate the anglesof thoracic and lumbar curvatures of the spine in the sagittal plane. Rehabil Res Pract 2012;2012:186156.

Deacon P, Flood BM, Dickson RA. Idiopathic scoliosis in three dimensions. A radiographic and morphometric analysis. J Bone Joint Surg Br 1984;66(4):509-12

Delorme S, Labelle H, Aubin CE, de Guise JA, Rivard CH, Poitras B, Coillard C, Dansereau J. Intraoperative comparison of two instrumentation techniques for the correction of adolescent idiopathic scoliosis. Rod rotation and translation. Spine 1999;24(19):2011-7

Denis F. The three column spine and its significance in the classification of acute thoracolumbar spinal injuries. Spine,1983;8(8):817-31

Deschênes S, Charron G, Beaudoin G, Labelle H, Dubois J, Miron MC, Parent S. Diagnostic imaging of spinal deformities: reducing patients radiation dose with a new slot-scanning X-ray imager. Spine 2010;35(9):989-94

Dickson RA, Lawton JO, Archer IA, Butt WP. The pathogenesis of idiopathic scoliosis. Biplanar spinal asymmetry. J Bone Joint Surg Br 1984;66:8-15

Dickson RA. The etiology and pathogenesis of idiopathic scoliosis. Acta Orthop Belg 1992;58:21-5

Diefenbach C, Lonner BS, Auerbach JD, Bharucha N, Dean LE. Is radiation-free diagnostic monitoring of adolescent idiopathic scoliosis feasible using upright positional magnetic resonance imaging? Spine 2013;38:576-80

Dimar JR, Carreon LY, Labelle H, Djurasovic M, Weidenbaum M, Brown C, Roussouly P. Intra- and inter-observer reliability of determining radiographic sagittal parameters of the spine and pelvis using a manual and a computer-assisted method. Spine 2008;17:1373-9

Doody MM, Lonstein JE, Stovall M, Hacker DG, Luckyanov N, Land CE. Breast cancer mortality after diagnostic radiography: findings from the U.S. Scoliosis Cohort Study. Spine 2000;25(16):2052-63

D'Osualdo F, Schierano S, Iannis M. Validation of clinical measurement of kyphosis with a simple instrument, the arcometer. Spine 1997;22(4):408-13

Driscoll C, Aubin CE, Canet F, Labelle H, Horton W, Dansereau J. Biomechanical study of patient positioning: influence of lower limb positioning on spinal geometry. J Spinal Disord Tech 2012;25(2):69-76

Dubousset J. Three-dimensional analysis of the scoliosis deformity. In: Weinstein S (ed) The pediatric spine: principles and practice. Raven 1994, New York, pp 479-96

El-Hawary R, Gauthier L, Ohlin A. Sagittal Plane alignment and deformities in growing children. The growing spine. 2016, Chapter 23. P.396-410

Eom KS, Kim TY, Moon SK. Extreme elongation of the transverse process of the fifth limber vertebra: An unusual variant. Turk Neurosurg, 2011;21(4):648-650.

Farcy JP, Schwab FJ. Management of flatback and related kyphotic decomposition syndromes. Spine 1997;22(20):2452-7

Farkas A. Physiological Scoliosis. J Bone Joint Surg 1941;23:607-27

Farley CW, Curt BA, Pettigrew DB, Holtz JR, Dollin N, Kuntz C 4th. Spinal cord intramedullary pressure in thoracic kyphotic deformity: a cadaveric study. Spine 2012, 37(4):E224-30

Fehlings MG, Tetreault LA, Wilson JR, Skelly AC. Cervical spondylotic myelopathy: current state of the art and future directions. Spine 2013;38:S1-8

Fenster A, Downey DB, Cardinal HN. Three-dimensional ultrasound imaging. PhysMed Biol,2001;46:R67-99

Fidler MW, Jowett RL. Muscle imbalance in the aetiology of scoliosis. J Bone Joint Surg Br 1976;58:200-1

Ford DM, Bagnall KM, McFadden KD, Greenhill BJ, Raso VJ. Paraspinal muscle imbalance in adolescent idiopathic scoliosis. Spine 1984;9:373-6

Frerich JM, Hertzler K, Knott P, Mardjetko S. Comparison of radiographic and surface topography measurements in adolescents with idiopathic scoliosis. Open Orthop J 2012;6:261-5

Gee AH, Prager RW, Treece GM, Berman L. Engineering a freehand 3D ultrasound system. Pattern Recognition Lett, 2003;24(12):757-7

Gelb DE, Lenke LG, Bridwell KH, Blanke K, McEnery KW. An analysis of sagittal spinal alignment in 100 asymptomatic middle and older aged volunteers. Spine 1995;20:1351-8

Glassman SD, Bridwell K, Dimar JR, Horton W, Berven S, Schwab F. The impact of positive sagittal balance in adult spinal deformity. Spine 2005;30(18):2024-9

Gocen S, Aksu MG, Baktirolu L, Ozcan O, Gocen S, Aksu MG, Baktirolu L, Ozcan O. Evaluation of computed tomographic methods to measure vertebral rotation in adolescent idiopathic scoliosis: an intraobserver and interobserver analysis. J Spinal Disord 1998;11:210-4

Goldberg CJ, Kaliszer M, Moore DP, Fogarty EE, Dowling FE. Surface topography, Cobb angles, and cosmetic change in scoliosis. Spine 2001; 26(4):E55-63

Good CR. The genetic basis of adolescent. J Spinal Res Found 2009;4 (1):15-64

Grabara M, Hadzik A. Postural variables in girls practicing volleyball. Biomedical Human Kinetics 2009;1:67-71

Grivas TB, Wade MH, Negrini S, O'Brien JP, Maruyama T, Hawes MC, Rigo M, Weiss HR, Kotwicki T, Vasiliadis ES, Sulam LN, Neuhous T. SOSORT consensus paper: school screening for scoliosis. Where are we today? Scoliosis 2007;2:17

Gum JL, Asher MA, Burton DC, Lai SM, Lambart LM. Transverse plane pelvic rotation in adolescent idiopathic scoliosis: primary or compensatory? Eur Spine J 2007;16(10):1579-86

Guo X, Chau WW, Chan YL, Cheng JC. Relative anterior spinal overgrowth in adolescent idiopathic scoliosis. Results of disproportionate endochondral-membranous bone growth. J Bone Joint Surg Br 2003;85(7):1026-31

Guo X, Chau WW, Hui-Chan CW, Cheung CS, Tsang WW, Cheng JC. Balance control in adolescents with idiopathic scoliosis and disturbed somatosensory function. Spine 2006;31:E437-40.

Hackenberg L, Hierholzer E, Bullmann V, Liljenqvist U, Götze C. Rasterstereographic analysis of axial back surface rotation in standing versus forward bending posture in idiopathic scoliosis. Eur Spine J 2006;15(7):1144-9

Hammerberg EM, Wood KB. Sagittal profile of the elderly. J Spinal Disord Tech 2003;16(1):44-50

Hardacker JW, Shuford RF, Capicotto RN, Pryor PW. Radiographic standing cervical segmental alignment in adult volunteers without neck symptoms. Spine 1997;22:1472-80

Harrison DD, Cailliet R, Janik TJ, Troyanovich SJ, Harrison DE, Holland B. Elliptical modeling of the sagittal lumbar lordosis and segmental rotation angles as a method to discriminatebetween normal and low back pain subjects. J Spinal Disord 1998;11(5):430-9

Harrison DD, Janik TJ, Troyanovich SJ, Holland B. Comparisons of lordotic cervical spine curvatures to a theoretical ideal model of the static sagittal cervical spine. Spine 1996;21(6):667-75

Harrison DE, Cailliet R, Harrison DD, Janik TJ, Holland B. Changes in sagittal lumbar configuration with a new method of extension traction: nonrandomized clinical controlled trial. Arch Phys Med Rehabil 2002;83(11):1585-91

Harrison DE, Cailliet R, Harrison DD, Janik TJ, Holland B. Reliability of centroid, Cobb, and Harrison posterior tangent methods: which to choose for analysis of thoracic kyphosis. Spine 2001;26(11):E227-34

Harrison DE, Cailliet R, Harrison DD, Janik TJ. How do anterior/posterior translations of the thoracic cage affect the sagittal lumbar spine, pelvic tilt, andthoracic kyphosis? Eur Spine J 2002;11(3):287-93

Hattori T, Sakaura H, Iwasaki M, Nagamoto Y, Yoshikawa H, Sugamoto K. In vivo three-dimensional segmental analysis of adolescent idiopathic scoliosis. Eur Spine J 2011;20:1745-50

Havey RM, Gavin TM, Patwardhan AG. Stability of the Scoliotic Spine: Effect of Scoliosis Braces. Spine 2016;41 Suppl 7:S18-9

Hayashi K, Upasani VV, Pawelek JB, Aubin CE, Labelle H, Lenke LG, Jackson R, Newton PO. Three-dimensional analysis of thoracic apical sagittal alignment in adolescent idiopathic scoliosis. Spine 2009;34(8):792-7

He C, To MK, Cheung JP, Cheung KM, Chan CK, Jiang WW, Zhou GQ, Lai KK, Zheng YP, Wong MS. An effective assessment method of spinal flexibility to predict the initial in-orthosis correction on the patients with adolescent idiopathic scoliosis (AIS). PLoS One. 2017;12(12):e0190141.

Hefti F. Pathogenesis and biomechanics of adolescent idiopathic scoliosis (AIS). J Child Orthop 2013;7(1):17-24

Helenius I, Remes V, Yrjonen T, Ylikoski M, Schlenzka D, Helenius M, Poussa M. Harrington and Cotrel-Dubousset instrumentation in adolescent idiopathic scoliosis. Long-term functional and radiographic outcomes. J Bone Joint Surg Am 2003;85-A(12):2303-9

Hilibrand AS, Tannenbaum DA, Graziano GP, Loder RT, Hensinger RN. The sagittal alignment of the cervical spine in adolescent idiopathic scoliosis. J Pediatr Orthop 1995;15:627-32

Ho EK, Upadhyay SS, Ferris L, Chan FL, Bacon-Shone J, Hsu LC, Leong JC. A comparative study of computed tomographic and plain radiographic methods to measure vertebral rotation in adolescent idiopathic scoliosis. Spine 1992;17:771-4.

Hoffman DA, Lonstein JE, Morin MM, Visscher W, Harris BS 3rd, Boice JD Jr. Breast cancer in women with scoliosis exposed to multiple diagnostic X-rays. J Natl Cancer Inst 1989;81(17):1307-12

Hogervorst T, Bouma HW, De Vos J. Evolution of the hip and pelvis. Acta Orthop 2009;80:1-39

Hong JY, Kim KW, Suh SW, Park SY, Yang JH. Effect of Coronal Scoliotic Curvature on Sagittal Spinal Shape: Analysis of Parameters in Mature Adolescent Scoliosis Patients. Clin Spine Surg. 2017;30(4):E418-22

Hsu JD. The natural history of spine curvature progression in the nonambulatory Duchenne muscular dystrophy patient. Spine 1983;8:771-5.

Hu P, Yu M, Liu X, Zhu B, Liu X, Liu Z. Analysis of the relationship between coronal and sagittal deformities in adolescent idiopathic scoliosis. Eur Spine J. 2016;25(2):409-16

Hu PP, Yu M, Liu XG, Chen ZQ, Liu ZJ. Correltation analysis between the sagittal and coronal parameters of spino-pelvic in Lenke type 1 adolescent idiopathic scoliosis. Beijing Da Xue Xue Bao 2015;47(2):248-52

Huang QH, Zheng YP, Lu MH, Chi ZR. Development of a portable 3D ultrasound imaging system for musculoskeletal tissues. Ultrasonics 2005;43(3):153-63

Hueter C. Anatomische Studien an den Extremitaetengelenken Neugeborener und Erwachsener. Virchows Archiv Path Anat Physiol 1862;25:572-99

Hung VW, Qin L, Cheung CS. Osteopenia: a new prognostic factor of curve progression in adolescent idiopathic scoliosis. J Bone Joint Surg Am 2005;87: 2709-16

Hwang SW, Samdani AF, Cahill PJ: The impact of segmental and en bloc derotation maneuvers on scoliosis correction and rib prominence in adolescent idiopathic scoliosis. J Neurosurg Spine 2012;16:345-50

Ilharreborde B, Pesenti S, Ferrero E, Accadbled F, Jouve JL, De Gauzy JS, Mazda K. Correction of hypokyphosis in thoracic adolescent idiopathic scoliosis using sublaminar bands: a 3D multicenter study. Eur Spine J 2018;27(2):350-7

Ishihara A. Roentgenographic studies on the normal pattern of the cervical curvature. Nihon Seikeigeka Gakkai Zasshi 1968;42(11):1033-44

Jackson RP, MacManus AC. Radiographic analysis of sagittal plane alignment and balance in standing volunteers and patients with low back pain matched for age, sex and size. Spine 1994;19:1611-8

James JI. Paralytic scoliosis. J Bone Joint Surg Br. 1956;38-B:660–85.

Janssen MM, Drevelle X, Humbert L, Skalli W, Castelein RM. Differences in male and female spino-pelvic alignment in asymptomatic young adults: a three-dimensional analysis using upright low-dose digital biplanar X-rays. Spine 2009;34(23):E826-32

Janssen MM, Kouwenhoven JW, Schlösser TP, Viergever MA, Bartels LW, Castelein RM, Vincken KL. Analysis of preexistent vertebral rotation in the normal infantile, juvenile, and adolescent spine. Spine 2011;36(7):E486-91

Janssen MM, Vincken KL, Kemp B, Obradov M, de Kleuver M, Viergever MA, Castelein RM, Bartels LW. Pre-existent vertebral rotation in the human spine is influenced by body position. Eur Spine J 2010;19(10):1728-34

Janssen MM, Vincken KL, van Raak SM, Vrtovec T, Kemp B, Viergever MA, Bartels LW, Castelein RM. Sagittal spinal profile and spinopelvic balance in parents of scoliotic children. Spine J 2013;13(12):1789-800

Journé A, Sadaka J, Belicourt C, Sautet A. New method for measuring acetabular component positioning with EOS imaging: feasibility study on dry bone. Int Orthop 2012; 36(11):2205-9

Kaplan SC, Eksi MS. Cervical Sagittal Alignment Parameters of Patients Admitted to Neurosurgery and Emergency Clinics in a State Hospital at Eastern Part of Turkey. Korean J Spine 2015;12(2):75-8

Kim H, Kim HS, Moon ES, Yoon CS, Chung TS, Song HT, Suh JS, Lee YH, Kim S. Scoliosis imaging: what radiologists should know. Radiographics. 2010;30(7):1823-42

Kim YJ, Bridwell KH, Lenke LG, Rhim S, Cheh G. An analysis of sagittal spinal alignment following long adult lumbar instrumentation and fusion to L5 or S1: can we predict ideal lumbar lordosis? Spine 2006 Sep 15;31(20):2343-52

Kim YJ, Lenke LG, Cho SK, Bridwell KH, Sides B, Blanke K. Comparative analysis of pedicle screw versus hook instrumentation in posterior spinal fusion of adolescent idiopathic scoliosis. Spine 2004;29:2040-8

King HA, Moe JH, Bradford DS, Winter RB. The selection of fusion levels in thoracic idiopathic scoliosis. J Bone Joint Surg Am 1983;65(9):1302-13

Knott P, Mardjetko S, Nance D, Dunn M. Electromagnetic topographical technique of curve evaluation for adolescent idiopathic scoliosis. Spine 2006;31(24):E911-5

Knott PT, Mardjetko SM, Techy F. The use of the T1 sagittal angle in predicting overall sagittal balance of the spine. Spine J 2010;10:994-8.

Koo TK, Guo JY, Ippolito C, Bedle JC. Assessment of scoliotic deformity using spinous processes: comparison of different analysis methods of an ultrasonographic system. J Manipulative Physiol Ther 2014;37(9):667-77

Kotwicki T, Napiontek M. Intravertebral deformation in idiopathic scoliosis: a transverse plane computer tomographic study. J Pediatr Orthop. 2008;28(2):225-9

Kouwenhoven JW, Bartels LW, Vincken KL, Viergever MA, Verbout AJ, Delhaas T, Castelein RM. The relation between organ anatomy and pre-existent vertebral rotation in the normal spine: magnetic resonance imaging study in humans with situs inversus totalis. Spine 2007b;32:1123-8.

Kouwenhoven JW, Castelein RM. The pathogenesis of adolescent idiopathic scoliosis: review of the literature. Spine 2008 Dec 15;33(26):2898-908

Kouwenhoven JW, Smit TH, van der Veen AJ, Kingma I, van Diee¨n JH, Castelein RM. Effects of dorsal versus ventral shear loads on the rotational stability of the thoracic spine: a biomechanical porcine and human cadaveric study. Spine 2007b;32:2545-50

Kouwenhoven JW, Vincken KL, Bartels LW, Castelein RM. Analysis of preexistent vertebral rotation in the normal spine. Spine 2006a;31:1467-72.

Krismer M, Chen AM, Steinlechner M, Haid C, Lener M, Wimmer C, Krismer. Measurement of vertebral rotation: a comparison of two methods based on CT scans. J Spinal Disord 1999;12:126-30

Kuntz C 4th1, Levin LS, Ondra SL, Shaffrey CI, Morgan CJ. Neutral upright sagittal spinal alignment from the occiput to the pelvis in asymptomatic adults: a review and re-synthesis of the literature. J Neurosurg Spine 2007;6(2):104-12.

Kuntz C IV, Shaffrey CI, Ondra SL, Durrani AA, Mummaneni PV, Levin LS, Pettigrew DB. Spinal deformity: a new classification derived from neutral upright spinal alignment measurements in asymptomatic juvenile, adolescent, adult, and geriatric individuals. Neurosurgery 2008;63(3 Suppl):25-39

La Grone MO. Loss of lumbar lordosis. A complication of spinal fusion for scoliosis. Orthop Clin North Am. 1988;19(2):383-93

La Maida GA, Zottarelli L, Mineo GV, Misaggi B. Sagittal balance in adolescent idiopathic scoliosis: radiographic study of spino-pelvic compensation after surgery. Eur Spine J 2013;22 Suppl 6:S859-67

Lafage V, Schwab F, Skalli W, Hawkinson N, Gagey PM, Ondra S, Farcy JP. Standing balance and sagittal plane spinal deformity: analysis of spinopelvic and gravity line parameters. Spine 32008;3:1572-8

Lam TP, Hung VW, Yeung HY, Chu WC, Ng BK, Lee KM, Qin L, Cheng JC. Quantitative ultrasound for predicting curve progression in adolescent idiopathic scoliosis: a prospective cohort study of 294 cases followed-up beyond skeletal maturity. Ultrasound Med Biol. 2013;39(3):381-7

Lam TP, Hung VW, Yeung HY, Tse YK, Chu WC, Ng BK, Lee KM, Qin L, Cheng JC. Abnormal bone quality in adolescent idiopathic scoliosis: a case-control study on 635 subjects and 269 normal controls with bone densitometry and quantitative ultrasound. Spine 2011;36(15):1211-7

Lazennec JY, Brusson A, Rousseau MA. Hip-spine relations and sagittal balance clinical consequences. Eur Spine J 2011;20 Suppl 5:686-98

Le Bras A, Laporte S, Mitton D, de Guise JA, Skalli W. Three-dimensional (3D) detailed reconstruction of human vertebrae with low-dose digital stereoradiography. Eur J Orthop Surg Traumatol 2003;91:286-90

Lee CS, Chung SS, Kang KC, Park SJ, Shin SK. Normal patterns of sagittal alignment of the spine in young adults radiological analysis in a Korean population. Spine 2011;36(25):E1648-54

Lee CS, Noh H, Lee DH, Hwang CJ, Kim H, Cho SK. Analysis of sagittal spinal alignment in 181 asymptomatic children. J Spinal Disord Tech 2012;25(8):E259-63

Lee ES, Ko CW, Suh SW, Kumar S, Kang IK, Yang JH. The effect of age on sagittal plane profile of the lumbar spine according to standing, supine, and varioussitting positions. J Orthop Surg Res 2014;9(1):11

Lee MC, Solomito M, Patel A. Supine magnetic resonance imaging Cobb measurements for idiopathic scoliosis are linearly related tomeasurements from standing plain radiographs. Spine 2013;38(11):E656-61

Lee WT, Cheung CS, Tse YK, Guo X, Qin L, Lam TP, Ng BK, Cheng JC. Association of osteopenia with curve severity in adolescent idiopathic scoliosis: a study of 919 girls. Osteoporos Int 2005;16:1924-32

Lee WT, Cheung CS, Tse YK, Guo X, Qin L, Ho SC, Lau J, Cheng JC. Generalized low bone mass of girls with adolescent idiopathic scoliosis is related to inadequate calcium intake and weight bearing physical activity in peripubertal period. Osteoporos Int 2005;16:1024-35

Legaye J, Duval-Beaupe`re G, Hecquet J, Marty C. Pelvic incidence: a fundamental pelvic parameter for three-dimensional regulation of spinal sagittal curves. Eur Spine J 1998;7:99-103

Lenke G. Lenke classification system of adolescent idiopathic scoliosis: treatment recommendations. Instr Course Lect 2005;54:537-42

Lenke L, SRS Working Group. 3-D Classification and the Terminology Committee. Revised Glossary of Terms [SRS Web site]. March 2000. Available at: http://srs.org/professionals/glossary. Accessed June 30, 2007

Lenke LG, Betz RR, Bridwell KH, Harms J, Clements DH, Lowe TG. Spontaneous lumbar curve coronal correction after selective anterior or posterior thoracic fusion in adolescent idiopathic scoliosis. Spine 1999;24:1663–71; discussion 72.

Lenke LG, Edwards CC 2nd, Bridwell KH. The Lenke classification of adolescent idiopathic scoliosis: how it organizes curve patterns as a template to perform selective fusions of the spine. Spine 2003;28(20):S199-207

Leroux MA, Zabjek K, Simard G, Badeaux J, Coillard C, Rivard CH. A noninvasive anthropometric technique for measuring kyphosis and lordosis: an application for idiopathic scoliosis. Spine 2000;25(13):1689-94

Lewis JS, Valentine RE. Clinical measurement of the thoracic kyphosis. A study of the intra-rater reliability in subjects with and without shoulder pain. BMC Musculoskelet Disord 2010;11:39

Li M, Cheng J, Ying M, Ng B, Zheng Y, Lam T, Wong W, Wong M. Could clinical ultrasound improve the fitting of spinal orthosis for the patients with AIS? Eur Spine J 2012;21(10):1926-35

Liljenqvist UR, Link TM, Halm HF. Morphometric analysis of thoracic and lumbar vertebrae in idiopathic scoliosis. Spine 2000;25(10):1247-53

Lin H. The correlation comparison of vertebral axial rotation relative to curvature and torsion in scoliosis by simplified 3D spine model. Conf Proc IEEE Eng Med Biol Soc. 2006;1:1517-20.

López-Miñarro PA, Muyor JM, Alacid F. Sagittal spinal curvatures and pelvic tilt in elite young kayakers. Medicine dello Sport 2010;63:509-19

López-Miñarro PA, Muyor JM, Alacid F. Sagittal spinal and pelvic postures of highly-trained young canoeists. J Hum Kinet 2011;29:41-8

Lowenstein JE, Matsumoto H, Vitale MG, Weidenbaum M, Gomez JA, Lee FY, Hyman JE, Roye DP Jr. Coronal and sagittal plane correction in adolescent idiopathic scoliosis: a comparison between all pedicle screw versus hybrid thoracic hook lumbar screw constructs. Spine 2007; 32:448-52

Lucas DB, Bresler B. Stability of the ligamentous spine. Vol 40. San Francisco, CA: University of California, Biomechanics Laboratory; 1961.

MacEwen GD. Cerebral palsy and scoliosis. In: Spinal Deformity in Neurological and Muscular Disorders. New York, NY: Mosby; 1974:191-9.

MacEwen GD. Experimental scoliosis. IsrJ Med Sci 1973;9:714-8.

Mac-Thiong JM, Labelle H, Berthonnaud E, Betz RR, Roussouly P. Sagittal spinopelvic balance in normal children and adolescents. Eur Spine J 2007;16(2):227-34

Mac-Thiong JM, Labelle H, Charlebois M, Huot MP, de Guise JA. Sagittal plane analysis of the spine and pelvis in adolescent idiopathic scoliosis according to the coronal curve type. Spine 2003;28:1404-9

Mac-Thiong JM, Labelle H, Roussouly P. Pediatric sagittal alignment. Eur Spine J 2011a;20 Suppl 5:586-90

Mac-Thiong JM, Roussouly P, Berthonnaud E, Guigui P. Age- and sex-related variations in sagittal sacropelvic morphology and balance in asymptomatic adults. Eur Spine J 2011;20 Suppl 5:572-7

Mac-Thiong JM, Roussouly P, Berthonnaud E, Guigui P. Sagittal parameters of global spinal balance: normative values from a prospective cohort of seven hundred nine Caucasian asymptomatic adults. Spine 2010;35(22):E1193-8

Madigan RR, Wallace SL. Scoliosis in the institutionalized cerebral palsy population. Spine 1981;6:583-90

Majdouline Y, Aubin CE, Robitaille M, Sarwark JF, Labelle H. Scoliosis correction objectives in adolescent idiopathic scoliosis. J Pediatr Orthop 2007;27(7):775-81

Malfair D, Flemming AK, Dvorak MF, Munk PL, Vertinsky AT, Heran MK, Graeb DA. Radiograph evaluation of scoliosis: Review. Am J Roentgenol 2010;194(3):S8-S22

Mannion AF, Knecht K, Balaban G, Dvorak J, Grob D. A new skin-surface device for measuring the curvature and global and segmental range of motion of the spine: reliability of measurements and comparison with data reviewed from the literature. Eur Spine J 2004;13(2):122-36

McKenna C, Wade R, Faria R, Yang H, Stirk L, Gummerson N, Sculpher M, Woolacott N. EOS 2D/3D X-ray imaging system: a systematic review and economic evaluation. Health Technol Assess 2012;16(14):1-188

McMaster MJ, Singh H. Natural history of congenital kyphosis and kyphoscoliosis. A study of one hundred and twelve patients. J Bone Joint Surg Am 1999; 81(10):1367-83

Mehta MH. Radiographic estimation of vertebral rotation in scoliosis. J Bone Joint Surg Br 1973;55:513-20

Mellado JM, Larrosa R, Martin J, Yanguas N, Solanas S, Cozcolluela R. MDCT of variations and anomalies of the neural arch and its processes: part 1— pedicles, pars interarticularis, laminae, and spinous process. AJR, 2011a;197:W104-13

Mente PL, Aronsson DD, Stokes IA, Iatridis JC. Mechanical modulation of growth for the correction of vertebral wedge deformities. J Orthop Res 1999;17:518-24

Mente PL, Stokes IA, Spence H, Aronsson DD. Progression of vertebral wedging in an asymmetrically loaded rat tail model. Spine 1997;22:1292-6

Michelsson JE. The development of spinal deformity in experimental scoliosis. Acta Orthop Scand 1965;(suppl 81):1-91

Middleditch A, Oliver J. Functional anatomy of the spine. 2e. Elsevier,2005;1-62

Mitulescu A, Skalli W, Mitton D, De Guise JA. Three-dimensional surface rendering reconstruction of scoliotic vertebrae using a non stereo-corresponding points technique. Eur Spine J 2002;11:344-52

Mok JM, Berven SH, Diab M, Hackbarth M, Hu SS, Deviren V. Comparison of observer variation in conventional and three digital radiographic methods used in the evaluation of patients with adolescent idiopathic scoliosis. Spine 2008;33:681-6

Muyor JM, López-Miñarro PA, Alacid F. A comparison of the thoracic spine in the sagittal plane between elite cyclists and non-athlete subjects. J Back Musculoskelet Rehabil 2011;24(3):12935

Muyor JM, Sánchez-Sánchez E, Sanz-Rivas D, López-Miñarro PA. Sagittal spinal morphology in highly trained adolescent tennis players. J Sports Sci Med 2013;12(3):588-93

Nachemson AL, Peterson LE. Effectiveness of treatment with a brace in girls who have adolescent idiopathic scoliosis: a prospective controlled study based on data from the brace study of the scoliosis research society. J Bone Joint Surg 1995;77A:815-21

Nam WD, Chang BS, Lee CK, Cho JH. Clinical and radiological predictive factors to be related with the degree of lumbar back muscle degeneration: difference by gender. Clin Orthop Surg 2014;6(3):318-23

Nash C, Moe JH. A study of vertebral rotation. J Bone Joint Surg Am 1969;51:223-9

Nault ML, Mac-Thiong JM, Roy-Beaudry M, Turgeon I, de Guise J, Labelle H, Parent S. Three-dimensional spinal morphology can differentiate between progressive and nonprogressive patients with adolescent idiopathic scoliosis at the initial presentation: a prospective study. Spine 2014;39(10):E601-6

Negrini S, Aulisa AG, Aulisa L, Circo AB, de Mauroy JC, Durmala J, Grivas TB, Knott P, Kotwicki T, Maruyama T, Minozzi S, O'Brien JP, Papadopoulos D, Rigo M, Rivard CH, Romano M, Wynne JH, Villagrasa M, Weiss HR, Zaina F. 2011 SOSORT guidelines: Orthopaedic and Rehabilitation treatment of idiopathic scoliosis during growth. Scoliosis 2012;7(1):3

Negrini S, Grivas TB, Kotwicki T, Rigo M, Zaina F; International Society on Scoliosis Orthopaedic and Rehabilitation Treatment (SOSORT). Guidelines on ''Standards of management of idiopathic scoliosis with corrective braces in everyday clinics and in clinical research'': SOSORT Consensus 2008. Scoliosis 2009;4:2

Nelson TR, Pretorius DH. Three-dimensional ultrasound imaging. Ultrasound Med Biol 1998;24(9):1243-70

Newton PO, Fujimori T, Doan J, Reighard FG, Bastrom TP, Misaghi A. Defining the "Three-Dimensional Sagittal Plane" in Thoracic Adolescent Idiopathic Scoliosis. J Bone Joint Surg Am 2015;97(20):1694-701

Newton PO, Yaszay B, Upasani VV, Pawelek JB, Bastrom TP, Lenke LG, Lowe T, Crawford A, Betz R, Lonner B; Harms Study Group. Preservation of thoracic kyphosis is critical to maintain lumbar lordosis in the surgical treatment of adolescent idiopathic scoliosis. Spine 2010;35(14):1365-70

Ni H, Zhu X, He S, Yang C, Wang C, Zhao Y, Wu D, Xu J, Li M. An increased kyphosis of the thoracolumbar junction is correlated to more axial vertebral rotation in thoracolumbar/lumbar adolescent idiopathic scoliosis. Spine 2010;35(23):E1334-8

Nissinen M, Heliövaara M, Seitsamo J, Poussa M. Trunk asymmetry, posture, growth, and risk of scoliosis. A three-year follow-up of Finnish prepubertal school children. Spine 1993;18(1):8-13

Nordwall A, Willner S. A study of skeletal age and height in girls with idiopathic scoliosis. Clin Orthop Relat Res 1975;6-10

Obeid I, Hauger O, Aunoble S, Bourghli A, Pellet N, Vital JM. Global analysis of sagittal spinal alignment in major deformities: correlation between lack of lumbar lordosis and flexion of the knee. Eur Spine J 2011;20(Suppl 5):681-5

Oe S, Togawa D, Nakai K, Yamada T, Arima H, Banno T, Yasuda T, Kobayasi S, Yamato Y, Hasegawa T, Yoshida G, Matsuyama Y. The influence of age and gender on cervical spinal alignment among volunteers aged over 50. Spine 2015; 40(19):1487-94

Öhlén G, Spangfort E, Tingvall C. Measurement of spinal sagittal configuration and mobility with Debrunner's kyphometer. Spine 1989;14(6):580-3

Ottander HG. Experimental progressive scoliosis in a pig. Acta Orthop Scand 1963;91-7

Parent S, Labelle H, Skalli W, Latimer B, de Guise J. Morphometric analysis of anatomic scoliotic specimens. Spine 2002;27(21):2305-11

Parvaresh KC, Osborn EJ, Reighard FG, Doan J, Bastrom TP, Newton PO. Predicting 3D Thoracic Kyphosis Using Traditional 2D Radiographic Measurements in Adolescent Idiopathic Scoliosis. Spine Deform. 2017;5(3):159-65

Patel PN, Upasani VV, Bastrom TP, Marks MC, Pawelek JB, Betz RR, Lenke LG, Newton PO. Spontaneous lumbar curve correction in selective thoracic fusions of idiopathic scoliosis: a comparison of anterior and posterior approaches. Spine 2008;33:1068-73

Petersen I, Sahlstrand T, Sellden U. Electroencephalographic investigation of patients with adolescent idiopathic scoliosis. Acta Orthop Scand 1979;50:283-93

Phillips FM, Reuben J, Wetzel FT. Intervertebral disc degeneration adjacent to a lumbar fusion. An experimental rabbit model. J Bone Joint Surg Br 2002;84:289-94

Piggott H. The natural history of scoliosis in myelodysplasia. J Bone Joint Surg Br 1980;62-B:54-8

Pincott JR, Taffs LF. Experimental scoliosis in primates: a neurological cause. J Bone Joint Surg Br 1982;64:503-7

Polly DW Jr, Kilkelly FX, McHale KA, Asplund LM, Mulligan M, Chang AS. Measurement of lumbar lordosis. Evaluation of intraobserver, interobserver, and technique variability. Spine 1996;21(13):1530-5

Ponrartana S, Fisher CL, Aggabao PC, Chavez TA, Broom AM, Wren TA, Skaggs DL, Gilsanz V. Small vertebral cross-sectional area and tall intervertebral disc in adolescent idiopathic scoliosis. Pediatr Radiol 2016;46(10):1424-9.

Pope MH, Stokes IAF, Moreland M. The biomechanics of scoliosis. CRC Crit Rev Biomed Eng 1984;11:157-88

Porter R. Idiopathic scoliosis: the relation between the vertebral canal and the vertebral bodies. Spine 2000;25:1360-6

Porter RW. Can a short spinal cord produce scoliosis? Eur Spine J 2001b; 10:2–9.

Porter RW. The pathogenesis of idiopathic scoliosis: uncoupled neuroosseous growth? Eur Spine J 2001a;10:473-81

Potter BK, Kuklo TR, Lenke LG. Radiographic outcomes of anterior spinal fusion versus posterior spinal fusion with thoracic pedicle screws for treatment of Lenke Type I adolescent idiopathic scoliosis curves. Spine 2005;30: 1859-66

Poussa MS, Heliovaara MM, Seitsamo JT, Könönen MH, Hurmerinta KA, Nissinen MJ. Development of spinal posture in a cohort of children from the age of 11 to 22 years. Eur Spine J 2005;14:738-42

Prince RL, Devine A, Dick IM. The clinical utility of measured kyphosis as a predictor of the presence of vertebral deformities. Osteoporos Int 2007;18(5):621-7

Pruijs JE, Hageman MA, Keessen W, van der Meer R, van Wieringen JC. Variation in Cobb angle measurements in scoliosis. Skeletal Radiol 1994;23(7):517-20

Purnama KE, Wilkinson MH, Veldhuizen AG, van Ooijen PM, Lubbers J, Burgerhof JG, Sardjono TA, Verkerke GJ. A framework for human spine imaging using a freehand 3D ultrasound system. Technol Health Care 2010;18(1):1-17

Qiu G, Zhang J, Wang Y, Xu H, Zhang J, Weng X, Lin J, Zhao Y, Shen J, Yang X, Luk KD, Lu D, Lu WW. A new operative classification of idiopathic scoliosis: a peking union medical college method. Spine 2005;30(12):1419-26

Rajabi R, Doherty P, Goodarzi M and Hemayattalab R. Comparison of thoracic kyphosis in two groups of elite Greco-Roman and free style wrestlers and a group of non-athletic subjects. British Journal of Sports Medicine 2007; 42, 229-32

Riddle HF, Roaf R. Muscle imbalance in the causation of scoliosis. Lancet 1955;268:1245-7

Ripani, M, Di Cesare A, Giombini A, Agnello L, Fagnani F, Pigozzi F. Spinal curvature: comparison of frontal measurements with the Spinal Mouse and radiographic assessment. J Sports Med Phys Fitness 2008;48(4):488-94

Roaf R. Vertebral growth and its mechanical control. J Bone Joint Surg Br 1960;42:40-59

Robin GC. Scoliosis of spina bifida and infantile paraplegia. Isr J Med Sci 1972;8:1823-9

Roth M. Idiopathic scoliosis caused by a short spinal cord. Acta Radiol Diagn (Stockh) 1968;7:257-71

Roussouly P, Berthonnaud E, Dimnet J. Geometrical and mechanical analysis of lumbar lordosis in an asymptomatic population: proposed classification. Rev Chir Orthop Reparatrice Appar Mot 2003;89(7):632-9

Roussouly P, Gollogly S, Noseda O, Berthonnaud E, Dimnet J. The vertical projection of the sum of the ground reactive forces of a standing patient is not the same as the C7 plumb line: a radiographic study of the sagittal alignment of 153 asymptomatic volunteers. Spine 2006 15;31(11):E320-5

Roussouly P, Labelle H, Rouissi J, Bodin A. Pre- and post-operative sagittal balance in idiopathic scoliosis: a comparison over the ages of two cohorts of 132 adolescents and 52 adults. Eur Spine J 2013;22 Suppl 2:S203-15

Roussouly P, Nnadi C. Sagittal plane deformity: an overview of interpretation and management. Eur Spine J 2010;19(11):1824-36

Roussouly P, Pinheiro-Franco JL. Biomechanical analysis of the spino-pelvic organization and adaptation in pathology. Eur Spine J 2011; 20(Suppl 5): 609-18

Roussouly P, Pinheiro-Franco JL. Biomechanical analysis of the spino-pelvic organization and adaptation in pathology. Eur Spine J 2011b;20 Suppl 5:609-18

Roussouly P, Pinheiro-Franco JL. Sagittal parameters of the spine: biomechanical approach. Eur Spine J 2011a;20 Suppl 5:578-85

Sahlstrand T, Petruson B, Ortengren R. Vestibulospinal reflex activity in patients with adolescent idiopathic scoliosis. Postural effects during caloric labyrinthine stimulation recorded by stabilometry. Acta Orthop Scand 1979;50:275-81

Salem W, Coomans Y, Brismée JM, Klein P, Sobczak S, Dugailly PM. Sagittal Thoracic and Lumbar Spine Profiles in upright standing and Lying Prone Positions among Healthy Subjects: Influence of various Biometric features. Spine 2015; 40(15):E900-8

Schlegel JD, Smith JA, Schleusener RL. Lumbar motion segment pathology adjacent to thoracolumbar, lumbar, and lumbosacral fusions. Spine 1996;21:970-81

Schlösser TP, Shah SA, Reichard SJ, Rogers K, Vincken KL, Castelein RM. Differences in early sagittal plane alignment between thoracic and lumbar adolescent idiopathic scoliosis. Spine J 2014;14(2):282-90

Schlösser TP, Vincken KL, Attrach H, Kuijf HJ, Viergever MA, Janssen MM, Castelein RM. Quantitative analysis of the closure pattern of the neurocentral junction as related to preexistent rotation in the normal immature spine. Spine J 2013;13(7):756-63.

Schmid S, Studer D, Hasler CC, Romkes J, Taylor WR, Brunner R, Lorenzetti S. Using Skin Markers for Spinal Curvature Quantification in Main Thoracic Adolescent Idiopathic Scoliosis: An Explorative Radiographic Study. PLoS One 2015;10(8):e0135689

Schmitz A, Ja¨ger U, Ko¨nig R, Kandyba J, Gieske J, Schmitt O. Sagittale Cobb–Winkel Messungen bei Skoliose mittels MR-Ganzwirbelsa¨ulenaufnahme. Z Orthop Ihre Grenzgeb 2001;139:304-7

Schmitz-Feuerhake I, Pflugbeil S. 'Lifestyle' and cancer rates in former East and West Germany: the possible contribution of diagnostic radiation exposures. Radiat Prot Dosimetry 2011;147(1-2):310-3

Schuler TC, Subach BR, Branch CL, Foley KT, Burkus JK; Lumbar Spine Study Group. Segmental lumbar lordosis: manual versus computer-assisted measurement using seven different techniques. J Spinal Disord Tech 2004;17(5):372-9

Schuller S, Charles YP, Steib JP. Sagittal spinopelvic alignment and body mass index in patients with degenerative spondylolisthesis. Eur Spine J 2011;20:713-719

Schwab F, Ungar B, Blondel B, Buchowski J, Coe J, Deinlein D, DeWald C, Mehdian H, Shaffrey C, Tribus C, Lafage V. Scoliosis Research Society-Schwab adult spinal deformity classification: a validation study. Spine 2012;37(12):1077-82

Sevastikoglou JA, Linderholm H, Lindgren U. Effect of the Milwaukee brace on vital and ventilatory capacity of scoliotic patients. Acta Orthop Scand 1976;47:540-5

Shamji MF, Ames CP, Smith JS, Rhee JM, Chapman JR, Fehlings MG. Myelopathy and spinal deformity. Spine 2013;38:S147-8

Shea KG, Stevens PM, Nelson M, Smith JT, Masters KS, Yandow S. A comparison of manual versus computer-assisted radiographic measurement. Intra-observer measurement variability for Cobb angles. Spine 1998;23(5):551-5

Shrout PE, Fleiss JL. Intraclass correlations: uses in assessing rater reliability. Psychol Bull 1979;86(2):420-8

Singer KP, Edmondston SJ, Day RE, Breidahl WH. Computer-assisted curvature assessment and Cobb angle determination of the thoracic kyphosis. An in vivo and in vitro comparison. Spine 1994;19(12):1381-4

Singer KP, Jones TJ, Breidahl PD. A comparison of radiographic and computer-assisted measurements of thoracic and thoracolumbar sagittalcurvature. Skeletal Radiol 1990;19(1):21-6

Skalli W, Vergari C, Ebermeyer E, Courtois I, Drevelle X, Kohler R, Abelin-Genevois K, Dubousset J. Early Detection of Progressive Adolescent Idiopathic Scoliosis: A Severity Index. Spine 2017;42(11):823-30

Smit TH. The use of a quadruped as an in vivo model for the study of the spine–biomechanical considerations. Eur Spine J 2002;11:137-44

Smith JS, Lafage V, Ryan DV, Shaffrey CI, Schwab FJ, Patel AA, Brodke DS, Arnold PM, Riew KD, Traynelis VC, Radcliff K, Vaccaro AR, Fehlings MG, Ames CP. Association of myelopathy scores with cervical sagittal balance and normalized spinal cord volume. Spine 2013;38:S161-70

Solomonow M, Zhou BH, Baratta RV, Burger E. Biomechanics and electromyography of a cumulative lumbar disorder: response to static flexion. Clin Biomech 2003;18(10):890-8

Somoskeöy S, Tunyogi-Csapó M, Bogyó C, Illés T. Accuracy and reliability of coronal and sagittal spinal curvature data based on patient-specific three-dimensional models created by the EOS 2D/3D imaging system. Spine J 2012a;12(11):1052-9

Srinivasalu S, Modi HN, Smehta S, Suh SW, Chen T, Murun T. Cobb angle measurement of scoliosis using computer measurement of digitally acquired radiographs. Intra-observer and inter-observer variability. Asian Spine J 2008;2(2):90-3

Stagnara P, De Mauroy JC, Dran G, Gonon GP, Costanzo G, Dimnet J, Pasquet A. Reciprocal angulation of vertebral bodies in a sagittal plane: approach to references for the evaluation of kyphosis and lordosis. Spine 1982;7:335-42

Stokes IA, Aronsson DD. Computer-assisted algorithms improve reliability of King Classification and Cobb angle measurement of scoliosis. Spine 2006;31(6):665-70

Stokes IA, Bigalow LC, Moreland MS. Three-dimensional spinal curvature in idiopathic scoliosis. J Orthop Res 1987;5(1):102-13

Stokes IA, Moreland MS. Measurement of the shape of the surface of the back in patients with scoliosis. The standing and forward-bending positions. J Bone Joint Surg Am 1987;69(2):203-11

Stokes IA, Spence H, Aronsson DD, Kilmer N. Mechanical modulation of vertebral body growth. Implications for scoliosis progression. Spine 1996;21: 1162-7

Stokes IAF, Gardner-Morse M. Analysis of the interaction between vertebral lateral deviation and axial rotation in rotation in scoliosis. J Biomech 1991;24(8):753-9

Sullivan TB, Bastrom T, Reighard F, Jeffords M, Newton PO. A Novel Method for Estimating Three-Dimensional Apical Vertebral Rotation Using Two-Dimensional Coronal Cobb Angle and Thoracic Kyphosis. Spine Deform 2017;5(4):244-9

Sullivan TB, Reighard FG, Osborn EJ, Parvaresh KC, Newton PO. Thoracic Idiopathic Scoliosis Severity Is Highly Correlated with 3D Measures of Thoracic Kyphosis. J Bone Joint Surg Am 2017;99(11):e54

Suzuki S, Yamamuro T, Shikata J, Shimizu K, Iida H. Ultrasound measurement of vertebral rotation in idiopathic scoliosis. J Bone Joint Surg Br 1989;71(2):252-5

Swank ML. Adjacent segment failure above lumbosacral fusions instrumented to L1 or L2. Paper presented at: 37th Annual Scoliosis Research Society Meeting 2002; Seattle, WA.

Takács M, Orlovits Z, Jáger B, Kiss RM. Comparison of spinal curvature parameters as determined by the ZEBRIS spine examination method and the Cobb method in children with scoliosis. PLoS One 2018;13(7):e0200245

Takács M, Rudner E, Kovács A, Orlovits Z, Kiss RM. The assessment of the spinal curvatures in the sagittal plane of children using an ultrasound-based motion analysing system. Ann Biomed Eng 2015;43(2):348-62

Tan KJ, Moe MM, Vaithinathan R, Wong HK. Curve progression in idiopathic scoliosis: follow-up study to skeletal maturity. Spine 2009;34(7):697-700

Tang JA, Scheer JK, Smith JS, Deviren V, Bess S, Hart RA, Lafage V, Shaffrey CI, Schwab F, Ames CP; ISSG. The impact of standing regional cervical sagittal alignment on outcomes in posterior cervical fusion surgery. Neurosurgery 2012;71:662-9

Tang SP, Cheng JCY, Ng BKW, Lam TP. Adolescent idiopathic scoliosis (AOS): An overview of the etiology and basic management principles. HK J Paediatr 2003;8:299-306

Thaler M, Kaufmann G, Steingruber I, Mayr E, Liebensteiner M, Bach C. Radiographic versus ultrasound evaluation of the Risser Grade in adolescent idiopathic scoliosis: a prospective study of 46 patients. Eur Spine J 2008;17(9):1251-5

Than P, Szuper K, Somoskeoy S, Warta V, Illes T. Geometrical values of the normal and arthritic hip and knee detected with the EOS imaging system. Int Orthop 2012;36(6):1291-7

Thawait GK, Chhabra A, Carrino JA. Spine segmentation and enumeration and normal variants. Radiol Clin North Am 2012;50(4):587-98

Thompson JP, Transfeldt EE, Bradford DS, Ogilvie JW, Boachie- Adjei O. Decompensation after Cotrel-Dubousset instrumentation of idiopathic scoliosis. Spine 1990;15(9):927-31

Thomsen M, Abel R. Imaging in scoliosis from the orthopaedic surgeon's point of view. Eur J Radiol 2006;58(1):41-7

Torell G, Nachemson A, Haderspeck-Grib K, Schultz A. Standing and supine Cobb measures in girls with idiopathic scoliosis. Spine 1985;10:425-7

Torlak G, Kiter E, Oto M, Akman A. Ultrasonographic evaluation of the Risser sign. Is it a reliable and reproducible method? Spine 2012;37(4):316-20

Ungi T, Abolmaesumi P, Jalal R, Welch M, Ayukawa I, Nagpal S, Lasso A, Jaeger M, Borschneck DP, Fichtinger G, Mousavi P. Spinal needle navigation by tracked ultrasound snapshots. IEEE Trans Biomed Eng 2012;59:2766-72

Ungi T, King F, Kempston M, Keri Z, Lasso A, Mousavi P, Rudan J, Borschneck DP, Fichtinger G. Spinal curvature measurement by tracked ultrasound snapshots. Ultrasound Med Biol 2014;40(2):447-54

Van Royen BJ, De Gast A, Smit TH. Deformity planning for sagittal plane corrective osteotomies of the spine in ankylosing spondylitis. Eur Spine J 2000;9(6):492-8

Van Royen BJ, Toussaint HM, Kingma I, Bot SD, Caspers M, Harlaar J, Wuisman PI. Accuracy of the sagittal vertical axis in a standing lateral radiograph as a measurement of balance in spinal deformities. Eur Spine J 1998;7(5):408-12

Van Schaik JP, Verbiest H, Van Schaik FD, Isolated spinous process deviation: a pitfall in the interpretation of AP radiographs of the lumbar spine. Spine 1989;14:970-6

Vaz G, Roussouly P, Berthonnaud E, Dimnet J. Sagittal morphology and equilibrium of pelvis and spine. Eur Spine J 2002;11(1):80-7

Velis KP, Healey JH, Schneider R. Peak skeletal mass assessment in young adults with idiopathic scoliosis. Spine 1989;14:706-11

Venn G, Mehta MH, Mason RM. Solubility of spinal ligament collagen in idiopathic and secondary scoliosis. Clin Orthop Relat Res 1983;294-301

Vidal C, Ilharreborde B, Azoulay R, Sebag G, Mazda K. Reliability of cervical lordosis and global sagittal spinal balance measurements in adolescent idiopathic scoliosis. Eur Spine J 2013;22(6):1362-7

Villemure I, Aubin CE, Grimard G, Dansereau J, Labelle H. Progression of vertebral and spinal three-dimensional deformities in adolescent idiopathic scoliosis: a longitudinal study. Spine 2001;26(20):2244-50

Volkmann R. Verletzungen und Krankenheiten der Bewegungsorgane. Pitha-Billroth, Handbuch der allgemeinen und speciellen Chirurgie Bd II Teil II. Stuttgart: Ferdinand Enke; 1882.

Vora V, Crawford A, Babekhir N, Boachie-Adjei O, Lenke L, Peskin M, Charles G, Kim Y. A pedicle screw construct gives an enhanced posterior correction of adolescent idiopathic scoliosis when compared with other constructs: myth or reality. Spine 2007;32:1869-74

Voutsinas S, MacEwen G. Sagittal profiles of the spine. Clin Orthop Relat Res 1986;210:235–242

Vrtovec T, Pernus F, Likar B. A review of methods for quantitative evaluation of spinal curvature. Eur Spine J 2009;18(5):593-607

Walter SD, Eliasziw M, Donner A. Sample size and optimal designs for reliability studies. Stat Med 1998;17(1):101-10

Wang Q, Li M, Lou EH, Chu WC, Lam TP, Cheng JC, Wong MS. 2016. Validity Study of Vertebral Rotation Measurement Using 3-D Ultrasound in Adolescent Idiopathic Scoliosis. Ultrasound Med Biol 42(7):1473-81

Wang Q, Li M, Lou EH, Wong MS. Reliability and Validity Study of Clinical Ultrasound Imaging on Lateral Curvature of Adolescent Idiopathic Scoliosis. PLoS One 2015;10(8):e0135264

Wang S, Qiu Y, Zhu Z, Ma Z, Xia C, Zhu F. Histomorphological study of the spinal growth plates from the convex side and the concave side in adolescent idiopathic scoliosis. J Orthop Surg 2007;2:19

Wang ZW, Wang WJ, Sun MH, Liu Z, Zhu ZZ, Zhu F, Qiu XS, Qian BP, Wang SF, Qiu Y. Characteristics of the pelvic axial rotation in adolescent idiopathic scoliosis: a comparison between major thoracic curve and major thoracolumbar/lumbar curve. Spine J 2014;14(9):1873-8

Waters RL, Morris JM. An in vitro study of normal and scoliotic interspinous ligaments. J Biomech 1973;6:343-8

Weinstein SL, Dolan LA, Cheng JC, Danielsson A, Morcuende JA. Adolescent idiopathic scoliosis. Lancet 2008;371:1527-37

Wessberg P, Danielson BI, Willen J. Comparison of Cobb angles in idiopathic scoliosis on standing radiographs and supine axially loaded MRI. Spine 2006;31:3039-44

Wilke HJ, Kettler A, Wenger KH, Claes LE. Anatomy of the sheep spine and its comparison to the human spine. Anat Rec 1997;247:542-55

Wilke HJ, Neef P, Caimi M, Hoogland T, Claes LE. New in vivo measurements of pressures in the intervertebral disc in daily life. Spine 1999;24(8):755-62

Willner S. Spinal pantograph – a non-invasive technique for describing kyphosis and lordosis in the thoraco-lumbar spine. Acta Orthop Scand 1981;52(5):525-9

Willner S. The proportion of legs to trunk in girls with idiopathic structural scoliosis. Acta Orthop Scand 1975;46:84-9

Winter R, Hall JE (1978) Kyphosis in childhood and adolescence. Spine 3:285-308

Winter R, Lovell WW, Moe J. Excessive thoracic lordosis and loss of pulmonary function in patients with idiopathic scoliosis. J Bone Joint Surg 1975;57: 972-7

Wojtys EM, Ashton-Miller JA, Huston LJ, Moga PJ. The association between athletic training time and the sagittal curvature of the immature spine. Am J Sports Med 2000;28(4):490-8

Wong MS, Cheng JC, Lo KH. A comparison of treatment effectiveness between the CAD/CAM method and the manual method for managing adolescent idiopathic scoliosis. Prosthet Orthot Int 2005;29(1):105-11

Wong MS, Lee JT, Luk KD, Chan LC. Effect of different casting methods on adolescent idiopathic scoliosis. Prosthet Orthot Int 2003;27(2):121-31

Wong MS, Mak AF, Luk KD, Evans JH, Brown B. Effectiveness and biomechanics of spinal orthoses in the treatment of adolescent idiopathic scoliosis (AIS). Prosthet Orthot Int 2000;24(2):148-62

Wren TA, Aggabao PC, Poorghasamians E, Chavez TA, Ponrartana S, Gilsanz V. Association between vertebral cross-sectional area and lumbar lordosis angle in adolescents. PLoS One 2017a;12(2):e0172844

Wright A. The conservative management of adolescent idiopathic scoliosis. Phys Ther Rev 1977;2:153-63

Wybier M, Bossard P. Musculoskeletal imaging in progress: the EOS imaging system. Joint Bone Spine 2013;80(3):238-43

Xiong B, Sevastik J, Hedlund R, Sevastik B. Sagittal configuration of the spine and growth of the posterior elements in early scoliosis. J Orthop Res 1994;12:113-8

Yagi M, Takeda K, Machida M, Asazuma T. Discordance of gravity line and C7PL in patient with adult spinal deformity-factors affecting the occiput-trunk sagittal discordance. Spine J 2015;15:213-21

Yang B, Yang C, Ondra S. A novel mathematical model of the sagittal spine. Spine 2007;32:466-70

Yazici M, Acaroglu ER, Alanay A, Deviren V, Cila A, Surat A. Measurement of vertebral rotation in standing versus supine position in adolescent idiopathic scoliosis. J Pediatr Orthop 2001;21(2):252-6

Yong Q, Zhen L, Zezhang Z, Bangping Q, Feng Z, Tao W, Jun J, Xu S, Xusheng Q, Weiwei M, Weijun W. Comparison of sagittal spinopelvic alignment in Chinese adolescents with and without idiopathic thoracic scoliosis. Spine 2012;37(12):E714-20

Young M, Hill DL, Zheng R, Lou E. Reliability and accuracy of ultrasound measurements with and without the aid of previous radiographs in adolescent idiopathic scoliosis (AIS). Eur Spine J 2015;24(7):1427-33

Yu J, Fairbank JC, Roberts S, et al. The elastic fiber network of the anulus fibrosus of the normal and scoliotic human intervertebral disc. Spine 2005;30:1815-20

Yu M, Silvestre C, Mouton T, Rachkidi R, Zeng L, Roussouly P. Analysis of the cervical spine sagittal alignment in young idiopathic scoliosis: a morphological classification of 120 cases. Eur Spine J 2013;22(11):2372-81

Zaleske DJ, Ehrlich MG, Hall JE. Association of glycosaminoglycan depletion and degradative enzyme activity in scoliosis. Clin Orthop Relat Res 1980;177-81

Zetterberg C, Hansson T, Lindström J, Irstam L, Andersson GB. Postural and time-dependent effects on body height and scoliosis angle in adolescent idiopathic scoliosis. Acta Orthop Scand 1983;54(6):836-40

Zheng R, Young M, Hill D, Le LH, Hedden D, Moreau M, Mahood J, Southon S, Lou E. Improvement on the Accuracy and Reliability of Ultrasound Coronal Curvature Measurement on Adolescent Idiopathic Scoliosis With the Aid of Previous Radiographs. Spine 2016;41(5):404-11

Zsidai, A, Kocsis L. Ultrasound based measuring diagnostic and muscle activity measuring system for spinal analysis. Technol Health Care 2006;14(4-5):243-50